2011

Investigation of Ultrasonics as a tool for energy efficient recycling of Lactic acid from postconsumer PLA products

Gowrishankar Srinivasan
Iowa State University

Investigation of Ultrasonics as a tool for energy efficient recycling of Lactic acid from postconsumer PLA products

By

Gowrishankar Srinivasan

A dissertation submitted to the graduate faculty

in partial fulfillment of the requirements for the degree of

DOCTOR OF PHILOSOPHY

Major: Biorenewable Resources and Technology

Program of Study Committee:

David Grewell, Major Professor

Thomas Brumm

Matthew J. Darr

Michael R. Kessler

Raj D. Raman

Iowa State University

Ames, Iowa

2011

TABLE OF CONTENTS

LIST OF TABLES

LIST OF FIGURES

LIST OF SYMBOLS

ΔH^o_m - Enthalpy of melting/ crystallization (J/g or J/mole)

T_g - Glass transition temperature (^oC)

T_m - Melting temperature (^oC)

Pa - Pascal (N/m^2)

MPa - Mega Pascal (10^6 x N/m^2)

GPa - Giga Pascal

t - Time(s)

E - Energy (J)

m - Mass (kg)

f - Frequency, Hz (1/s)

A - Amplitude (m)

V - Volume (m^3)

ρ - Density (kg/m^3)

I - Intensity (W/m^2)

c - Speed of sound (m/s)

ω - Angular frequency (rad/s)

Q - Quality factor

R - Rayleigh number

λ - Wavelength(m)

M - number of moles(mol)

C_p - Specific heat (J/mol. K)

ACKNOWLEDGMENTS

I would like to express my sincere gratitude to the Mr. Steve Devlin and the USDA –Biopreferred program for providing the financial support for this research work and hope the outcome of this work is useful in the field of biobased polymers.

I would also like to thank Dr. Lawrence Johnson and the staff members of Center for Crops Utilization and research for allowing me to use their equipment and extending their support for the work discussed in this thesis.

I would like to express my sincere gratitude to Dr. Robert Stephenson for his help with the statistical analysis of the results.

Last but not the least I would express my sincere thanks to my major professor Dr. David Grewell, my committee members Dr. Thomas Brumm, Dr. Mathew Darr, Dr. Michael Kessler and Dr. Raj Raman for providing valuable guidance and providing me with the opportunity to do research in the field of Biopolymers.

ABSTRACT

The growing use of “ecofriendly,” biodegradable polymers have created a need for a suitable recycling technique because, unlike petroleum derived plastics, their properties deteriorate during conventional recycling. These new techniques must be cost efficient and yield material properties same as virgin polymer. This research investigates the effectiveness of high-power ultrasonics as an efficient technique to recover lactic acid from postconsumer polylactic acid (PLA) products. Polylactic acid is a commercially available bioplastic derived from corn starch and/or sugar cane that is biorenewable and compostable (biodegradable). The various ongoing researches to recover lactic acid from PLA employ a common platform of high temperature, high pressure (HTHP) to effect polymer hydrolysis. The energy intensiveness of these HTHP processes prompted this work to investigate ultrasonics as an low energy alternative process to cause PLA depolymerization. The energy consumption and the time required for depolymerization were utilized as the metrics to quantify and compare depolymerization enhanced by ultrasonics with hot-bath technique. The coupled effect of catalysts concentration and different solvents, along with ultrasonic were studied based on preliminary trial results. In addition, the correlation between the rates of de-polymerization was analyzed for ultrasonic amplitude, treatment time, and catalyst concentration and types. The results indicate that depolymerization of

PLA was largely effected by heating caused by ultrasonic-induced cavitations. Other effects of ultrasonics, namely cavitations and acoustic streaming, were shown to have minimal effects in enhancing depolymerization. In fact, thermal energy predominately affected the reaction kinetics; the heat introduced by conventional method (i.e., electrical heaters) was more efficient than ultrasonic heating in terms of energy (for depolymerization) per unit mass of PLA and depolymerizing time. The degree of crystallinity also was an important factor that affected the reaction kinetics of depolymerization. It was found that amorphous PLA de-polymerized faster compared to semi-crystalline PLA under the same conditions. While the depolymerization of PLA was anticipated to require 15 to 30 minutes, or extreme conditions [41,43], it was determined that with K2CO3 or NaOH catalysts and methanol media as the conditions, PLA could be fully de-polymerized within a few minutes. This information provided insight for effective pathways for the depolymerization of PLA, reducing the environmental impact of material use on the environment.

The effects of the ultrasonics were modeled with finite element analysis based on fundamental concepts. The predictions from the modeling were confirmed by studying real-time streaming and fluid flow inside the treatment cell utilizing particle image Velocimetry (PIV). The FEA (finite element analysis) models of ultrasonic streaming were verified and were in reasonable

agreement with the experimental values, validating simple assumptions for future researchers.

CHAPTER 1: INTRODUCTION

Since the advent of polymers in twentieth century, people have become increasingly reliant on this class of materials. Plastics have become an integral part of everyday life, used in products ranging from cutlery to automobiles. Historically, plastics have been derived from petroleum feedstock; thus, their price and availability have been largely dictated by crude oil prices. Over the last decade, the exponential growth in global petroleum demand, coupled with the Middle-East crisis, have driven crude oil prices up by 500%, as seen Figure 1 [1]. Thus, the cost of polymers and other products derived from petroleum feedstock have also increased. Traditionally, plastics synthesized from hydrocarbons have been engineered for properties such as high-temperature stability and mechanical strength.

Figure 1 World crude oil prices weighted by estimated export volume [1]

As a result of achieving these properties petroleum plastics are innately non-biodegradable and durable, making their, disposal without causing environmental pollution difficult. Recently, multiple approaches have been proposed to solve this problem. The prominent ones include thermal recycling, blending petroleum plastics with biorenewable, biodegradable components, such as starch, to assist structural disintegration and, recently, the use of biodegradable plastics as a substitute. Thermal recycling is the most widely practiced of these solutions. The latest statistics published by the Environmental Protection Agency (EPA), however, reveal concerns with waste stream plastics recovery and disposal. During 2009, the total Municipal Solid Waste (MSW) in the United States amounted to 243 million tons, 12.3% (29.8 million tons) of which was plastic waste, as illustrated in Figure 2. The MSW plastic waste stream is comprised of durable goods (appliances, furniture battery casings, etc), bags, packaging, and polyethylene terephthalate (PET) bottles, as depicted in Figure 3. From the total mass of plastics waste generated (29.8 million tons), only 7.1% was recovered for reuse or recycling during 2009. This leaves 27.7million tons of plastics waste to be discarded. It is important to note that the larger portions of plastic recovered from the waste stream are from the categories of durable goods, PET, and HDPE bottles. Over the last five decades, the rate of plastic recovery from MSW stream has not been in tandem (i.e., proportional) with the amount of waste generated (see Figure 4). The widening gap between the

waste generation line and the recovery line has led to a steady increase in the amount of plastic waste

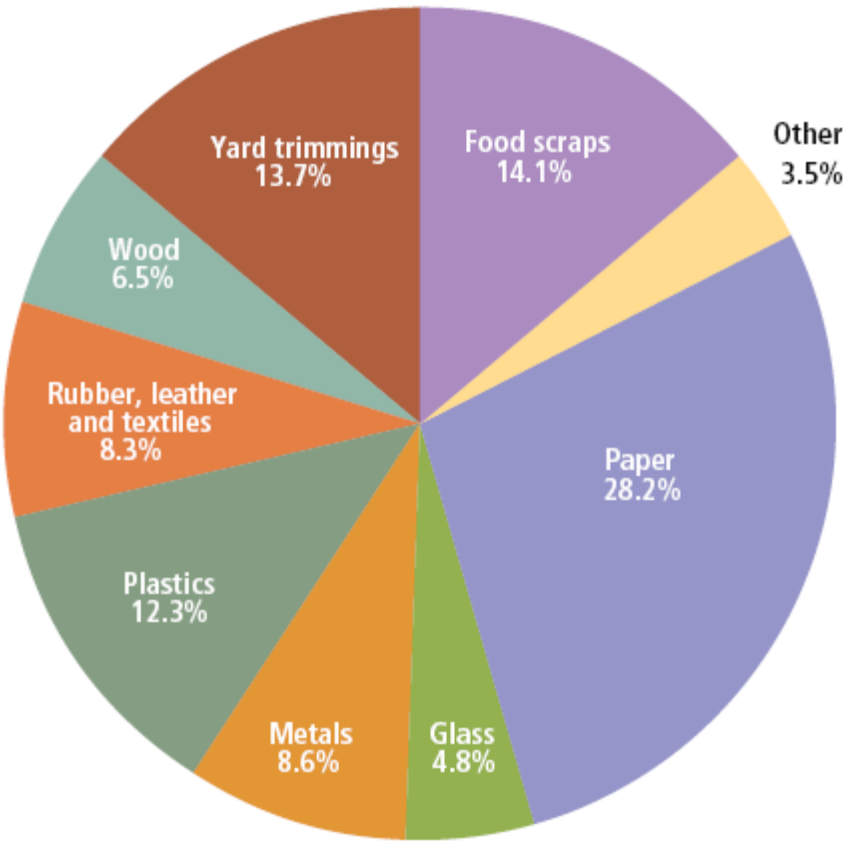

Figure 2 Total municipal solid waste generation (by material), 2009, was a total of 243 million tons before recycling [2]

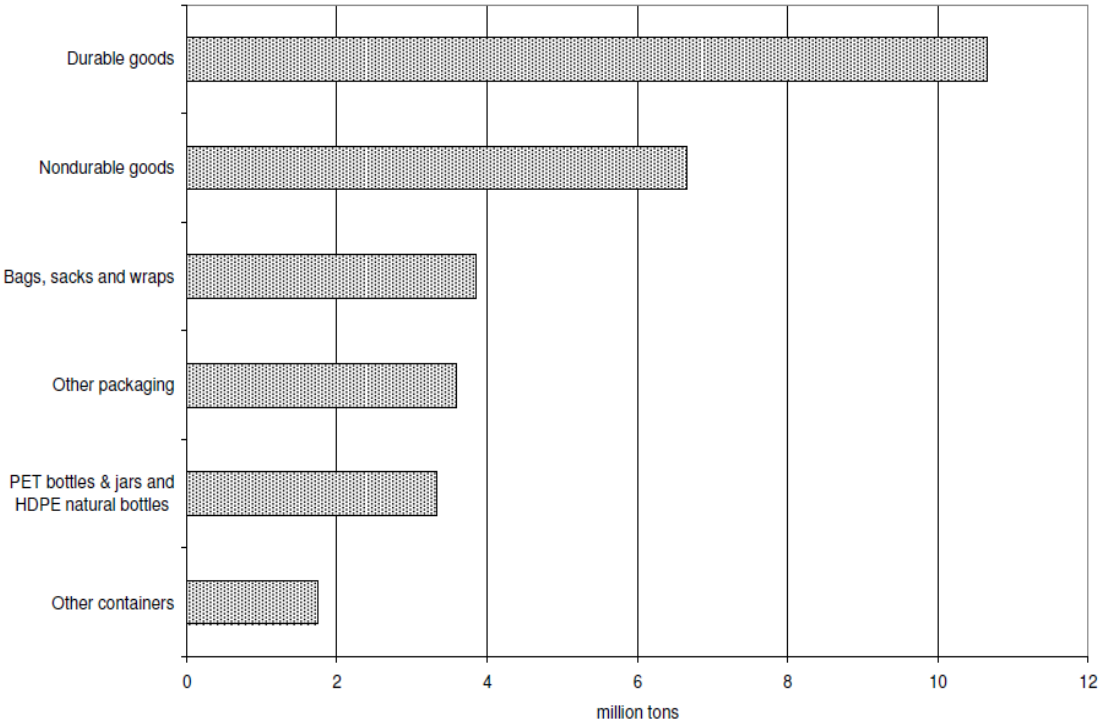

Figure 3 Plastics products generated in MSW, 2009[3]

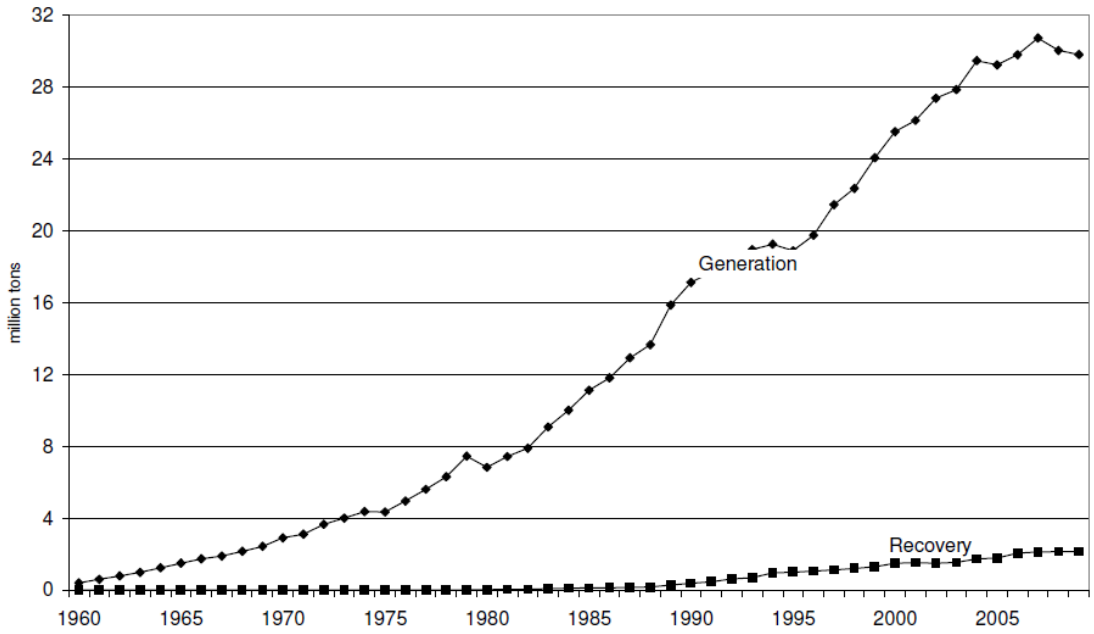

Figure 4 Plastics generation and recovery, 1960 to 2009 [3]

being discarded. During 2009, 27.7 million tons of plastic waste was discarded, thereby adding further to the pollution caused by landfill or incineration. Petroleum plastics blended or filled with biodegradable additives, such as starch and corn cobs, reduce the overall amount of plastics. But such fillers make it difficult to recycle these blended plastic because of their lower thermal stability. In addition, the degradation of these additives after disposal will leave a highly fragmented plastic residue that poses even greater problems of soil contamination and long-term pollution because of their non-biodegradability[4]. The accumulation of such fine non-biodegradable plastic particles in the soil over time will affect the bioactivity of the soil and will release chemical additives as a result of leeching.

The adverse effects of petroleum plastics on environmental pollution has recently led to increased utilization of biorenewable and degradable bio-polyesters (polymers), such as poly(lactic acid) (PLA) and poly-hydroxyl butyrate (PHB). The growing use of PLA as a widely accepted resin in the plastics and packaging industries has enabled companies such as Nature Works, Naturally Iowa, and PepsiCo to manufacture and utilize “ecofriendly” water bottles and food packaging products. This growth is largely due to the reduced cost of PLA resin [5], which is comparable to that of conventional polymers, such as polyethylene, and strong marketing of its claimed environmental benefits. Despite being biorenewable and biodegradable,

issues related to the processability and mechanical properties of PLA have been a major hurdle in achieving widespread acceptance by industry. The latest setback for PLA has been the corporate decision of PepsiCo to partly withdraw its PLA food packaging for its Sunchips® product line, citing customer complaints about the loudness of the packaging[6]. This is attributed to the stiffness/brittleness of PLA, which has been one of the many issues raised when comparing PLA with conventional plastics. Amid such controversies, the preexisting concern regarding contamination of the conventional plastic recycling stream has resurfaced. The discussion below begins with introductions to lactic acid and PLA. Then, it details the need to recycle PLA by developing a method that would both improve PLA's the long-term viability and make it more attractive in terms of energy savings.

1.1 Lactic acid

Lactic acid, according to International union of Pure and Applied Chemistry (IUPAC) nomenclature: 2-Hydroxy propionic Acid [7], is also commonly known as “milk acid”. Lactic acid is one of many organic acids commonly found in nature, most familiarly in milk products, human muscle, bloodstreams, and various fermented beverages and liquids.

1.1.1History

Lactic acid was first discovered by Swedish experimental chemist Carl Wilhelm Scheele in 1780 in sour milk [8].Over time, the acid was also found to be present in fruits and animals. It was understood that depending on oxygen levels, muscles produced lactic acid by breaking down sugars or carbohydrate. In 1860, French chemist and microbiologist, Louis Pasteur, discovered the production of lactic acid by a microorganism (lactobacilli) through the anaerobic process called fermentation [9]. Since its discovery, the food industry has used lactic acid in various fermented products, and many attempts were made to patent it as a food additive. Although the historical record is not clear about the start of commercial lactic production [10,11] the first commercial production of synthetic lactic acid started in 1950 in Japan, where acetaldehyde and hydrogen cyanide were used as the precursors for the lactic acid. Currently, almost all the lactic acid in the world is produced by fermentation of sugars and carbohydrates [12]. Until recently, Purac, Netherlands was the largest manufacturer of lactic acid, but during the last decade, Cargill Dow (now Nature works PLL®) has taken over that position, as it produces lactic acid for in-house production of polylactic acid polymer at its Nebraska plant in the United States.

1.1.2 Structure and properties of lactic acid

Chemically, lactic acid is a chiral three-carbon carboxylic acid (lacking in-plane symmetry, non-superimposable mirror images) and exists in two optically active isomeric forms, L- and D-Lactic acid, as shown in Figure **5**. Lactic acid is commonly found in the L+(-)lactic acid(L-lactic acid) isomeric form in nature and is vital for biological function in animals and humans [13]. The other optical isomer is D(-) lactic acid, also known as R-lactic acid. Either of these isomers can be produce with high levels of purity by using specific microbes in the sugar fermentation process, which is the commercial method of lactic acid production [6,13] **Error! Bookmark not defined.Error! Bookmark not defined.**.

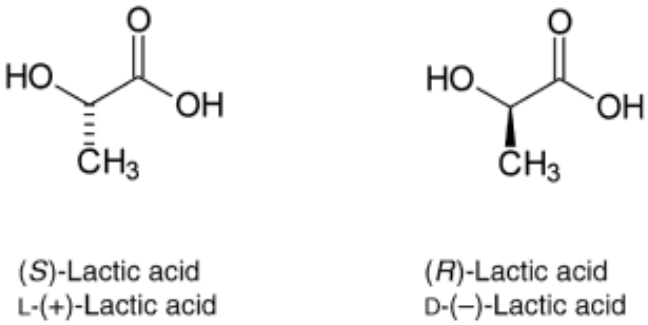

Figure 5 Lactic acid isomers

The ratio of these isomeric forms in a racemic mixture plays a vital role in polymerization of lactic acid into poly (lactic acid) [20]. The racemic purity of lactic acid also partially defines its physical properties, such as density and melting point. The racemic mixture of lactic acid has a melting point of 18 ℃, with a specific gravity of 1.22 at 20 ℃ in the liquid form. The chirally pure lactic acid exists in the solid white crystalline (orthorhombic configuration) powder form, with a melting point of 58 ℃ and a solid density of 1.33 g/cc [12]. The common form L-lactic acid exists in a viscous transparent liquid state and is soluble in water, ethanol, and methanol. The presence of both hydroxyl and carboxylic groups classifies it as alpha hydroxy acid, which can be polymerized into linear polymeric chains. Lactic acid in solution with water tends to undergo polycondensation to form oligomers and intermediate molecules. This makes purification of lactic acid difficult.

1.1.3 Lactic acid production process

Historically, fermentation has been the preferred technique for producing lactic acid because of its simplicity and cost effectiveness compared to other non-biological synthesis routes. Although earlier and current commercial lactic acid production is achieved primarily through fermentation, it is important to review the alternative commercial processes to understand the evolution of commercial lactic acid production. As previously mentioned,

synthesis of lactic acid was conceptualized with various reaction routes, among them the use of aldehydes and lactic acid intermediates as the raw material was one. Then, in 1863, the Monsanto chemical company developed a new process for the commercial synthesis of lactic acid that used cyanation of acetaldehyde to form lactonitrile, which was hydrolyzed into lactic acid, as described in Eqs. 1 and 2 [14,15].

$$CH_3\,CHO + HCN \xrightarrow{HCl} CH_3\,CHOH\,CN \qquad \text{[Eq. 1]}$$

(Acetaldehyde) (Lactonitrile)

$$CH_3\,CHOH\,CN + 2H_2O \xrightarrow{HCl} CH_3\,CHOH\,COONH_4 \rightarrow CH_3CHOHCOOH \qquad \text{[Eq. 2]}$$

(Ammonium lactate) (Lactic acid)

Another approach to lactic acid synthesis was nitrification of alkenes, such as propene, to obtain nitropropionic acid as an intermediate product [14]. These products were further hydrolyzed to obtain lactic acid as depicted by Eqs. 3 and 4.

$$CH_3CH_2CH_3 + HNO_3 + O_2 \longrightarrow CH_3CH(NO_2)COOH \quad \text{[Eq. 3]}$$

(α-Nitropropionic acid)

$$CH_3CH(NO_2)COOH + H_2O \longrightarrow CH_3CHOHCOOH \quad \text{[Eq. 4]}$$

(Lactic acid)

In the past two decades, the process of industrial fermentation of lactic acid from sugars, which had been established during early 20th century in Germany and the United States [12,15], regained prominence because of interest in its use as a monomer for polylactic acid. The fermentation of lactic acid is completed by utilizing the bacterial species Lactobacillus, which is commonly found in such fermented products as wine, cheese, and yogurt. The lactic acid bacterium metabolizes sugars to release energy that the bacterium uses for further propagation; lactic acid as yielded as a byproduct [15]. Fermentation of sugars into lactic acid occurs through two primary routes: homolactic and hetrolactic fermentation, as depicted by Eqs. 5 and 6 in the simplified form. The former is the conversion of a single six-carbon hexose, such as glucose, into two molecules of lactic acid; the latter is the conversion of glucose into one molecule each of lactic acid, ethanol, and carbon dioxide [16, 15,17].

$C_6H_{12}O_6 \longrightarrow 2\ CH_3CHOHCOOH$ [Eq. 5]

(Glucose) (Lactic acid)

$C_6H_{12}O_6 \longrightarrow CH_3CHOHCOOH + C_2H_5OH + CO_2$ [Eq. 6]

(Glucose) (Lactic acid) (Ethanol)

To improve the efficiency of industrial fermentation, various bacterial strands have been developed to follow a homolactic fermentation pathway by using a variety of carbon sources as raw material. These sources range from sugars, such as lactose and glucose, to complex carbohydrates, such as starches. In addition to following a homolactic pathway, the different strands of bacteria yield either D(-) or L(+) optically pure/stereospecific lactic acid, which reduces the need for purification in the production process. As an example, the bacterium strands "Lactobacillus rhamosus" and "Lactobacillus delbrueckii" yield large amounts of L(+) and D(-) optically pure lactic acid from glucose under controlled temperature and pH conditions [15].

Some prominent producers of lactic acid by fermentation have been Archer Daniel Midland (Illinois), Conagra foods (Wisconsin), and Cargill inc. (Minneapolis) in the United States and Purac in The Netherlands. Until 2001,

Purac was the largest producer of lactic acid, but it was later surpassed by Cargill Inc for the production of biopolymer polylactic acid (PLA). A common challenge faced during fermentation of lactic acid is the reduction in pH level (< 3) as lactic acid increases in concentration in the broth. This creates an unfavorable environment for lactic acid bacteria. To counter this, Purac uses a traditionally employed batch production process that includes lime (calcium carbonate) as a pH controller throughout the fermentation phase. This yields a calcium salt of lactic acid as show in Figure 6. Lactic acid is then regenerated from the calcium lactate by reacting the salt with concentrated sulfuric acid. In addition to being a batch process, another problem is that every unit mass of lactic acid produced results in the generation of one unit mass of salt/gypsum. These large quantities of gypsum, along with the use of sulfuric acid, poses a waste disposal issue [14,15]. Further, the lactic acid obtained by this process has a low level of purity and needs to be fractionated by distillation or another filtration-based purifying technique [14]. In contrast, the lactic acid production by Cargill Dow employs a continuous fermentation process. The process involves the removal of lactic acid from the fermentation broth by using a membrane filtration system that is coupled with electrodialysis. This avoids the generation of gypsum and the use of sulfuric acid [15].

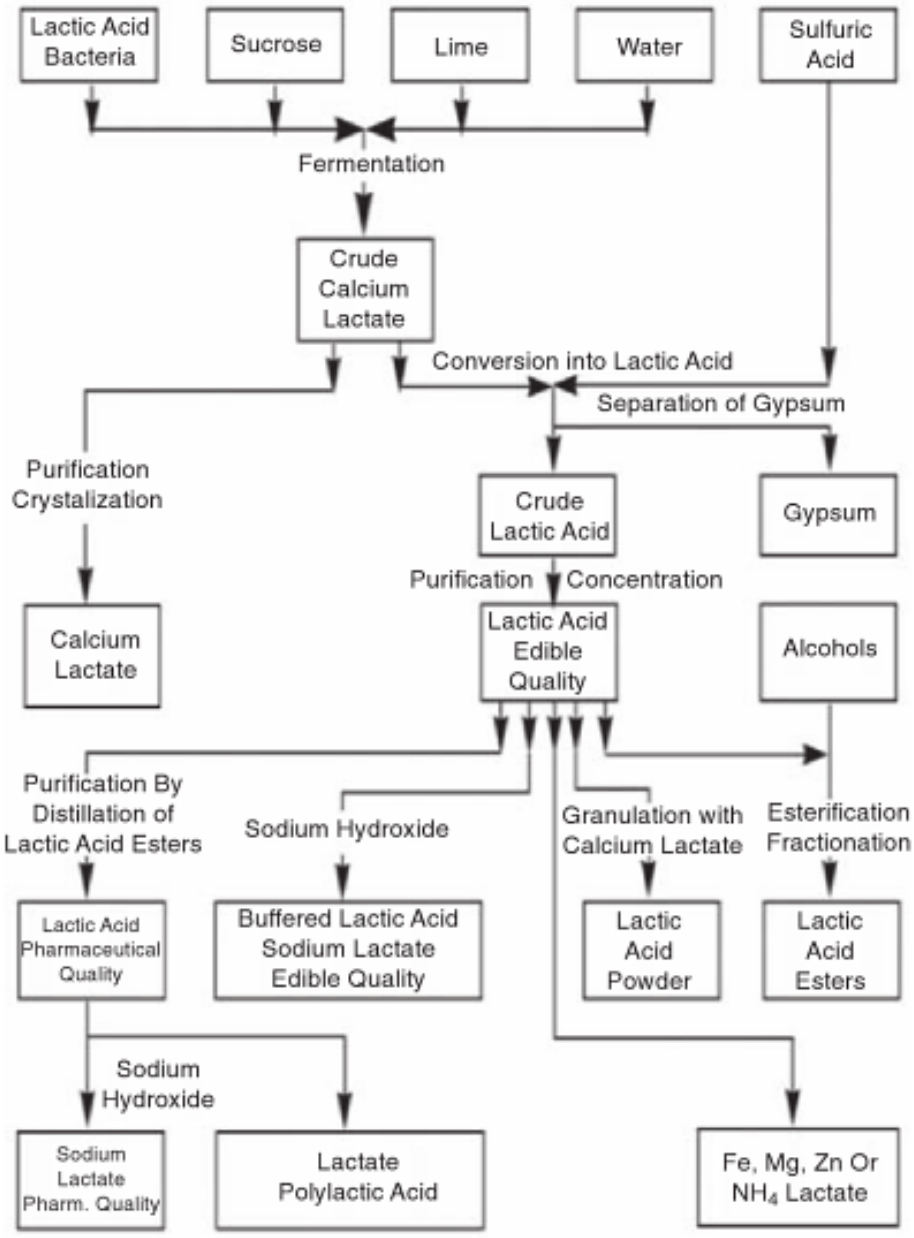

Figure 6 Process flow of lactic acid production by Purac [15]

1.1.4 Commercial end use for lactic acid

Lactic acid is widely used in the food industry and is naturally produced in fermented products, such as yogurt and wine. In its pure form, lactic acid is used as a solvent, as an antimicrobial agent, and for pH control. It is also used for pickling, curing, and flavoring of bread in the food industry. The major consumption of lactic acid in the food industry is in its salt and fatty ester forms. In particular, sodium, potassium, and ferrous and calcium lactate are used as flavor enhancers, emulsions, and whip stabilizers. In addition, lactyle esters and fatty acids are used as emulsifiers and surface active agents in food products. These salts are also used in, pharmaceuticals, such as acne treatment and moisturizing lotions. The most recent use of lactic acid has been as a monomer for the production of polylactic acid polymer. The recent identification of PLA as a suitable bio-alternative for petroleum plastics has catapulted the production and use of lactic acid worldwide. The next sections discuss the development of PLA and its prominence in the current industrial environment.

1.2 Poly (Lactic acid)-PLA

Polylactic acid is the polymeric form of the organic acid, lactic acid, and falls under the polymeric class of polyesters. Polylactic acid has gained popularity during recent years because of its innate properties, such as biodegradability

and thermoplastic processability. Most importantly, the raw material for PLA production comes from biorenewable sources, such as corn and sugars, thereby making it a candidate to replace petroleum-based plastics and to support the advocacy of petroleum independence.

1.2.1 History of poly (lactic acid)

Wallace Carothers first synthesized PLA in 1932 during his exploratory research to produce aliphatic polyesters. It was identified as a low molecular weight polymer with inferior mechanical properties [18]. The polymer was produced by dehydration of lactic acid by heating it under vacuum to yield low molecular weight PLA. Although patented by DuPont in 1954, further research on PLA was discontinued, because of the inability to achieve higher molecular weight and the material's nature to undergo hydrolytic degradation [19]. Further research was reinvigorated in the 1970s, when lactic acid was used along with glycolic acid as monomers to produce high- strength copolymers for bio-absorbable medical suture applications [18, 19]. Then, during 1990s, the identification of PLA as a suitable biodegradable alternative for petroleum plastics, along with developments in cost-effective lactic acid production, paved the way to current PLA production.

1.2.2 Commercial production of PLA

One of the major portions of landfilled non-degradable waste comes from high- volume petroleum plastic products, such as water bottles [3], disposable cups, cutlery, and mulch films. PLA was adopted for these applications because of its biodegradability, which led to an exponential rise in demand for the resin over the last decade. This section details the evolution of lactic acid polymerization and production technologies developed to keep up with these demands. This extensive effort to produce PLA leads to the necessity for recycling the lactic acid for the production of “virgin” PLA so as to increase the utilization of lactic acid and ultimately the efficiency of the process.

Although PLA was originally used for such applications as absorbable medical sutures, the advent of new uses demanded high molecular weight PLA. The effort to achieve high molecular weight in industrial-scale production of PLA has had its own limitations. Because lactic acid is an α-hydroxy/carboxylic acid, the primary mechanism of polymerization is poly-condensation reaction. Fundamentally, polycondensation of lactic acid releases a water molecule for every reaction site polymerized. This has been the challenge to overcome. The presence of water during polymerization of PLA inhibits the growth of the polymer chain, making it difficult to obtain high molecular weights. In contrast, the removal of water becomes difficult with an

increase in molecular weight because of the increased viscosity of the polymerizing reactants. [12] The increase in viscosity reduces the ability to continue mixing the reaction adding in transport phenomena.

Traditionally, polymerization of lactic acid into PLA has been achieved by two different routes. The first is direct polycondensation of lactic acid. The second requires intermediate steps to form cyclic lactide, which is later polymerized into PLA by ring opening in the presence of catalyst, as shown in Figure **7** [20].

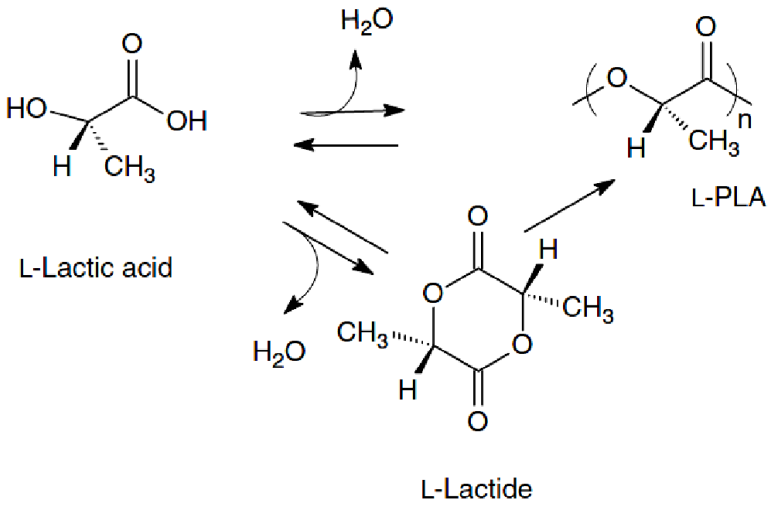

Figure 7 Routes of polylactic acid synthesis [20]

Polymerization of PLA by direct polycondensation is normally carried out under high temperature and in a vacuum to ensure continuous removal of the

water formed during the reaction. The disadvantage is that this process produces low to medium molecular weight PLA as a result of the inefficient removal of the water. The rate of water removal is primarily affected by the increase in the viscosity of polymerizing reactants, as mentioned earlier. Japanese scientists developed a modified process that employs azeotropic distillation to continuously remove the water formed from polycondensation. However, although this process is efficient at water removal and yields high molecular weight PLA, it has no control over the molecular weight distribution of the polymerized PLA [18,19].

The major hurdle in industrial commercialization (nonmedical) of PLA was its high cost because of the limitations of the polymerizing process, discussed previously [20]. This issue was overcome with a high-volume polymerizing three-step process developed by Cargill and Dow [21], as detailed in Figure 8. The first step polymerizes lactic acid into low molecular weight pre-polymers, or oligomers, by polycondensation. The second step is the catalytic depolymerization of the oligomers to form stereo specific cyclic lactides. The ratio of L-, D-, and Meso lactide (depicted in Figure 9) produced is determined by the racemic purity of the lactic acid feedstock used for polymerization. The purity level of stereo-specific lactides directly translates to superior thermal and mechanical properties of the final polymer, and meso lactide is the least favored, as depicted in Figure 9 [12, 19].

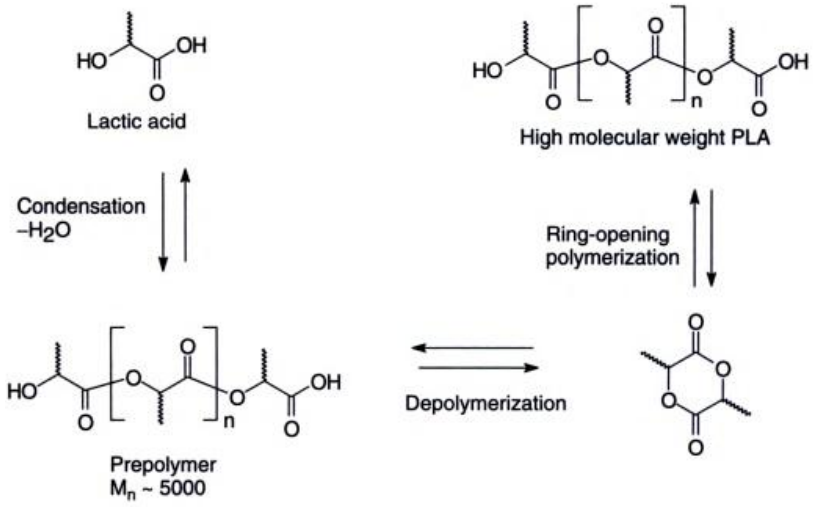

Figure 8 Dow Cargill process: PLA production via polycondensation of pre-polymers (oligomer) and ring-opening polymerization [20]

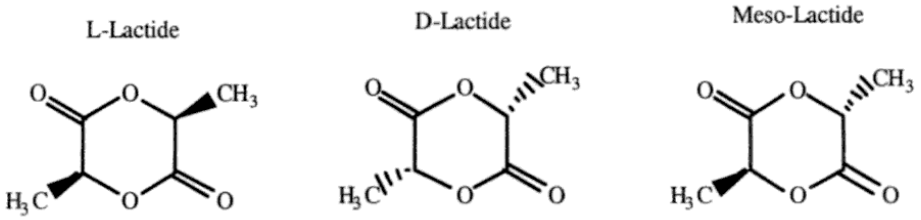

Figure 9 Structural representation of stereo-specific lactides [19]

The catalytic depolymerization and lactide formation results in a molten lactide mixture that is further purified by vacuum-assisted distillation. The third and final step involves the ring-opening polymerization (ROP) of the lactide in

the presence of an organic metallic catalyst, such as stannous octate (tin), to form the high molecular weight poly(lactic) acid polymer (see Figure 10). However, tin-based organic compounds are toxic in nature. As a result, nontoxic catalysts have been developed for the ROP of lactides. Ring-opening polymerization has been investigated with various other organometallic compounds, using aluminum, lead, zinc, bismuth, iron, and yttrium as catalysts. The type of catalyst used determined whether the mechanism of polymerization was ionic, coordination, or free radical growth[20]. Different types of catalyst also exhibit different stereo selectivity of lactides, affecting the optical (spatially) symmetry of the polymerized PLA molecule. The final level of symmetry affects the overall crystallinity of PLA.

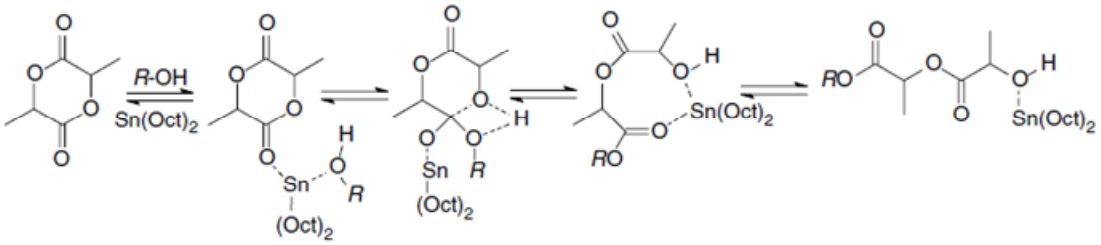

Figure 10 Generalized coordination-insertion chain growth mechanism of lactide to PLA: *R,* growing polymer chain [20]

The process developed by Cargill & Dow was based on the use of L-lactide to finally produce poly(L-lactic)acid (PLLA). This process uses lactic acid fermented from sugars that are derived from corn starch. This makes it

biorenewable. In addition, PLA is inherently biodegradable and completely compostable. Currently, the majority of the PLA available in the market is manufactured by this process of lactide formation and ring-opening polymerization. Because the process achieved commercial success as a result of its cost effectiveness, the PLA division has been spun off as separate company, which is known as NatureWorksLLC. The company manufactures and distributes PLA under the brand name Ingeo®. Various grades of Ingeo® resin are offered to cater the needs of the product-specific plastics market.

1.2.3 Properties of PLA

The physical properties of PLA closely resemble those of petroleum plastics. Similar to all the conventional polymers, the properties of PLA depend on the level of crystallinity, processing conditions, fillers, and other factors. The level of crystallinity is affected by the stereo purity of the lactic acid; the lactide feed stock used for polymerization, and thermal history. The distortion in symmetry of side groups on the backbone of the PLA molecule inhibits coiling of the polymeric chain and, hence, inhibits crystal growth [12, 20]. Such an effect is caused by the presence of meso-lactide or the opposite stereo symmetric lactide. PLA can either be amorphous or semicrystalline depending on the stereo purity of the lactic acid. It has been reported that Poly(L-Lactic acid)

PLLA is found to be semicrystalline by up to 40 percent crystallinity with a 93 percent L-lactic acid concentration/purity in the feed stock [20,21]. The density of PLA is also dependent on the stereo purity and crystallinity of PLA. To gain insight into the various properties of PLA, the next section provides a brief review of PLA properties and processing/production pathways.

1.2.3.1 Thermal properties of PLA

Stereo/enantiomerically-pure PLA is reported to have a glass transition temperature (T_g) of 55 ºC and a melting point(T_m) of 180ºC [20, 21]. The T_g and T_m values for amorphous and semicrystalline PLA can be broadened to a range of 52ºC to 58ºC and 130ºC to 230ºC, as they depend on the molecular weight, crystallinity, and thermal history of the polymer. The values drop when the PLA is produced with meso-lactide [20,21]. The relative change in the value of T_g can be calculated, provided the molar ratio of meso-lactide in the polymer is known. Thermal properties of PLA are also subject to change depending on the crystallinity induced by mechanical stretching. It has been reported that PLA crystallizes into a left handed α-helix coiled structure that further transforms into the more stable β-form under high-draw ratios. The enthalpy of melting (ΔH^o_m) for 100 percent crystalline PLA has been estimated to be 93 J/g, which is a universally used value for melt calculations.

1.2.3.2 Physical and mechanical properties of PLA

The densities of PLA in its amorphous and purely crystalline states have been reported to be 1.25 g/cm^3 and 1.37 g/cm^3 to 1.49 g/cm^3 respectively [20,21]. The mechanical properties similar to thermal properties depend on the molecular weight and crystallinity of PLA. The overall mechanical properties of semicrystalline PLA are between the value ranges, with tensile strength of 50 MPa to 70 MPa and a modulus of 2 GPa to 3.5 GPa. Studies on the effect of molecular weight on mechanical properties of PLA indicate a linear relationship until a certain limit is reached in terms of molecular weight. Other properties, such as flexural strength, lie below 100 MPa. Polylactic acid in its homolactic form is very brittle, and enormous amounts of research have been done to address this issue. Some of the popular methods investigated are the use of copolymers and blends, such as glycolic acid and poly-caprolactone, to improve the flexibility and toughness of the polymer.

1.2.3.3 Interaction and chemical properties of PLA

The study of interaction/ miscibility of PLA with other polymers have been one of the important research areas. Over the last three decades, researchers have been trying to blend PLA with other similar polyesters, such as Polycaprolactone (PCL) and poly(glycolic) acid(PGA) to obtain improved mechanical properties [19]. Studies indicate that PLA is not miscible with

these polymers unless a copolymer, such as poly (LA-co-CL), is used as a compatibilizer. Because this incompatibility is recognized, the majority of the research on PLA blends has involved enantiopure/stereo pure polymers PLLA and Poly (D-Lactic acid) (PDLA) rather than different polymers [19,20,21].

As with other properties, the solubility of PLA also depends on the molecular weight and the crystallinity of the polymer. Some of the solvents for pure PLLA or PDLA are halogenated organic solvents, such as chloroform, methylene chloride, and other organic compounds, including furan, pyridine, diaoxane, and dioxalane [20,22]. In addition, PLA polymerized with meso-lactide can dissolve in less harsh solvents, such as acetone, ethyl lactate, acetate, Tetrahydrofuran (THF), and other ketones. Poly(lactic) acid does not dissolve in water, but it does hydrolyze under certain pH, temperature, and pressure conditions. The lactic acid polymer is insoluble in alcohols, typically methanol, ethanol, and alkanes such as hexane [20].

A prominent reason for PLA to gain popularity as an ecofriendly material is its innate biodegradability, a characteristic that is largely related to the stability of the polymer. Compared to all other aliphatic polyesters, the stability of PLA is relatively poor at elevated temperatures [20]. Various research groups that

have studied the melt stability of PLA determined determine that PLA under goes degradation through hydrolysis, chain scission, and lactide formation through back biting or unzipping of the polymer in the molten state. The maintenance of dry conditions during melt processing or drying the resin prior to processing has been determined to minimize degradation PLA through hydrolysis [20]. Although hydrolytic degradation of PLA is detrimental to its properties at melt processing, it is highly favored during its application stage as a biodegradable polymer. The uptake of water into the PLA matrix under certain conditions of pH, temperature, and pressure accelerates the hydrolytic chain scission with no preference to sites causing bulk erosion of the polymer. Researchers have identified hydrolytic depolymerization as an effective route to recover lactic acid from PLA, and this topic is the focus of the research discussed in the following sections of this thesis.

At this juncture in literature we need to learn about ultrasonic technology which is a prospective alternative for deconstruction/pulverizing of particulates. Ultrasonics mostly used in the medical field for sterilization has been proven to be an effective source of mechanical energy to pulverize microbes and particulates. Such a technology is envisioned to be an effective too to effect PLA degradation. The following section introduces the basic concepts of ultrasonics and its application.

1.3 Ultrasonics: High-frequency sound waves

Ultrasonics is the branch of acoustics that deals with high-frequency sound waves. The first prominent use of ultrasound in recorded history occurred during World War I, when underwater high-frequency sound waves were used to detect submarines [23]. Ultrasonics also exist in nature; animals such as bats generate ultrasound for navigation and hunting, while dolphins use high-frequency sound under water to communicate, locate prey, and coordinate activities during hunting [24].The use of ultrasonics, however, has vastly expanded since World War II, particularly in the fields of medical diagnosis and power engineering. To better comprehend the mechanism and the effects of ultrasonics, it is crucial to establish the basics of sound and its interaction with the media it moves through.

1.3.1 Sound

There are two types of mechanical waves, longitudinal and transverse, which are distinguished by how they displace matter (a media) as they travel through it. If a wave traveling through a media causes oscillatory displacement of the media/ matter in the direction perpendicular to the direction of wave propagation, as seen in Figure 11, then these waves are called transverse waves. Some examples of transverse waves are ripples observed over water, a vibrating rod, wave traveling through a whip or a string

[24]. In contrast, longitudinal waves are those which cause displacement of particle/ media in the same direction the wave propagation, as depicted in Figure 12. Sound is a longitudinal wave.

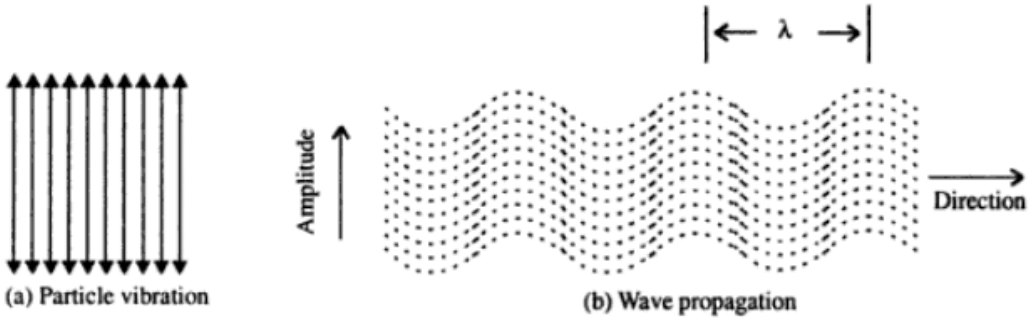

Figure 11 Schematic representation of transverse waves [25]

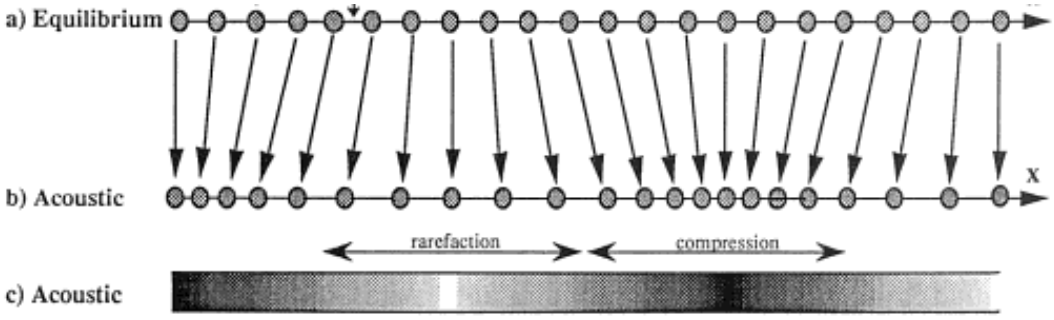

Figure 12 Schematic representation of compression and decompression as result of local particle displacement in a media. These are longitudinal waves [24]

The wave traveling on the surface of the sea (e.g., as in a tsunami) is not to be mistaken for transverse waves. Rather, they are Rayleigh waves, which are a combination of both transverse and longitudinal waves. Some other complex waves are Lamb and Love waves, which will not be discussed here [25].

Authors have defined sound in different ways, but all definitions have been based on the common principles of waves. Sound is a mechanical vibration form within a certain frequency. When it passes through matter/media, it causes density variation through compression and decompression. The propagation of sound, or any mechanical vibration through a medium, occurs by transfer of vibration/energy from particle to particle. The energy transfer can be further understood from the expression for energy E, of a vibrating particle and its relation to the intensity I, of a wave through a medium as seen in Eqs. 7 and 8 respectively.

$$E=2\pi^2 m f^2 A^2 \qquad \text{[Eq.7]}$$

Where m, f, and A are the mass, frequency of vibration, and amplitude of the vibrating particle, respectively. The intensity of a wave traveling through a medium is basically the cumulative energy of all the vibrating particles, n, in a particular medium with volume V, where ρ is the density of the material.

$$I = 2\pi^2 \rho f^2 A^2 V \qquad \text{[Eq.8]}$$

Further, the vital relationship between the velocity of sound C and material/media properties is given in Eq. 9, where E and ρ are the elastic modulus and the density of the media. Speed of sound in air and water are 343m/s and 1484 m/s, respectively.

$$C = \sqrt{(E/\rho)} \qquad \text{[Eq. 9]}$$

From Eq.9, it can be said that sound waves do not travel through a vacuum because of a lack of matter/particles that can transfer the energy forward. This is unlike electromagnetic (light) waves, which are energy packets and do not require a medium to travel through [25]. This means that sound waves travel faster through a dense medium, such as steel, and slower through rare

media, such as air and gases [23, 24]. Similar to other waves, the primary characteristics of sound waves are speed, amplitude, and frequency, and it is the last in which we are interested. The sound wave frequency range can be split into three divisions, which are infrasound/infra sonic (<20 Hz), sonic/acoustics (20Hz-20,000Hz), and ultrasound/ultrasonic (>20 KHz) respectively [23,24]. Human hearing falls in the acoustic frequency range, which is also affected by a person's age and gender. The ultrasonic frequency range lies above 20 KHz and is employed/generated by animals, such as bats, dolphins, and whales, for echolocation and communication. Based on the same principle. ultrasound has been used in the medical field for both destructive and nonlethal uses, such as ultrasonic stone removal from kidneys and ultrasound imaging of pregnant babies or internal organs. The next sections will elaborate on the basics of ultrasonic generation and its interaction with various media.

1.3.2 Ultrasonics and generation of ultrasonics

Ultrasonics can be generated in many different ways. The two prominent methods are the piezoelectric and the magnetostrictive. Both convert electrical energy into mechanical energy (a motor). The selection of source depends primarily on the energy level of the required output. The magnetostrictive method operates at low frequencies and high-power output,

while the piezoelectric can be designed to operate at a wide range of frequencies. [26].

1.3.2.1 Piezoelectric method

The most common method of ultrasonic generation is the piezoelectric method, which is based on the piezoelectric class of materials. This class typically consists of crystals of ceramics. Since the discovery of quartz and Rochelle salt as piezoelectric materials by the Curie brothers in 1880, many different materials have been identified as ultrasonic generators or receivers [26]. A common ceramics used in transducers is lead zirconate titanate (PZT). The method depends on the basic property of dipole moments that exist between the two layers/ atoms. When an electric charge/potential is applied across the two surfaces of the crystal, the atoms in the material move closer to or away from each other depending on the polarity of the charge. The relative movement of atomic planes causes the crystal to expand or contract in the direction of the net dipole moment. Similarly, when pressure is applied, the crystal will generate an electric charge between its surfaces. These materials resonant at a required frequency when stacked together and separated by electrodes to form a transducer, which is often called the converter, as shown in Figure 13 A high voltage (~ 900V) supplied at the resonant frequency of the stack will generate mechanical vibrations of a

certain peak to peak amplitude. The achievement of value depends on the voltage gradient in the discs, the peak voltage, and the converter design. Transducer design is a much more intricate and mathematical process and will not be discussed here.

Note that the stack of piezoelectric discs are held together by a fastener, so that the discs are tightly packed with no gap between them during the compressional (shortening) phase.. In addition, the ceramic discs are stacked

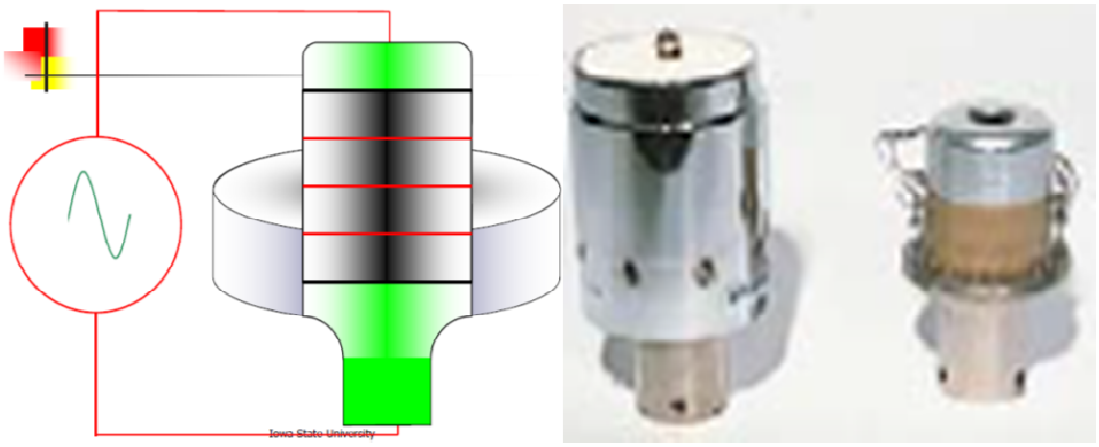

Figure 13 (Left) Schematic representation of a transducer made with a ceramic piezoelectric stack connected to an AC power source. (Right) A actual half wavelength transducer stack [27]

so that the two surfaces of two discs with the same polarity face each other and share the electrode of the same polarity. Transducers are typically half wave length of the resonance frequency in length and typically are 90% to 97% efficient at converting electrical to mechanical energy.

1.3.2.2 Magnetostrictive method

Similar to the piezoelectric method, this method uses electrical energy, but only to generate a magnetic field that is converted into mechanical vibrations. The conversion of energy forms is effected by ferromagnetic properties of magnetic metals, such as iron, cobalt, and nickel. Discovered in 1847 by Joule, magnetostirction is a phenomenon in which a change in dimension of a magnetic material is observed when the material is exposed or placed in a magnetic field of varying magnitude [23,26]. The construction of a magnetostrictive transducer is similar to that of an electromagnet, as depicted in Figure **14**. A rod of ferromagnetic material is wrapped with a loose coil and the inductance of the coil is proportional to the number of turns as well as to its size and the magnetic properties of the material within the coil.

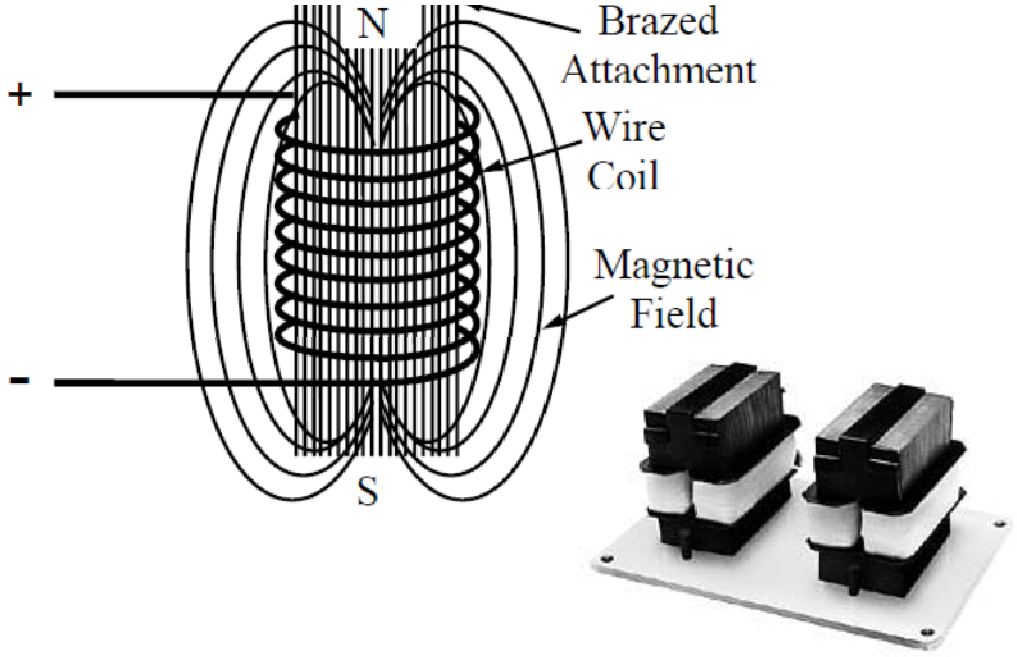

Figure 14 Schematic depiction of magnetostrictive transducer. Commercial magnetostrictive transducers for tank cleaning (bottom right)[28]

Magnetostirction was the one of the first methods to be used industrially to generate ultrasonics until the development of the piezoelectric method. Currently, piezoelectric transducers are preferred for an array of reasons. Magnetostrictive transducers are comparatively inefficient because of the high amounts of current required and the added step in conversion of electrical to mechanical energy through a magnetic field. The second disadvantage is that the magnetostrictive method is frequency limited (18KHz-80KHz), whereas the piezoelectric method is capable of working in wide frequency range (20

KHz to 20 GHz) [28]. Finally, the magnetostrictive method has been historically unpopular because of the change in magnetic permeability of the rod material caused by hysteresis. Over time, changes in the magnetism of the rod material result in less effective magnetostirction [29].

1.3.3 Resonance and Q factor

The design of transducers is a crucial process that requires consideration of the resonant frequencies of the material/ceramic used for its construction. Systems have their own distinct resonant frequency ranges that depend in part on the geometric dimensions of the material used [26]. The system is operated/vibrated at its resonant frequency to obtain maximum vibrational amplitude with the least amount of input voltage applied. The purpose of operating at a material's resonant frequency is to attain maximum efficiency, which is also expressed as the quality (Q) factor. The Q factor is a measure of resonance quality expressed as the ratio of stored energy in the transducer per unit time (frequency, ω) to the dissipated power, or power loss . It is expressed by Eq. 10 [27].

$$\mathbf{Q = \omega \left(E_{strored}/P_{dissipated}\right)} \qquad \text{[Eq. 10]}$$

The Q factor is a dimensionless number that represents how sharp the resonance signal is. The higher the Q value, lower the loss; the lower the Q value, the higher the loss [27,30]. The band width of an operational resonant frequency is calculated by dividing the resonant frequency by the Q value, as depicted in Figure 15 [30]. In other words the "Q factor of a vibrating system is inversely related to the logarithmic dampening decrement of the system" [30]. It is also stated that "the important characteristics of a resonant system are the extent of amplitude decrease caused by deviation of its frequency form its resonant value" and the Q factor is a measure that can be used to rectify the system.

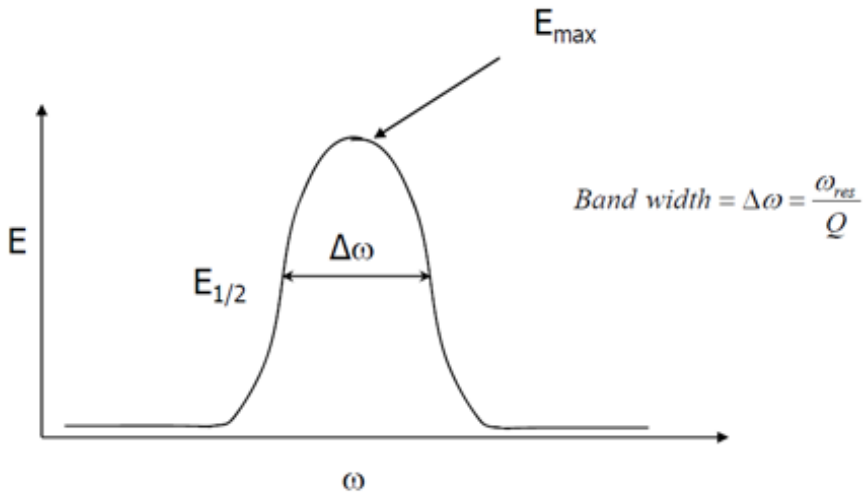

Figure 15 Plot of energy against frequency, depicting the maximum energy at ω_0 and the frequency bandwidth at half or a reduction in energy [27]

1.3.4 Tooling

An ultrasonic tooling typically consists of three components: the transducer, booster, and sonotrode, which is also known as the ultrasonic horn. When coupled together, they are often referred to as the stack. The transducer is the source of vibration. When passed on to the booster, the vibrations are either amplified or de-amplified based on the ratio of volume on either side of the midpoint (nodal plain) of the booster. Finally, the vibrations are further amplified as they pass through an ultrasonic horn. A typical ultrasonic stacked is shown in Figure 16. The system is also designed and tuned so that vibrations are only in the axial mode and not in the flexural radial mode which would reduce the efficiency of the system as well as result in stack failure. The booster and the horn must be made of relatively strong materials with a high modulus-to-density ratio, such a titanium alloys or aluminum. This allows them to withstand the high-frequency cyclic stresses (as well as minimize hysteresis heating) caused by ultrasonic vibrations.

The stack in Figure 16 is a typical ultrasonic system that can be used for various applications, such as welding systems, ultrasonic sewing, and chemical processing. In hand-held, ultrasonic systems, as well as cell disruptor systems, sometimes the booster is replaced with horns that have a relatively higher amplitude gain.

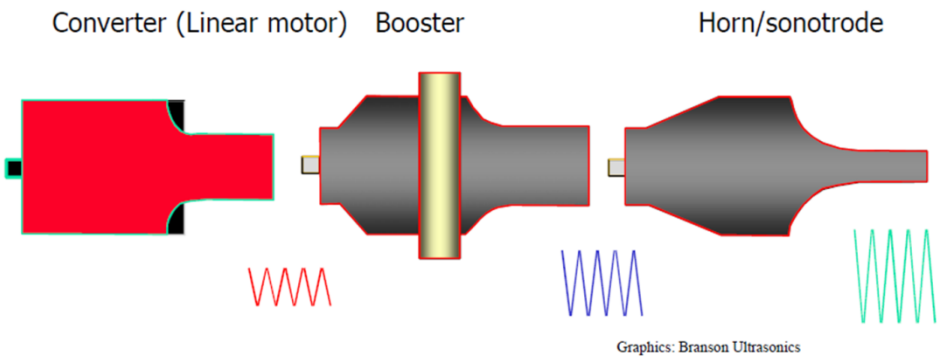

Figure 16 Depiction of a typical ultrasonic stack [27]

Manufacturers of ultrasonic systems cater to markets with specific applications. Each application requires different levels of energy output for different cycle times. To provide systems for a wide range of applications, manufacturers produce machines with different operational frequencies, as shown in Figure 17 [27]. Because these systems are designed to resonate, their maximum power is typically inversely related to frequency. Higher frequencies require the converter, as well as the remaining components of the stack, to be shorter in length to match the wavelength, which is shorter at higher frequencies. Thus, higher frequencies have smaller converters and. to keep the power density (W/m^3) below a critical threshold, the maximum power is limited. While it would be possible to increase the diameter of the converter to increase its volume, this usually introduces flexural modes of vibrations that promote bending of the converter, which can result in structural failure. It is

possible to couple multiple converters together to increase the maximum deliverable power into a single tool either in parallel or in series depending on the tooling design.

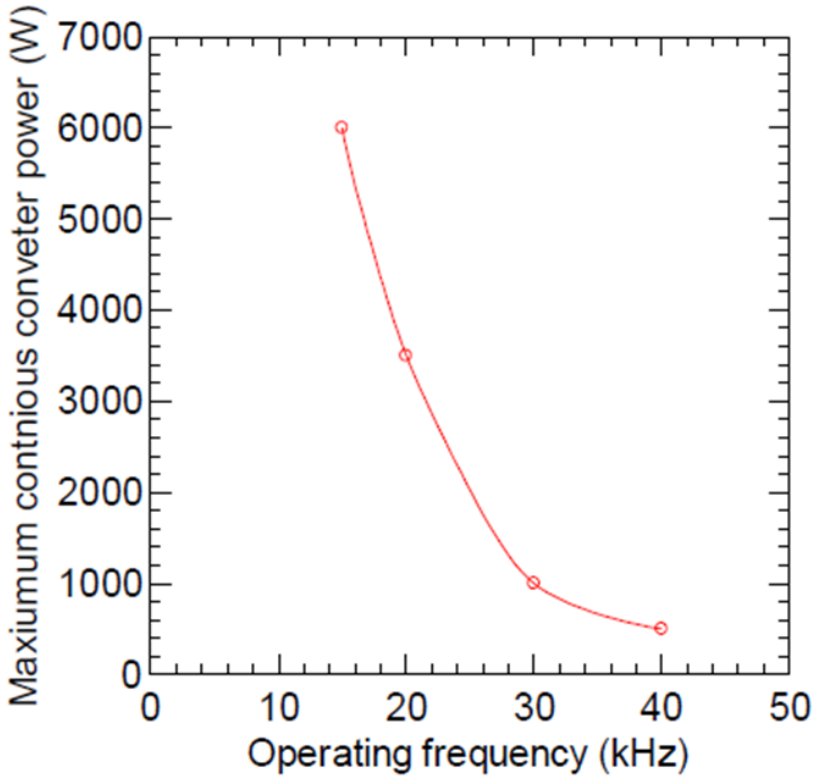

Figure 17 Plot relating maximum available power as a function of operational frequency of the system [27]

It can be seen from Figure 17 that lower frequency systems 10 kHz to 20 kHz generate a high level of power output and are generally used for high- energy applications, such as joining and welding of materials. For frequency ranges

30KHz and above, medium and low power output capacity, are typically used for delicate parts [27].

1.3.5 Interaction of ultrasonics with different medias

As a high-frequency longitudinal wave, ultrasonics causes stretch and compression in the media through which the waves travel. Depending on the density and purity of the medium, various effects, such as (a) Hysteresis heating in solids, (b) Cavitation in liquids, and (c) Modal accumulation of particles in gases, can be observed. This section discusses these effects and elaborates on the various parameters and factors that affect the outcome.

1.3.5.1 Ultrasonics in liquid: Cavitation

Myriad numbers of industrial applications that employ ultrasonic liquid processing rely on one primary phenomenon called cavitation. When an ultrasonic wave travels through a liquid, an alternating pressure gradient is created throughout the medium. This puts the liquid under varying stress, as seen in Figure 12. In practical terms, the liquid undergoes cyclic tensile loading and compression loading. At a certain load, a bubble is nucleated. This bubble entraps dissolved gases and vapors from the liquid and, on reaching a critical size, the bubble implodes. This compresses all the gases

and vapors and creates one massive local energy release with a shock wave or jetting, as depicted in Figure 18 and Figure 20 respectively. This section details the different mechanisms of nucleation, along with the types of collapse and the effects of ultrasonics in liquid.

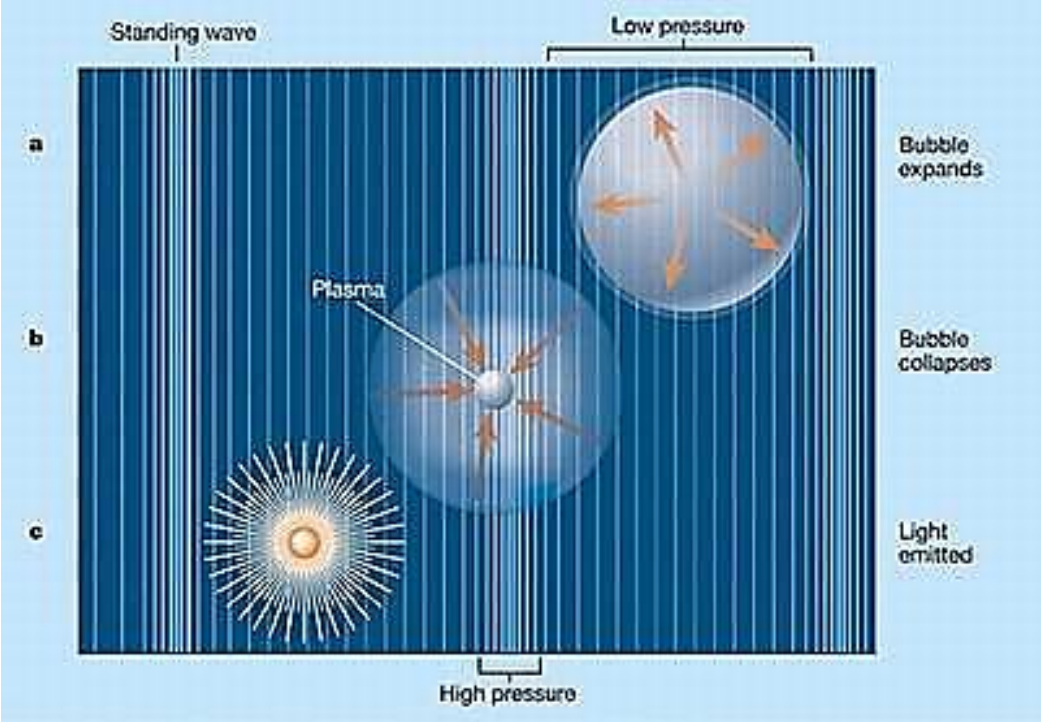

Figure 18 Depiction of sequential growth and collapse of a bubble with a shock wave in a liquid media under a gradient of pressure [31]

1.3.5.1.2 Homogeneous and heterogeneous nucleation

Cavitation by homogeneous nucleation principally occurs because of the fracture/tearing of pure water under very high stress conditions. This is created in the medium as a result of the pressure gradient seen in Figures

12,18 and 19 [32]. Under real-life conditions, homogeneous nucleation does not occur because of the presence of particulate impurities, such as dust and sand in the water, or surface roughness near interfaces. Rather, the impurities act as stress concentrators that reduce the effective strength of the medium leading to nucleation under relatively low stress values [24,27,32]. This mechanism of nucleation that occurs due to the presence of impurities is called heterogeneous nucleation, and it is the type of nucleation observed under practical conditions.

1.3.5.1.3 Bubble growth: rectified diffusion

Upon nucleation, the bubble containing the dissolved gases and vapor freed from the liquid expands and contracts under the dynamic pressure gradient traveling through the liquid medium. Due to certain effects, the net diffusion of gas into the bubble increases with time. This can be explained by the phenomenon called rectified diffusion [27,32].

Rectified diffusion can be explained by two mechanisms. One is surface area effect, and it can be detailed with the aid of one full cycle of bubble contraction and expansion. The concentration of gases inside the bubble during compression increases with respect to the medium immediate to the

bubble surface. This results in a net outward diffusion of gases from the bubble into the medium. However, because the bubble is compressed, its surface area is relatively small, thereby limiting the outward diffusions. During the expansion cycle, the bubble's surface area increases, and the increased volume causes a reduction in the concentration of gases inside the bubble. In this situation, inward diffusion of gases occurs and is relatively high because of the increased amount of surface area. With the cyclic pressure and mass transfer in and out of the bubble, the net mass of gases inside the bubble grows continuously until reaching a critical size [27, 32].

The second mechanism is the shell effect. Consider a contracted bubble, with the media immediate to the surface of the bubble is deficient of gases resembling a shell. This results in a net diffusion of gases towards the bubble. When the bubble expands, the relative concentration of gases is lower inside the bubble when compared with the new shell, thus resulting in a net inward diffusion of gases. Similar to the surface area effect, the bubble keeps increasing in size until reaching a critical size [27,32].

1.3.5.1.4 Bubble collapse: symmetric and asymmetric collapse

With bubble growth occurring because of rectified diffusion, upon reaching a critical size, the balance between forces/pressures exerted by the medium on the surface and the internal gas pressure is broken. This results in the collapse of the bubble and can be understood with the aid of Figure 19, in which the bubble collapse is the sum of the inward pressures P_σ (surface tension pressure) and liquid pressure near the bubble P_L are greater than P_i (internal gas pressure). The bubble can collapse symmetrically or asymmetrically. In the symmetrical mode, the bubble's radius reduces uniformly and implodes on itself. Thereby sending an explosive shock wave (a wave traveling faster than the speed of sound) through the medium, as seen in Figure 18 . The collapse of the bubble and the shock wave generation are accompanied by free radical formation, the generation of which was found to be proportional to ultrasonic amplitude [32]. In the asymmetrical mode, which is caused by the instability of the bubble and the surrounding medium, caving of the bubble surface occurs to form an intermediate donut shape before collapsing by jetting as seen Figure 20. Even though symmetrical implosion sends a shock wave, jetting is equally destructive in power.

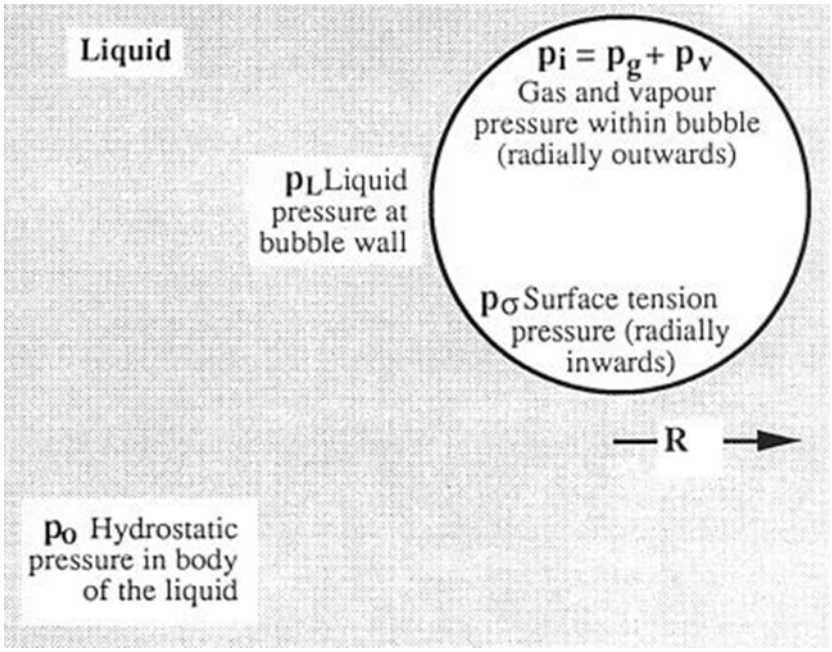

Figure 19 Schematic representation of pressures in a static gas bubble [24]

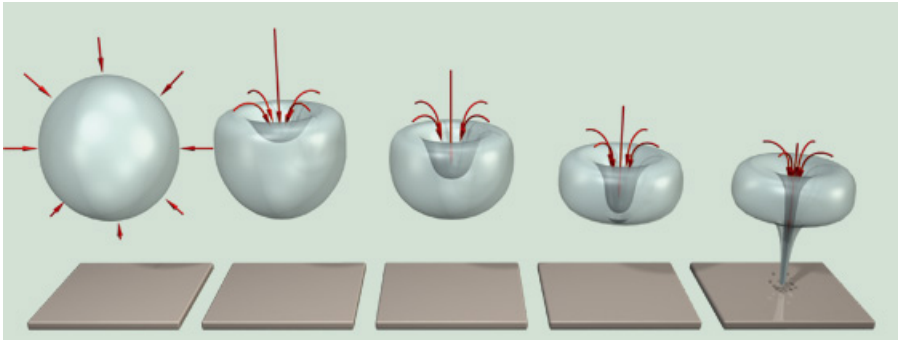

Figure 20 Asymmetric collapse of bubble via jetting [33]

1.3.5.1.5 Nonlinear Acoustic effects - Streaming

Many of the industrial applications of ultrasonics, such as mass transport, mixing, and emulsification, rely on an acoustic phenomena called streaming.

Streaming is “the time independent flow of fluid induced by a sound field” [32]. A simple explanation is that when a sound wave travels through a medium, not only is the energy of the wave is absorbed, but the momentum of the sound wave is also absorbed by the medium. This results in fluid flow in the direction of sound wave propagation. Based on earlier discussions, sound wave propagation can be better realized as energy transfer through a medium. The energy gradient that is set up by a traveling wave that was absorbed by the medium translates to a change in force per unit volume of the media [24]. This can also be referred to as the pressure gradient in the direction of wave propagation. Another sub-effect of streaming is microstreaming, which is fluid flow occurring near the surface of obstacles/particles arising as a result of the frictional forces between the medium and the surface of the obstacle. The application of acoustic streaming is most noticeable in the fields’ food industry and in biological research, where the bioactivity of microbes are altered with streaming fluid flows with speeds up to 10m/s. The bioeffects and increase in rate of reactions on use of ultrasonics in various applications are attributed to the turbulent mixing and mass transport caused by ultrasonic streaming. Other sophisticated end applications are thermoacoustic streaming in metals, which is utilized for heat transfer in solids.

1.4 Recovery of lactic acid

As mentioned previously, PLA made from renewable resources has the innate characteristic of biodegradability. As a result, it is a good candidate for high-volume disposable plastic products, such as water bottles, milk jugs, and other food packaging. Recent controversial arguments, such as "food versus fuel," have compounded the difficulties faced by proponents of biorenewable and degradable materials [34]. One frequent criticism faced by advocates of biomaterials is the question of recycling stream contamination by biopolymers, and its detrimental effects on the final properties recycled product. In order to make PLA a successful product, a widespread consensus by industry is that issues related to disposal of PLA (despite its biodegradable nature) need to be addressed. The following sections discuss these issues in depth, as well as the recycling solutions that will increase the value of PLA.

Thermal recycling of petroleum thermoplastics has been one of the primary solutions to reducing the pollution caused by their disposal. With the recent increase in the use of “ecofriendly” plastics for food packaging, recycling experts had expressed concerns regarding PLA entering the recycling stream. In recognition of the incompatibility between petroleum and biobased plastics, such as PLA, studies were conducted to determine the effect of PLA

entering the conventional plastics recycling stream. These studies indicated that PLA contamination in PET, PVC, and rubber recycling streams deteriorated the final properties of the recycled resin [35,36]. The latter discussion has been the primary reasoning for developing alternate PLA recycling techniques. Further studies on biodegradation of these plastics have shown that disposal of these materials might alter soil composition because of the accumulation of residues. The argument is supported by the fact that metal catalysts, such as stannous octate, utilized during ring-opening polymerization of PLA (see Figure 21) are found in trace amounts in the final polymer [37].

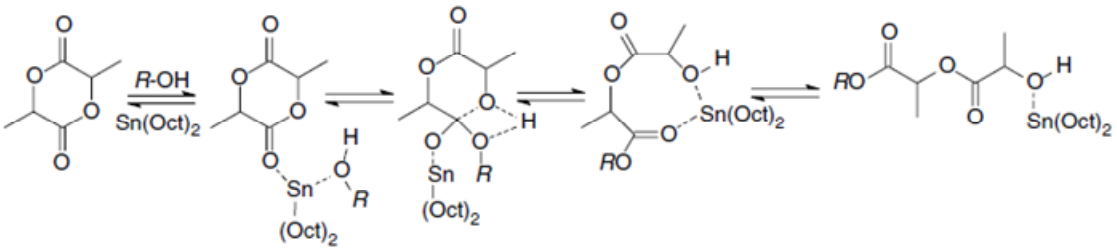

Figure 21 Generalized coordination-insertion chain growth mechanism of lactide to PLA. *R,* growing polymer chain[20]

During degradation, PLA releases metal compounds into the soil that affect the soil's composition [34,38]. To complicate the issue, studies indicate that higher concentrations of fragmented residue in the soil from biodegradation

will result in increased carbon concentration, This, in turn, leads to microbial activity that ultimately increases the overall BOD (Biochemical Oxygen Demand) of the local water system in the soil [39].

The complexity of disposing of renewable plastics can be seen in Figure 22, which details the assay of tests required to be conducted to characterize environmental impacts of plastics (materials). The arguments discussed so far were criticisms of PLA disposal. However, some positive arguments supporting PLA recycling are based on energy and economics. Depolymerization of PLA for monomer regeneration (lactic acid) and subsequent polymerization has been identified as a possible route to recycle the polymer with respect to traditional thermoplastic recycling. Recycling PLA by monomer regeneration not only reduces the consumption of lactic acid made from corn, but also yields virgin PLA. This virgin PLA can be used again for food packaging, unlike plastics recycled by thermal reprocessing. This addresses the concerns of contamination in mainstream recycling and competing with food for utilizing renewable feedstock. Thus, the recycling of PLA is a "necessity" and not just a "desire".

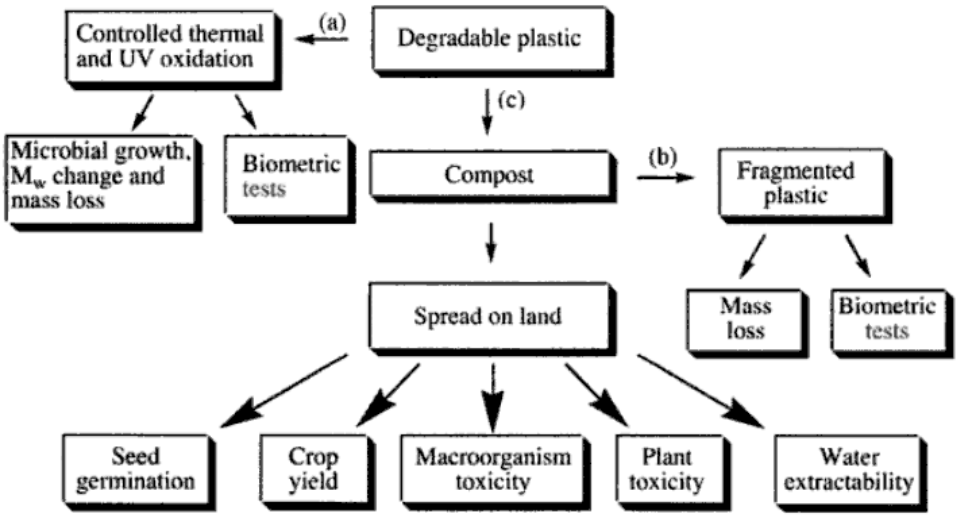

Figure 22 Schematic representation of tests to determine the effects of plastics degradation: (a) and (b) material characterization and (c) ecotoxicity tests [34]

CHAPTER 2: LITERATURE REVIEW

2.1 Research on PLA recycling techniques

Because of the increased use of PLA as a replacement for petroleum plastics, researchers have investigated various methods of lactic acid recovery from PLA. Most of these depolymerization techniques employ either one or a combination of pressure, heat, and catalysts, which pose a disadvantage to the energy economics of lactic acid recovery process. The following sections review the various PLA depolymerization approaches that have been investigated. The various techniques are detailed in chronological order of their development.

2.1.1 Thermal catalytic depolymerization- Organometallic catalysts (1999)

This research, conducted in 1999, investigated various metal compounds as replacements for stannous octate ($Sn(oct)_2$) in the depolymerization of poly(L-Lactic acid) oligomers into stereospecific lactides for intramolecular transesterification of high molecular weight poly(L-lactic acid). The study evaluated aluminum-, titanium-, zinc-, and zirconium-based compounds for their individual catalytic performance in terms of LL-, meso- and DD-lactide yields respectively. The catalytic depolymerization of oligomers was

conducted at a low pressure (4-5mmHg) distillation process at a temperature range of 190ºC to 245ºC. Results indicated that zinc-based compounds exhibit catalytic action similar to that of stannous octate in terms of stereospecific lactide levels, but at higher concentrations of the compound. The overall efficiency of the metal catalysts were rated as follows; Sn >Zn >Zr >Ti >Al. The primary reason for this work was to find a nontoxic catalyst as an alternative for $Sn(oct)_2$ (which is highly toxic) to avoid the pollution/hazard caused by disposal of PLA in the soil/compost [37]. The primary disadvantage of the technique proposed by these researchers is that it employs an energy intensive process, such as distillation for cracking of the oligomer at 190ºC to 245ºC, which adds to the cost and complexity of the process on scaling up. In addition, the depolymerization times are as long as 160 min for the best organozinc compounds.

2.1.2 High-temperature high-pressure (HTHP) depolymerization/degradation (2006)

From 1999 to 2006, a large number of Japanese researchers worked on the recovery of lactic acid from PLA. They investigated the feasibility of using high-temperature high-pressure (HTHP) conditions in water for depolymerizing PLLA into lactic acid. The method employed a miniature

HTHP stainless steel batch reactor (capacity 8.4 ml), which was filled with PLLA and water at specific ratios (1:10 and 1:20). The depolymerization was conducted at temperatures ranging from 250ºC to 350ºC, with reaction times varying from 5 min to 30 min and at internal vessel pressures of up to 4 MPa (~580 psi). The efficiency of the process was determined by evaluating the percentage of stereospecific L-lactic acid recovered from the PLA. The results indicated that HTHP depolymerization at 250ºC yielded the highest level of L-lactic acid. Even though temperature and reaction time were found to be linearly related to lactic acid yield, the percentage yield of stereospecific L-lactic acid reduced with an increase in reaction temperature. Because depolymerization at 350ºC produced the lowest overall lactic acid yield, it was argued that depolymerization at higher temperatures would result in direct degradation of PLA into carbon dioxide (CO_2) and methane (CH_4). They also reported that degradation at temperatures higher than 250ºC produced lower levels of stereopurity in the recovered lactic acid [39]. The overall process, despite the use of a benign agent such as water, has a great disadvantage in its high-energy requirements. In particular, scaling up HTHP vessels could render the process energy inefficient and might ultimately prove cost inhibiting.

2.1.3 Controlling racemization/ stereo specificity during lactic acid recovery with base catalysts (2007)

Researchers also investigated the effectiveness of magnesium oxide (MgO) as a catalyst to control the generation of stereospecific L-lactide during thermal degradation of PLLA. The study involved preparing solution-casted PLLA samples with MgO particles of various sizes mixed in the solution. The samples were later subjected to thermal degradation with a pryrolizer equipped with an inline gas chromatography to analyze the products generated. The pyrolysis was completed at various temperatures and heating rates ranging from 60ºC to 500 ºC and 1ºC to 9ºC/min respectively. The results indicated that the smaller particle size of MgO yielded higher levels of L-lactic acid, which was attributed to the increased surface area for catalytic action. The secondary goal of the study was to verify the effects of heat treatment of MgO on the stereospecific lactide generation during thermal degradation/depolymerization. Researchers observed that heat treatment initiated certain unfavorable side reactions leading to the generation of mesolactide and DD-lactide [42]. The study did not provide any detail on depolymerization and the percentage of lactic acid recovery. The work focused more on efficient generation of L-lactic acid, which is a favorable result for repolymerization of recovered lactic acid.

2.1.4 Enzymatic depolymerization of PLLA (2007)

Researchers have also studied enzymatic depolymerization of PLLA to develop the kinetics and simulate depolymerization. The study conducted enzymatic depolymerization to determine which depolymerization rates that should be used to develop kinetics of enzymatic action on PLLA. The depolymerization of PLLA involved forming an emulsion of PLLA to dissolve in chloroform using sonication as an emulsifying mechanism. The emulsion obtained was mixed with the enzyme proteinase K, and the depolymerization was allowed to occur at room temperature. A residual amount of 40% PLLA was observed after 5 hrs of incubation [40]. Though enzymatic depolymerization of PLLA is not energy intensive, the depolymerization rates are slow compared to hydrolytic degradation.

2.1.5 Hydrolytic degradation of PLLA in the solid and melt state (2008)

This work was a continuation of efforts to depolymerize PLLA by HTHP process with water as the media. The research is distinct from the previously discussed work in terms of the temperature range utilized. The primary objective of the work was to investigate the degradation/depolymerization at temperatures where PLLA is in the solid (120ºC, 140ºC, and 160ºC) and melt

state (160ºC and 180ºC).The lactic acid yield levels from depolymerization was evaluated by using high performance liquid chromatography (HPLC) and gel permeation chromatography (GPC). Results revealed that irrespective of solid or melt state, the depolymerization of PLLA at a temperature range of 120ºC to 190 ºC occurs by bulk erosion mechanism[43]. The degradation/depolymerization times to reach LA recovery > 95% in the sold state (120ºC) and the melt state (180ºC) were 4,000 min and 130 min, respectively. Based on the energy used to begin degradation of PLLA, it was evaluated that activation energy for PLLA depolymerization was 69.6 KJ/mol and 49.6 KJ/mol at temperature ranges from 120ºC to 170ºC and 170ºC to 250ºC respectively [43]. Recognizing the energy intensiveness of the HTHP process discussed earlier, this research was an attempt to achieve depolymerization at lower temperatures. The use of lower a temperature range (120ºC to 190ºC) resulted in a 100-fold increase in depolymerization/degradation times with respect to the higher temperature range (250ºC to 350 ºC).

2.1.6 Hydrolytic degradation of PLLA in the presence of sodium hydroxide (2010)

Research in 2010 studied the depolymerization of PLA similar to the batch reactor methodology discussed in Section 2.1.5. The degradation of PLLA in a water medium was compared with degradation in a 0.6M sodium hydroxide (NaOH) medium. However, in the 2010 study, the batch reactor vessel was designed so that the PLLA polymer was slowly introduced into the hydrolyzing media under a constant pressure level of 10 MPa. The degradation process with NaOH and water media were conducted at varying temperatures of 353 K to 453 K (80ºC to 180ºC) and 453 K to -573 K (180ºC to 300ºC) respectively. Complete degradation/depolymerization of lactic acid was observed for NaOH media (PLLA sample mass: 60 mg) at degradation times of 20 min and 60 min at degradation temperatures of 433 K (160ºC) and 453 K (180ºC) respectively [41]. The ratio of NaOH concentration per unit mass of sample was 2 ml of 0.6 M NaOH per 60 mg of PLLA amounts to 8 g of NaOH per 10 g of PLLA. It is important to note that this is a relatively large quantity of sodium hydroxide, which may be an inhibiting factor for scale-up of the process.

2.1.7 Inference

The review above indicates that hydrolytic depolymerization has been one of the popular techniques in which researchers often employ pressures of approximately 10 MPa (~1500 psi), coupled with temperatures ranging from 120ºC to 350℃ to depolymerize PLA in small quantit ies [39,41,43]. Although the inexpensive treatment media used in this technique is water or an alkaline solution, scale up of such high-pressure processes make the technique energy intensive/costly. In addition, the batch-wise process of hydrolytic depolymerization of PLA will be a challenge to overcome to achieve scale up and meet the needs of the industry. Other techniques that have been investigated include selective enzymatic depolymerization [40] and metal organic salt catalytic depolymerization [42]. These methods have limitations, such as slower conversion rates and a higher residue of metal ions, which make them unattractive as recycling techniques. Thus, the development of an alternate recycling technique that satisfies all the needs of the recycling industry (which is economically viable), is critical to the continued acceptance of PLA by industry.

2.2 Alternative concept: Introduction to ultrasonics as a depolymerizing tool

Previous research has shown that degradation/depolymerization of PLA occurs as a bulk erosion mechanism [43] and that the activation energy for depolymerization is temperature dependent. This suggests that PLA depolymerization is dependent on the energy level (temperature) of its treatment medium as well as the PLA. Thus, this study proposes to investigate different treatment media for depolymerization and to use an approach other than heat and pressure to initiate depolymerization. In microbiology and medicine, a common technique used for sterilization is ultrasonics (high frequency sound waves), which is a form of mechanical energy [44]. Ultrasound is sound waves at a frequency above the hearing range of humans (> 18 kHZ to 20 kHz). When the ultrasound wave propagates in a liquid or slurry, it produces cavitation [45], acoustic streaming [46], and other mechanisms, such as localized heating and particle collision. High-power ultrasonics, when passed through a liquid medium, causes molecular vibration of dissolved gases. The localized periodic compression and decompression caused by the ultrasonic source initiates cavitation bubbles which grow because of rectified diffusion of dissolved gases and implode upon reaching critical size (see Figure 23). The cavitation generates powerful hydromechanical shear forces in the bulk liquid [47], which

disintegrate nearby particles by extreme shear forces. The streaming effect, as seen in Figure 23, helps promote mixing and mass transfer. The main benefit of streaming in slurry/suspension processing is enhanced mixing, which facilitates the uniform distribution of ultrasound energy within the suspension/slurry mass, convection of the liquid, and dissipation of any heating that occurs. In summary, the use of high-powered ultrasound has the potential to reduce the particle size and break down.

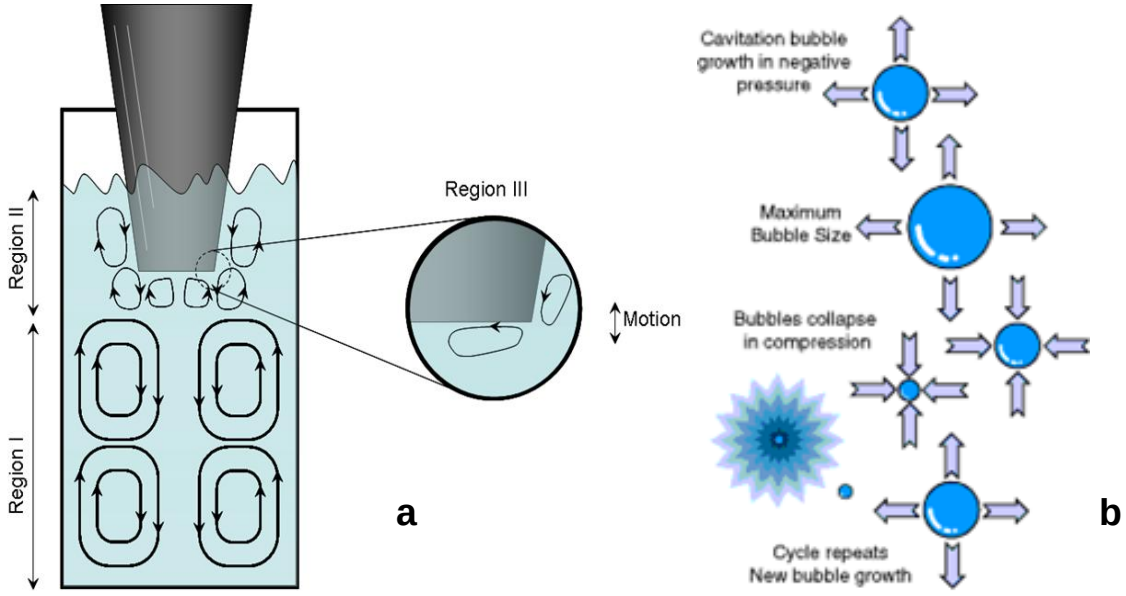

Figure 23 Schematics of (a) acoustic streaming and convection currents generated by ultrasonics, (b) cavitation bubble growth-collapse cycle

Ultrasonication has been widely applied in various biological and chemical processes. High-powered ultrasonics has been used for cell disruption, as well as the extraction of amino acid polymers from DNA and proteins. In many applications, glass microbeads added to the bulk act as “microhammers” that mechanically break cell walls and membranes. One of the latest uses of ultrasonics in the medical field has been to break down fat cells [48]. An example relevant to the research proposed here is the use of ultrasonics in the rubber recycling field, where it is used to devulcanize rubber without damaging the elastomer [49,50].

Numerous mechanisms have been attributed to the enhanced chemical pathways, including cavitation, acoustic streaming, shock waves, jetting, free radical production, agglomeration, surface activation, and thermal gradient. However, their relative contributions to the outcome of the application are not well known. In this research it is envisioned that ultrasonics can be efficiently utilized to depolymerize PLA, and recover lactic acid for effective repolymerization. In order to develop and materialize the technology, an investigation was completed to determine the ideal parameter set and chemistry. This research work was an attempt to study and identify the fundamental predominant mechanisms needed to achieve energy efficient depolymerization and high yields of lactic acid.

2.2.1 Near and far field

As with any propagating wave from a source, there are two major factors, attenuation and diffraction, that define the wave field. These factors are critical in determine the design of the tooling and reaction chamber for the desired chemical reaction. If the reactants are near the source of the ultrasonics, then the field intensity is relatively uniform. The Rayleigh distance (R_0) is often used to determine the maximum distance between the source with a radius (a) and the substrate while in the near field condition. The Rayleigh distance is based on the wavelength (λ) of the sound wave in the fluid and is defined as seen in Eq. 11.

$$R_0 = \frac{\pi a^2}{\lambda} \qquad \text{[Eq. 11]}$$

Beyond this distance, diffraction patterns are generated which produce constructive and destructive (minimum and maximum) intensity patterns. It is important to note that diffraction can also be generated by reflected waves from the reaction chamber and the Rayleigh distance assumes an infinite, uniform body. The Rayleigh distance assumes that the only diffraction patterns are generated by edge effects of the ultrasonic source as seen in Figure 24 Any interface with a different impedance (Z) will produce a reflection (R), that can produce complex diffraction patterns. The relative

intensity of the reflective wave can be determined using Eq. 12, where Z_1 and Z_2 are the impendence of the liquid and the material of the interfacial material, such as a glass beaker or stainless reaction chamber.

$$R = \frac{(Z_2 - Z_1)}{(Z_2 + Z_1)} \qquad \text{[Eq. 12]}$$

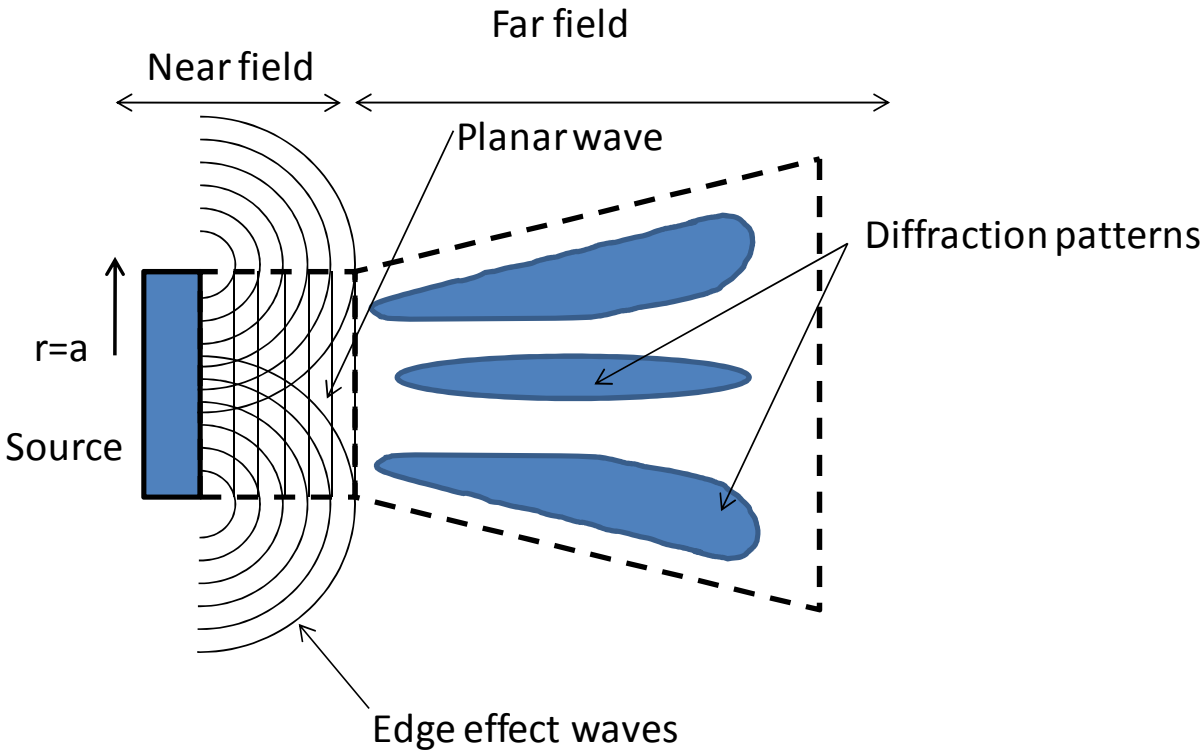

Figure 24 Schematic of near and far field distances and generation of diffraction patterns

The formation of diffractive is further illustrated in Figure 25 with a common example of a planar wave passing through two slits.

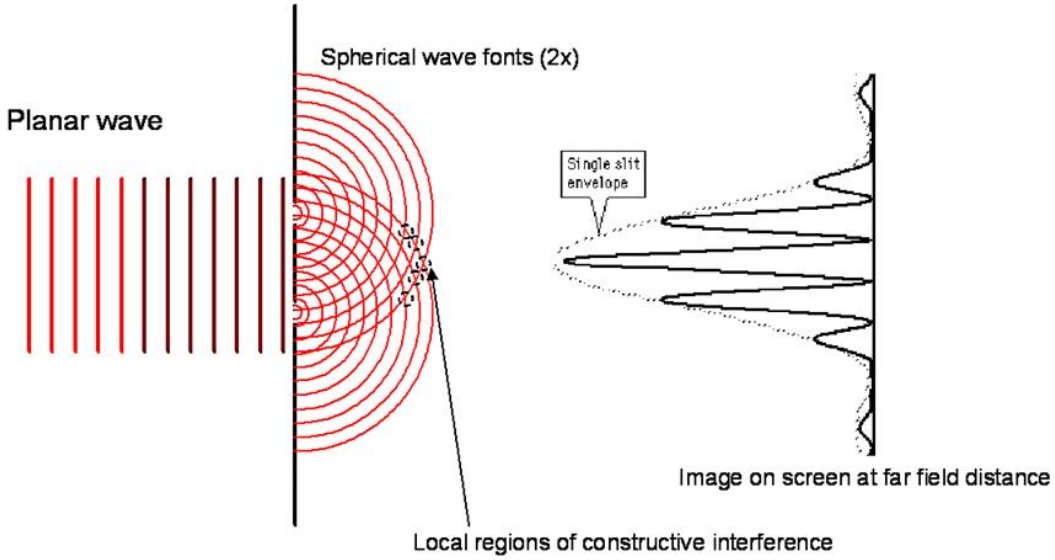

Figure 25 Schematic generation of diffraction patterns

In a practical means, it is common to treat substrates outside the near field condition and still assume uniform treatment as long as the substrate is mixed, either internally by streaming (detailed below) or externally by a mixing system.

In addition to diffraction, attenuation can reduce the effective distance between the source and the substrate, that can be used while efficiently treating the substrate.

2.3 Impetus for the research

This research was designed to enhance the overall economics of PLA products by demonstrating the energy efficient recycling of lactic acid from PLA. It was proposed to use ultrasonics (high frequency sound waves) in conjunction with salts to depolymerize postconsumer PLA products. Existing companies, such as BioCor and Galactic51, depolymerize PLA for recovery of lactic acid and repolymerize it into virgin PLA for food contact applications. although this approach is considered viable, the strategy is to further improve the recycling process with ultrasonics. The primary objective of the research was to study and characterize the effectiveness of ultrasonics as a tool to enhance the recovery of lactic acid by depolymerizing PLA. The goal was to achieve efficient recycling of PLA from postconsumer products and further reduce the carbon footprint of PLA.

2.4 Proof of concept experiments preliminary trials

As a proof of concept, two samples were prepared. Both had 1 g of chopped PLA samples from water bottles that were suspended in methanol as the treatment medium and potassium carbonate (K_2CO_3) as the catalyst. One sample was exposed to ultrasonics, while the other was agitated in a hot bath. The process was able to depolymerize PLA in methanol in 12 min using ultrasonics and the catalyst as compared to the conventional method, which

required 30 min using a hot water bath (heat source) and catalysts, as seen in Figure 26. The conversion of PLA into lactic acid was confirmed using high performance liquid chromatography (HPLC). For example, in the sample treated with ultrasonics, the lactic acid peaks were observed at approximately 12 min to 13 min in the timeline of the analysis. This was consistent with the control solution (lactic acid), as seen in Figure 27.

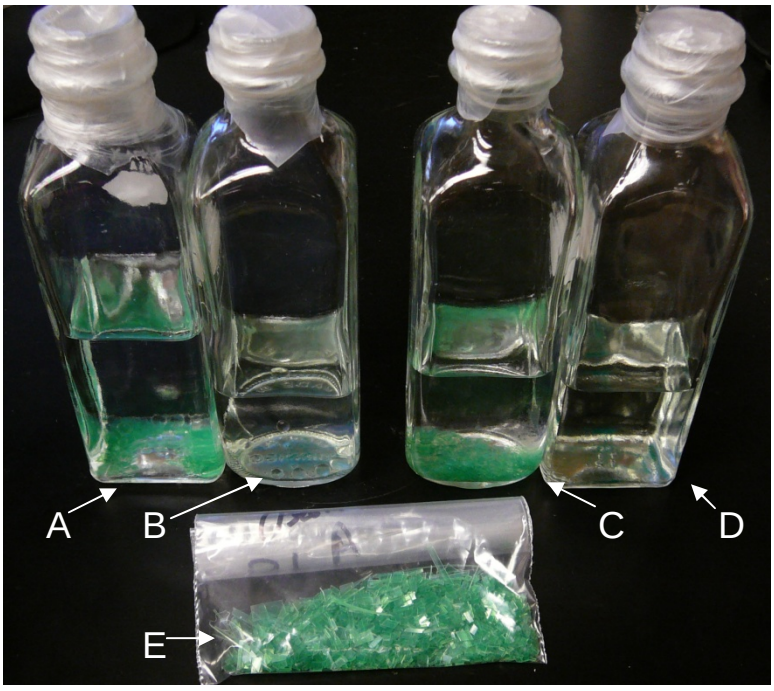

Figure 26 Sample details and treatments: A- heated bath w/o catalyst, B – heated bath with catalyst, C- ultrasonics w/o catalyst, D-ultrasonics with catalyst, E-chopped PLA

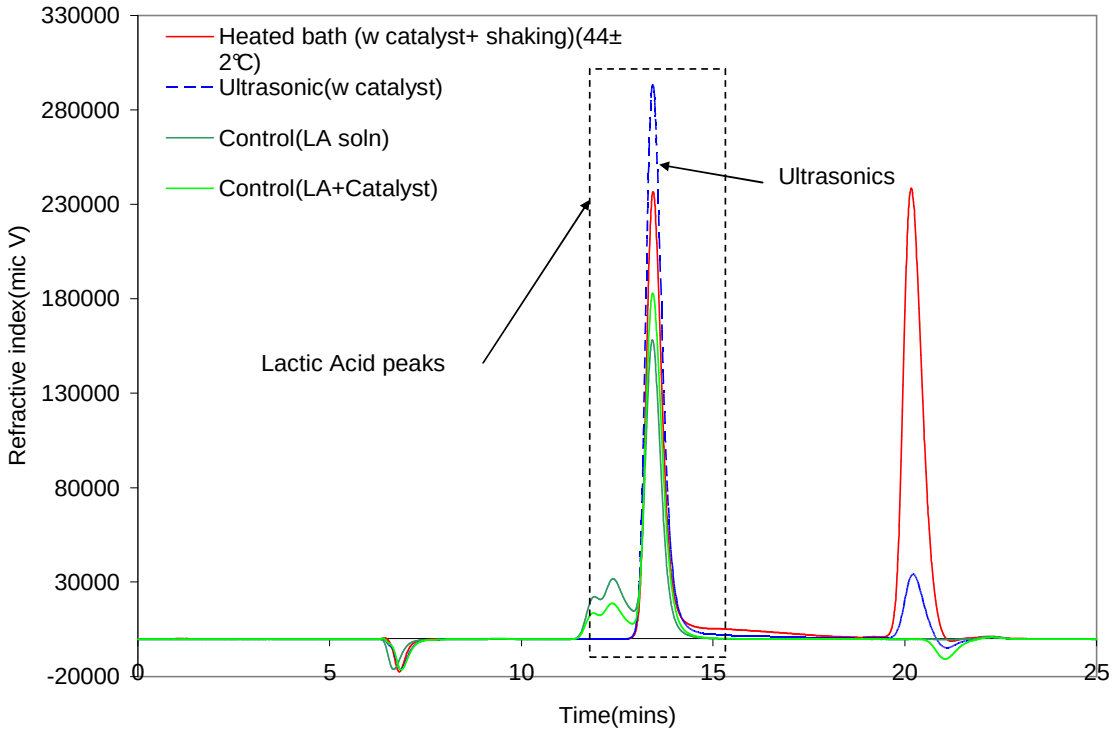

Figure 27 HPLC analysis of the control solutions and depolymerized PLA solutions using heated bath and ultrasonics respectively

It was observed that the area under the lactic acid peak (integration of the HPLC curves) of the ultrasonics sample was higher when compared to the hot bath hydrolysis. This suggested a higher yield of lactic acid for the ultrasonic treatment with respect to the hot bath process for the same mass of PLA depolymerized.

CHAPTER 3: RESEARCH QUESTIONS

This research was designed to address the following three primary questions:

1) Will depolymerization of PLA to lactic acid be enhanced with ultrasonics in a liquid medium?

2) What are effective catalysts and conditions for depolymerization of PLA within a scope of screening experiments with various proposed catalysis?

3) What is the correlation between the experimentation (operating) parameters and the effectiveness of depolymerization of PLA?

CHAPTER 4: MATERIALS AND METHODOLOGY

The initial experimental design was constructed based on results from the proof of concept trials and the literature review. The first phase of trials involved an array of screening experiments. Based on the outcome of these trials, further confirming tests were designed and conducted. These outcomes were compared to identify the design space for process optimization of th operating parameters. The various experimental materials, methods, and testing equipment used in the research are detailed in the following sections.

4.1 Materials

4.1.1 Raw Material and preparation: Post consumer poly lactic acid polymer

The raw PLA material for this work was sourced from Totally Green Inc., IA, previously known as "Naturally Iowa". The source was postconsumer PLA water bottles from the company's packaged water product brand "Green Bottle Spring Water". It should be noted that the bottles were made with the IngeoTM PLA resin, which is manufactured by NatureWorks LLC (Blair, NE). The PLA bottles were washed and rinsed with warm water (45ºC) to remove the dirt and beverage residues. Further, the bottles were steeped in room temperature water for approximately 3 hrs to facilitate the removal of the

brand label on the bottle. Following label removal, the bottles were rubbed with denatured ethanol to complete the removal of residual adhesive from the product label. Further, the bottles were air dried for 2 days to remove any residual water from the washing process.

The bottles were then chopped into PLA chips with standard dimensions. The thickness of the chips was limited by the capacity of the chopping equipment used to cut the samples. To avoid variation in the thickness of the PLA chips, the uniformly thick tubular section of the bottle was utilized, discarding the bottom and the neck sections which were it was found to be uneven in thickness. Further, the tubular portion was cut open into sheets and fed to a strip-cut paper shredder that produced strips with a standard width of ~6 mm. These strips were chopped into chips of 6 mm x 2 mm dimension, as seen in Figure 25, using a BT-25 strand pelletizer from Scheer Bay Plastics machinery, MI.

Figure 28 Chopped PLA chips from postconsumer water bottles (Picture showing unused neck and bottom portions)

4.1.2 Chemical compounds and treatment media

The ultrasonic treatment of PLA chips, was completed with various salts and treatment media. The various salts and compounds used were based on the findings in literature and on theorized chemical pathways. They were potassium carbonate (K2CO3), calcium carbonate (CaCO3), and sodium hydroxide(NaOH), all obtained from Fischer Scientific in Pittsburg, PA; aluminum carbonate (AL2(CO3)3) from Alfa Aesar, MA; zinc carbonate basic [ZnCO3]2 • [Zn(OH)2]3, magnesium oxide(MgO), and zirconium(IV)oxide (ZrO2) catalyst from Sigma Aldrich MO; and copper(II) carbonate, basic(CuCO3·Cu(OH)2) from Strem Chemical, MA. Most of these

compounds are carbonates and oxides of alkali, alkaline earth, and transition metals. They were selected because they are weak electronegative metals. When ionized, they yield cations that should produce a reactive species that will react with the PLA intramolecular bonding. In addition, in proof of concept trials, carbonate salt of potassium proved to be effective with the medium as methanol. The three media used for this research were water, methanol, and ethanol. Though none of these media are solvents of PLA, they were selected because LA is soluble or miscible in them. It was envisioned that if depolymerization of PLA into lactic acid occurred, the collection and purification of the lactic acid would be easier utilizing these media. The separation of lactic acid from these media can be achieved by low temperature distillation due to their relatively low boiling point temperatures (except for water). L(+)-Lactic acid (90%) from Acros organics NJ. Was utilized for the construction of the standard curve to measure the Lactic acid concentration in samples

4.2 Methods

4.2.1 Methods: Ultrasonic treatment

Ultrasonic treatment of PLA samples were conducted with a Branson 2000ea series 20 KHz ultrasonic system (2200 W), as shown in Figure 29. The

system was equipped with an ultrasonic stack that consisted of a PZT transducer (20 KHz, maximum amplitude of 20μm_{p-p}), a booster with a gain of 1:0.6 signal multiplying factor (a reducing booster), and a horn (1:2.17 multiplying factor) with a 39 mm diameter flat face. The stack assembly produced an amplitude of 26$m\mu_{p-p}$ at 100% power. All the samples were treated in a 150 ml quartz beaker. Every sample consisted of the PLA sample mass (1g to 5g), catalyst compound (0.125 g to 0.5 g), and 50 ml of the treatment medium respectively. The temperatures of the sonicated samples were recorded during treatments. All the experiments were conducted in three phases, as discussed in the following sections.

4.2.2 Thermo-gravimetric analysis

In order to gain insight of material composition and thermal properties PLA analysis was carried out on a thermo gravimetric analyzer (TGA) from TA Instruments, New Castle, Delaware. A heating rate of 10ºC/min was used for TGA analysis.

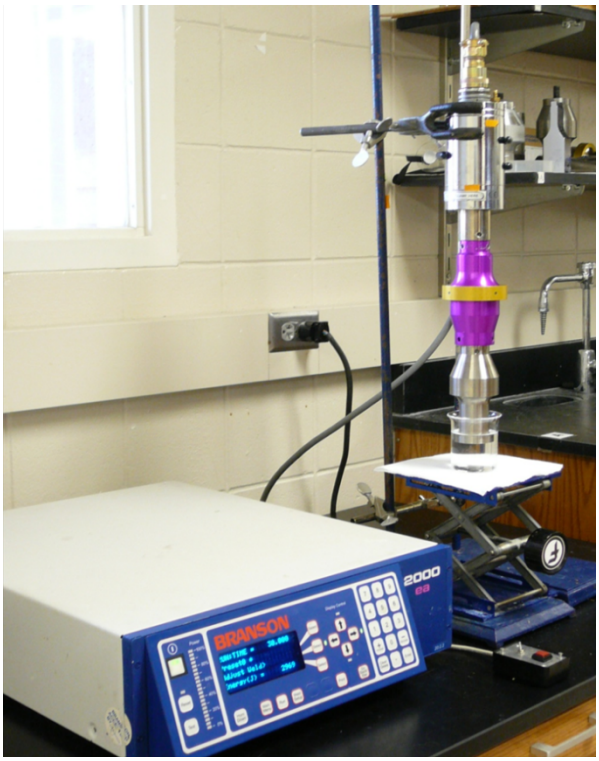

Figure 29 Branson 2000ea 20 KHz ultrasonic system with an ultrasonics stack

4.2.1.1 Ultrasonic treatment: Phase-I (screening experiments)

Ultrasonic treatment of PLA samples were conducted with all possible permutations of the parameters listed in Table 1 (chemical compounds and treatment media). The table also displays the code structure used for the nomenclature of individual experiments. For example, experiment "1MK(1)15X" indicates that 1g of PLA chips in treatment media methanol "M" with catalyst potassium carbonate (0.5 g) "K(1)" was treated for a time of 15 min at an amplitude of 13$\mu m_{p\text{-}p}$, or a power level of 50%. It should be noted

that the treatment parameters, amplitude, and time were fixed at 13μm_{p-p} and 15 min respectively. This was because during screening experiments no acoustic streaming or mixing was observed at an amplitude below 7μm_{p-p}. Conversely, at an amplitude above 19μm_{p-p}, a vapor barrier was observed to develop between the horn tip and the PLA chips with methanol and ethanol as the media. These effects prevented experiments from being conducted at amplitudes below and above 7μm_{p-p} and 13μm_{p-p}, respectively. The treatment time was limited to 15 min for the screening phase, as lower depolymerization times were observed during the proof of concept trials.

The array of experiments was completed to identify the combinations that effected PLA degradation/depolymerization. The degradation/ depolymerization of PLA was recognized and quantified by relative weight loss (as a percentage) of the treated sample, which was calculated as defined by Eq 10.

$$\text{Degree of depolymerization} = \frac{(\text{Initial weight} - \text{Post ultrasonic treatment weight})}{\text{Initial weight}} \times 100$$

Eq.10

Further confirmation and quantification of lactic acid was completed with high performance liquid chromatography (HPLC) as a characterization tool. The lactic acid concentration in a treated sample was determined using a calibration coefficient based on the area of LA peaks of known concentration from HPLC as seen in Figure 30. It is seen that the linear fit is reasonably good with an r^2 value of 0.95.

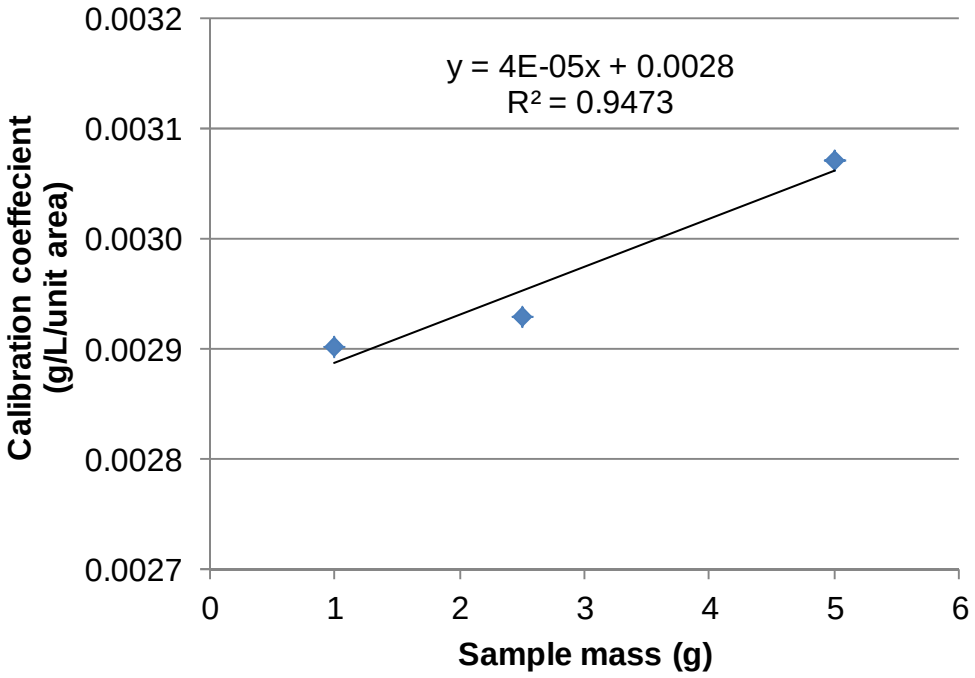

Figure 30 Calibration coefficient as a function of samples mass

The relation between area of LA peak from HPLC and concentration was established by constructing a standard curve with L(+)-Lactic acid (90%) at concentrations of 1, 2.5 and 5g per 50 ml.

4.2.1.2 Ultrasonic treatment: Phase-II (effect of sample mass)

At the completion of Phase-I, the respective combinations of salts and media that resulted in a PLA degradation (mass loss) value greater than 5% were selected for further investigation. Phase-II experiments were conducted by varying PLA chips mass/concentration (1 g to 5 g), along with the respective salt and media combinations identified from Phase-I. The objective of Phase-II experiments was to investigate the effect of initial PLA mass fraction on depolymerization. Based on the results of the PLA mass fraction study, a detailed study of depolymerization as a function of treatment time was conducted.

Table 1 Matrix of variables used during Phase-I

Variable / S.No	Sample Mass		Treatment Media		Catalyst		Time		Amplitude	
	Mass	Code (Pos #1)	Media	Code (Pos #2)	Type	Code (Pos#3)	Min	Code (Pos #4)	μ_{p-p}	code (Pos #5)
1	1g	1	Methanol	M	K_2CO_3(0.5g)	K(1)	15 min	15	$7\mu_{p-p}$	W
2			Water	W	K_2CO_3(0.25g)	K(2)	20 min	20	$13\mu_{p-p}$	X
3			Ethanol	E	AL_2CO_3	Al	10 min	10	$19\mu_{p-p}$	Y
4					Zn_2CO3	Zn	25 min	25		
5					NaOH(0.5g)	Na(1)	30 min	30		
6					NaOH(0.25g)	Na(2)				
7					NaOH(0.125g)	Na(3)				
8					ZrO	Zr				
9					MgO	Mg				
10					$CaCO_3$	Ca				
11					$CuCO_3$	CU				

Table 2 Matrix of variables used during Phase-III

Sample Mass	Code (Pos #1)	Treatment Media	Code (Pos #2)	Catalyst/ chemical	Code (Pos#3)
5g	1	Methanol	M	K_2CO_3(0.5g)	K(1)
		Ethanol	E	K_2CO_3(0.25g)	K(2)
				NaOH(0.5g)	Na(1)
				NaOH(0.25g)	Na(2)
				NaOH(0.125g)	Na(3)

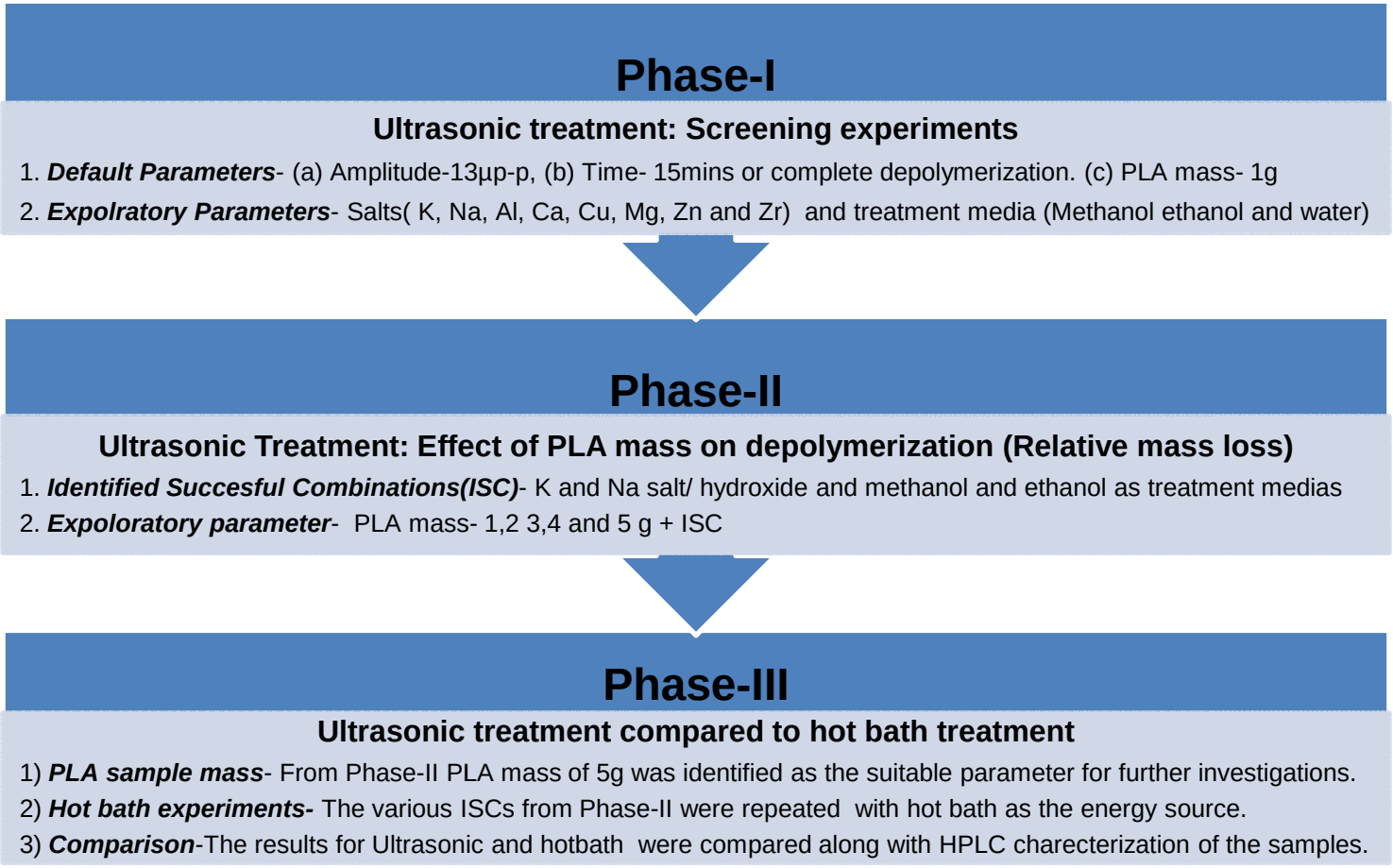

Figure 31 Flow diagram of overall experimental design

4.2.1.3 Ultrasonic treatment and hot bath: Phase-III (Degradation as a function of treatment time)

The best PLA mass fraction (of the ranges studied) from Phase II experiments was identified to be 5 g/(50 ml of media). All further replicates and experiments were conducted with 5 g PLA as the sample mass. The progressive depolymerization of PLA was traced by completing experiments with evenly spaced treatment times (0, 2.5, 5, 7.5…15 min). The parameters used for Phase-III experiments were derived from the results of Phase-II and are detailed in Table 2. A full factorial experimentation of these parameters was conducted to complete the data collection for the ultrasonic treatment experiments.

Further experiments were completed for the parameters in Table 2 using a hot bath in place of ultrasonics as the energy source (a control group). The hot bath experiments were conducted at the same temperature values observed during the ultrasonics treatment. These temperatures were 55ºC and 65ºC for methanol and ethanol respectively. Because there was fluctuation in the temperatures measured during ultrasonic treatment (±10 ºC), the effect of temperature on depolymerization/degradation of PLA was further investigated with the hot bath at temperatures of ±10 ºC (above and below) the observed ultrasonic treatment temperatures. A visualization of all

three phases and the process flow of the experimentation can be seen in Figure 31.

4.2.1.4 Lactic acid detection and quantification – High performance liquid chromatography

The liquid samples from both ultrasonic treatment and hot bath experiments were filtered with Whatman paper (spec #1). The filtrate was further centrifuged at 6,000 rpm to settle any suspended PLA or salt particles. These centrifuged samples were diluted by a factor of 10 prior to HPLC analysis. The samples were diluted to suppress the peaks that correspond to treatment media concentration (methanol/ethanol) at HPLC. The analysis was completed with a Varian HPLC and Varian-356-LC Ri detector. The column used was Aminex HPX-87H Column #125-0140 for organic acids from Biorad. Standard chemical grade LA samples were used for calibration.

4.2.1.5 Modeling fluid flow caused by ultrasonics

The modeling of fluid flow (acoustic streaming) caused by ultrasonics was completed using both real-time tracking with particle image velocimetry (PIV) and virtual modeling with finite element analysis (FEA), Ansys®. Both

approaches used water at room temperature and atmospheric pressure as the medium.

4.2.1.5.1 Tracking fluid flow caused by ultrasonics: Particle image velocimetry (PIV)

The fluid flow caused by ultrasonics in water was tracked by adding titanium dioxide (TiO_2) beads (Ø 1µm) to the media. A laser was pulsed through the water to track the movement of the. The water was contained in a transparent acrylic tank of dimensions (L X W X D) of 584 mm X 280 mm X 278 mm. The setup for the experiment is illustrated in Figure 32. The ultrasonic horn had a 39 mm dia. flat-faced standard horn, and the ultrasonic system was a 20 kHz system manufacture by Branson Ultrasonic (Danbury, CT).

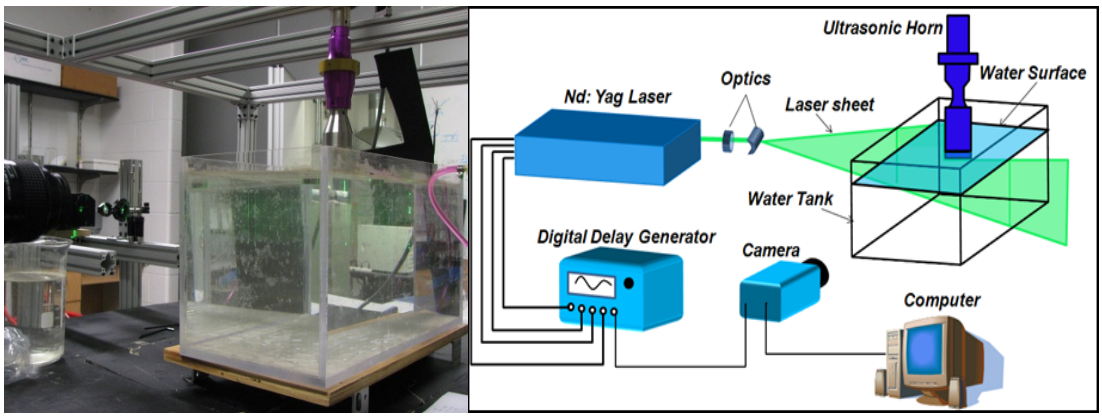

Figure 32 Photograph and schematics of experimental setup of ultrasonics with PIV investigation

In further detail, the system functions by passing a double-pulsed Nd:YAG laser (NewWave Gemini 200) through a medium, adjusted on the second harmonic and emitting two pulses of 200 mJ at the wavelength of 532 nm with a repetition rate of about 1 Hz. The laser beam was shaped to a sheet by a set of optics with spherical and cylindrical lenses. The thickness of the laser sheet in the measurement region was approximately 1.0 mm. A high-resolution 14-bit CCD camera (PCO2000, 2048×2048 pixels, Cooke Corp) was used for PIV image acquisition, with the axis of the camera perpendicular to the laser sheet. The CCD camera and the double-pulsed Nd:YAG lasers were connected to a workstation (host computer) through a digital delay generator (Berkeley Nucleonics, Model 565), which controlled the timing of the laser illumination and the image acquisition. Instantaneous PIV velocity vectors were obtained by a frame-to-frame cross-correlation technique involving successive frames of patterns of particle images in an interrogation window of 32 $\times$ 32 pixels. An effective overlap of 50% of the interrogation windows was employed in PIV image processing. Because the FPS (frame per second) of the camera was relative low (approximately 1 Hz), the resulting sampling rate of PIV was approximately 0.97Hz. The time interval between two sequential images was 600 μs. The image of the illuminated particles captured with a CCD collecting the sequential images were processed with a proprietary software package. Based on spatial locations of

the particles from frame to frame, the software calculates the velocities of the particles. These velocities are then plotted as contour plots, which were later used for validating with results from fluid flow simulation results from finite element analysis.

4.2.1.5.2 Modeling fluid flow caused ultrasonics: Finite element analysis (FEA) package

Finite element analysis (FEA) was used to predict acoustic streaming velocities, and the model was verified with natural buoyancy particle tracking. The FEA was completed with ANSYS Workbench of (Canonsburg, PA) version 12.1. The model was constructed in a quasi-2-dimensinal (2D) domain. A 2-D element type was used with an extruded thickness of 1 mm, and the constraints (properties) of the element were defined so that there was no gradient through the thickness of the element. A full-scale model was constructed (2D) through center of the experimental setup, as is detailed in Figure 33.

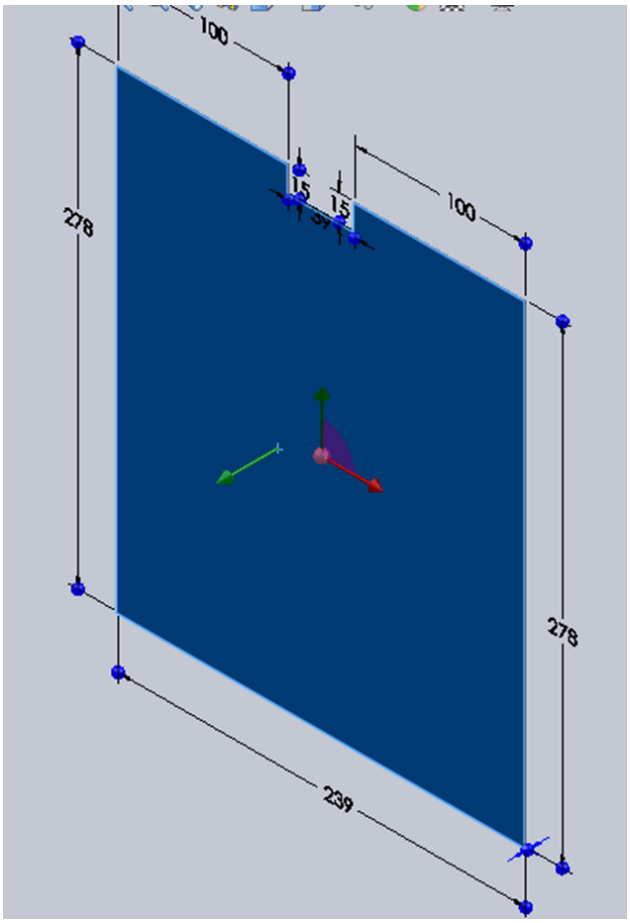

Figure 33 One element thick beaker model utilized for FEA (units: mm)

The model was used to predict the velocity fields in a water bath, as shown in Figure 34.

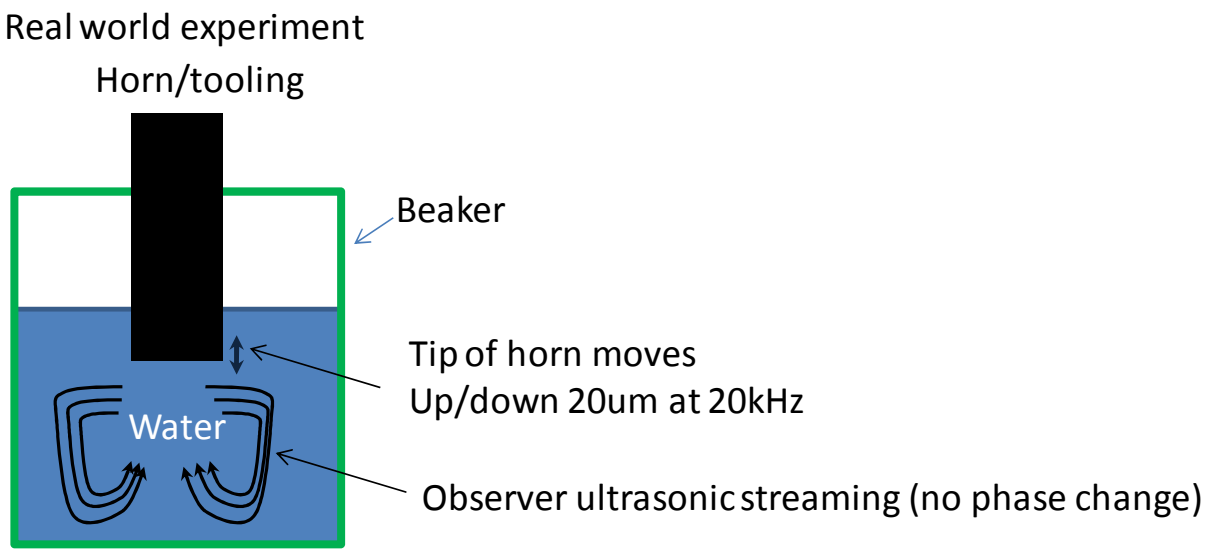

Figure 34. Illustration of experimental setup that was modeled to predict acoustic streaming

The assumptions of the model were:

1) No slip conditions at all interfaces
2) Newtonian fluid flow with properties defined as water (ANSYS default values)
3) Density of water for fluid
4) No thermal effects
5) No phase changes
6) Atmospheric pressure at the water/air interface

7) Horn interface displaces as a function of time to match experimental conditions

The model was calculated from a static condition and ran for 200 mS. Figure 35 details some of the assumptions, as well as where some of the boundary conditions were applied.

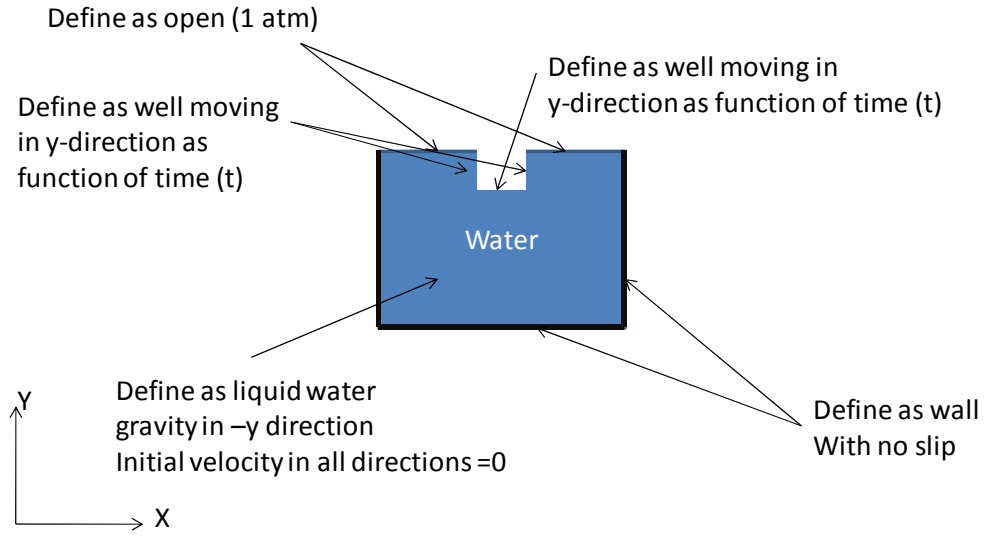

Figure 35 Details of FEA model assumption and application of these assumptions

Contour plots of the predicted velocity fields were generated with three varying ultrasonic amplitudes 7, 13, and 19 µm.

4.2.1.6 Scanning Electron Microscopy

Characterization was done using a Hitachi S-2460N variable pressure scanning electron microscope (VP-SEM). Variable pressure mode allows for examination of insulating samples with minimal sample preparation. A residual atmosphere of 40 Pa (0.3 Torr) of helium is adequate to eliminate charging from most samples while allowing reasonably high magnifications (up to 3000x). (The actual pressure is indicated in the lower right of the images.) (The scope may also be operated in high vacuum (high resolution) mode like a conventional SEM.)

Samples were examined at 20 kV using the backscattered electron (BSE) signal. (It is less sensitive to topography than the secondary electron signal, but it is the only signal available with operating this microscope in V-P mode.) Images were collected at 50x and 300x magnifications to show the gross and finer details of the texture. Note that some of the low magnification images show little structure, but the structure consists of broad, concave depressions on the surface.

CHAPTER 5: RESULTS AND CONCLUSIONS

As a brief review, the three phases of experiments, including the screening phase, were completed as detailed in Figure 31. As previously mentioned, these experiments were conducted to refine the design space of the independent parameters. It is important to note that the results from the ultrasonic experiments were compared with hot bath experiments (Phase III) that served as the control group. The results are detailed in the following sections in chronological order of the research phases conducted.

5.1 Results-Phase I

Phase I experiments were conducted with a default ultrasonic treatment parameter set of amplitude 13 μm_{p-p} and treatment time of 15 min. These parameters were based on the results of preliminary data. For all experiments the amplitude was fixed at a value of13 μm_{p-p}. In amplitude screening experiments, for amplitudes below 13 μm_{p-p}, (7 μm_{p-p}) no streaming was observed. In order to record the effects of amplitude experiments with methanol and potassium carbonate with various ultrasonic amplitudes (7,13 and 19 μm_{p-p}) were completed and the results of which are as depicted in Figure 36. It is seen that at generally LA yield is generally proportional to treatment time and amplitude. However, because of issues related to vapor

barriers limitation amplitudes above 19 μm_{p-p} were not possible to investigate. Thus, the center value of amplitude (13 μm_{p-p}) was selected as experimental value for the balance of screening experiments.

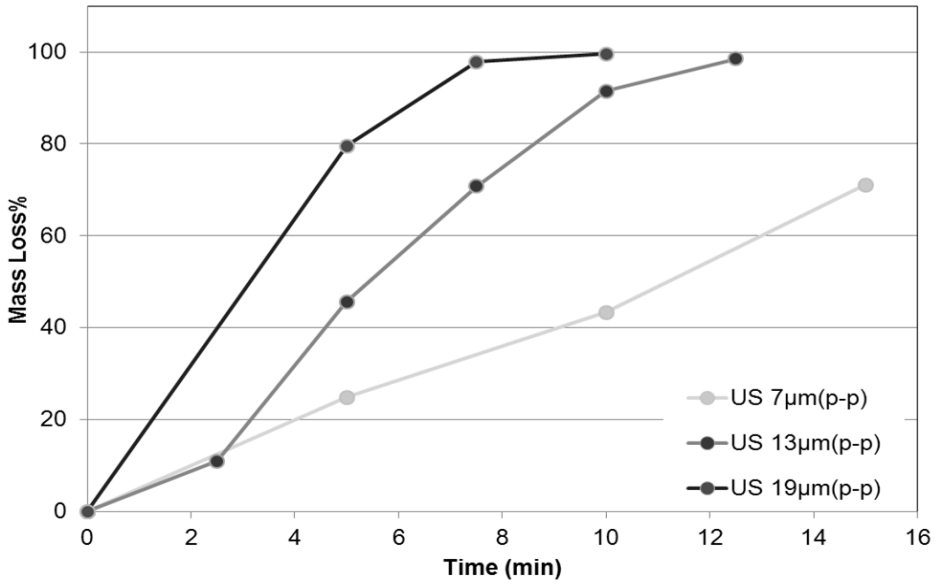

Figure 36 Relative mass loss (%) as a function of time treatment time for MK experiments using ultrasonic amplitudes of 7,13 and 1 9 μm_{p-p}

The various exploratory parameters were investigated in different combinations, as detailed in Table 3. As a reminder, the notations MK and MNa indicate that the experiments both had methanol "M" as the treatment medium, with K and Na denoting potassium carbonate and sodium hydroxide as the salt/catalyst respectively. The numbers indicated in parenthesis after the salt notation denotes the mass of the salt. The notations (1), (2), and (3)

indicate that the mass of salt/catalyst was 0.5, 0.25, and 0.125g respectively. As an example, MK(1) denotes the experiment had methanol "M", potassium carbonate with a mass of 0.5 g and "K(1)" as the treatment medium and catalysts respectively. It was observed that potassium carbonate with masses of 0.25 g and 0.5 g, was effective with methanol (MK) in depolymerizing 1 g of PLA but not with ethanol (EK) as the treatment medium. Sodium hydroxide was effective with either methanol (MNa) or ethanol (ENa) as the treatment medium. Both potassium carbonate and sodium hydroxide were ineffective with water as the medium.

It should be noted that the experiments with 0.5 g of sodium hydroxide with a methanol medium was not conducted because complete depolymerization of PLA was observed within 5 min of treatment time at a lower mass of 0.25 g of sodium hydroxide. That is, because the lower mass of catalysts resulted in effective depolymerization, it was assumed that higher masses (concentrations) would not be justified in terms of optimization. In addition, experiment ENa with a mass of 0.125 g of sodium hydroxide was omitted because the depolymerization was similar to that with the potassium carbonate in that lower masses of the catalysts were effective in depolymerization of PLA.

Table 3 Phase1 results: Various combinations of catalysts and treatment media (with codes) marked +ve (effected PLA mass loss), –ve (no mass loss observed), and n.a. (not applicable or not conducted). Default ultrasonic treatment parameters amplitude: 13 μm_{p-p}, treatment time-15 min or complete depolymerization, PLA mass- 1 g

Media / **Catalyst**	**Code**	Methanol M	Water W	Ethanol E
K_2CO_3(0.5g)	K(1)	+ve	-ve	-ve
K_2CO_3(0.25g)	K(2)	+ve	-ve	-ve
AL_2CO_3	Al	-ve	-ve	-ve
Zn_2CO3	Zn	-ve	-ve	-ve
NaOH(0.5g)	Na(1)	n.a.	-ve	+ve
NaOH(0.25g)	Na(2)	+ve	-ve	+ve
NaOH(0.125g)	Na(3)	+ve	-ve	n.a.
ZrO	Zr	-ve	-ve	-ve
MgO	Mg	-ve	-ve	-ve
$CaCO_3$	Ca	-ve	-ve	-ve
$CuCO_3$	CU	-ve	-ve	-ve

Thus, overall, methanol and ethanol as treatment media with sodium hydroxide and potassium carbonate as catalysts were selected as the design space for further optimization.

5.2 Results-Phase II

Similar to Phase-I experiments, the default ultrasonic treatment parameter set of amplitude 13 μm_{p-p} and maximum treatment time of 15 min were used in Phase–II experiments. Again, based on the phase I experiments, the combinations of potassium carbonate with methanol media (MK) and sodium hydroxide with both methanol and ethanol media (MNa and ENa) were used. Phase-II experiments investigated the effect of PLA mass (concentration) from 1 g to 5 g, with 1 g increments. The MK experiments were observed to result in 100% mass loss of PLA at all masses of PLA (1 g to 5 g). In more detail, as seen in Figure 37 (a) and (b), the results with methanol and at two mass levels 0.5 g (a) and 0.25 g (b) of potassium carbonate suggest that higher levels of catalyst (0.5 g) resulted in 100% mass loss over the entire range of PLA masses studied. In contrast, the lower catalysts mass 0.25 g only resulted in levels of mass loss, with less than 2 g of PLA. It is important to note that a trend line is added to the mass loss data points for visualization purposes only.

The relative mass loss (relative degree of depolymerization) is consistent with lactic acid concentration measures from HPLC. As expected the relative mass loss of PLA is generally directly proportional to LA concentration (% conversion of PLA to LA). The percent conversion values are calculated by

comparing HPLC results of treated samples with a standard curve plotted with known concentration values.

Similarly, as seen in Figure 38(a), the experiments (MNa) with 0.25 g sodium hydroxide as the catalyst depolymerized all masses of PLA (1 g to 5 g), within the reaction time of 5 min. However, with 0.125 g of NaOH, only PLA masses below 4 g were fully depolymerized, as seen in Figure 38 (b), at the end of 15 min treatment time.

In contrast with previous (MK and MNa) experiments, the results with ethanol and sodium hydroxide (ENa) resulted in a decrease in relative mass loss, with an increasing PLA sample mass independent of NaOH mass levels (0.5 g and 0.25 g), as seen in Figure 39 (a) and (b). This suggests that these combinations of media (solvent) and catalysts are limited in terms of effectiveness of depolymerization of PLA. It is seen that there is some divergence between the HPLC and mass loss at the lower PLA mass values and it is believed that at these low concentration, the divergence is related to experimental error.

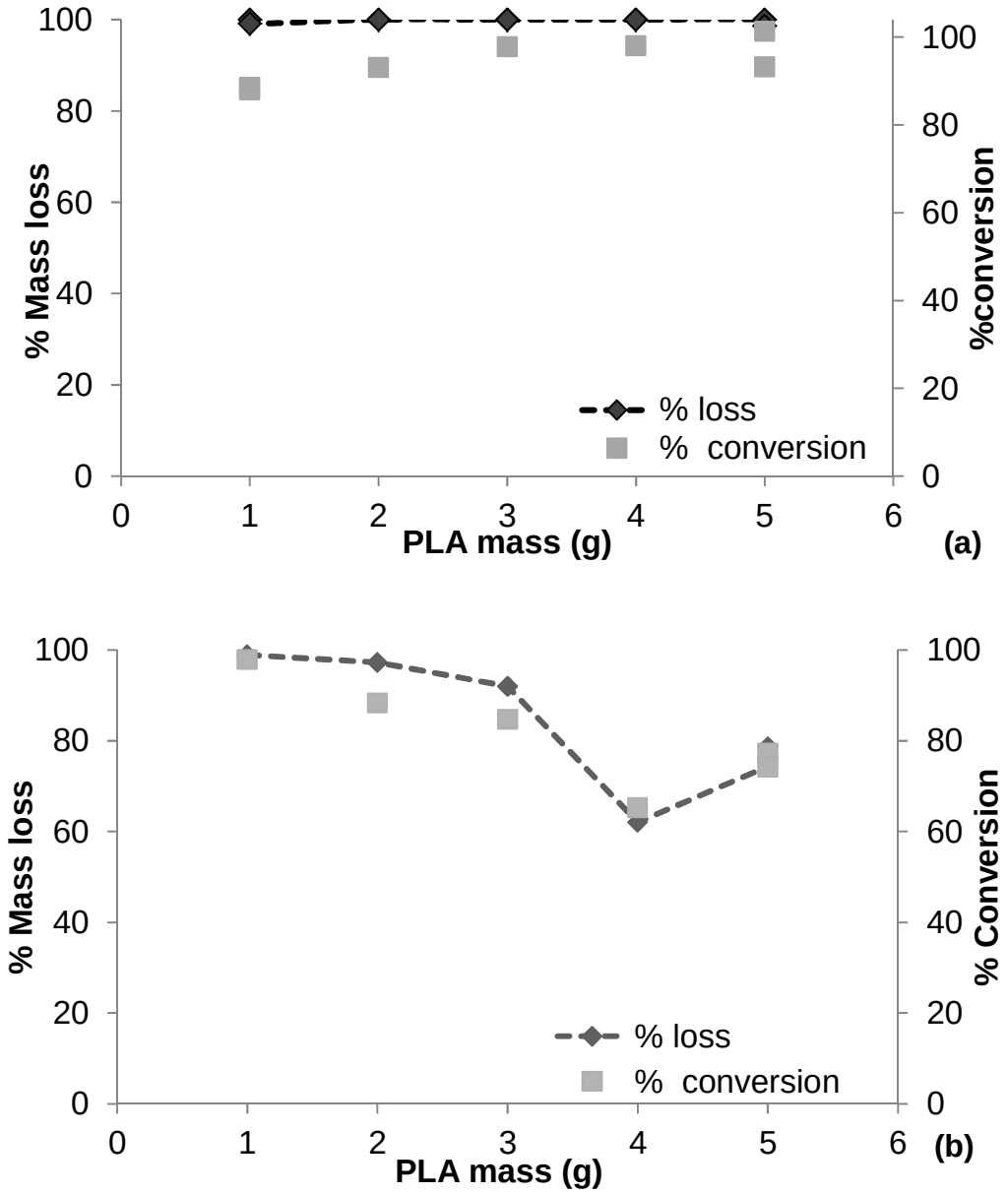

Figure 37 Relative mass loss (%) as a function of PLA mass for MK experiments (a) for 0.5 g potassium carbonate and (b) 0.25 g potassium carbonate

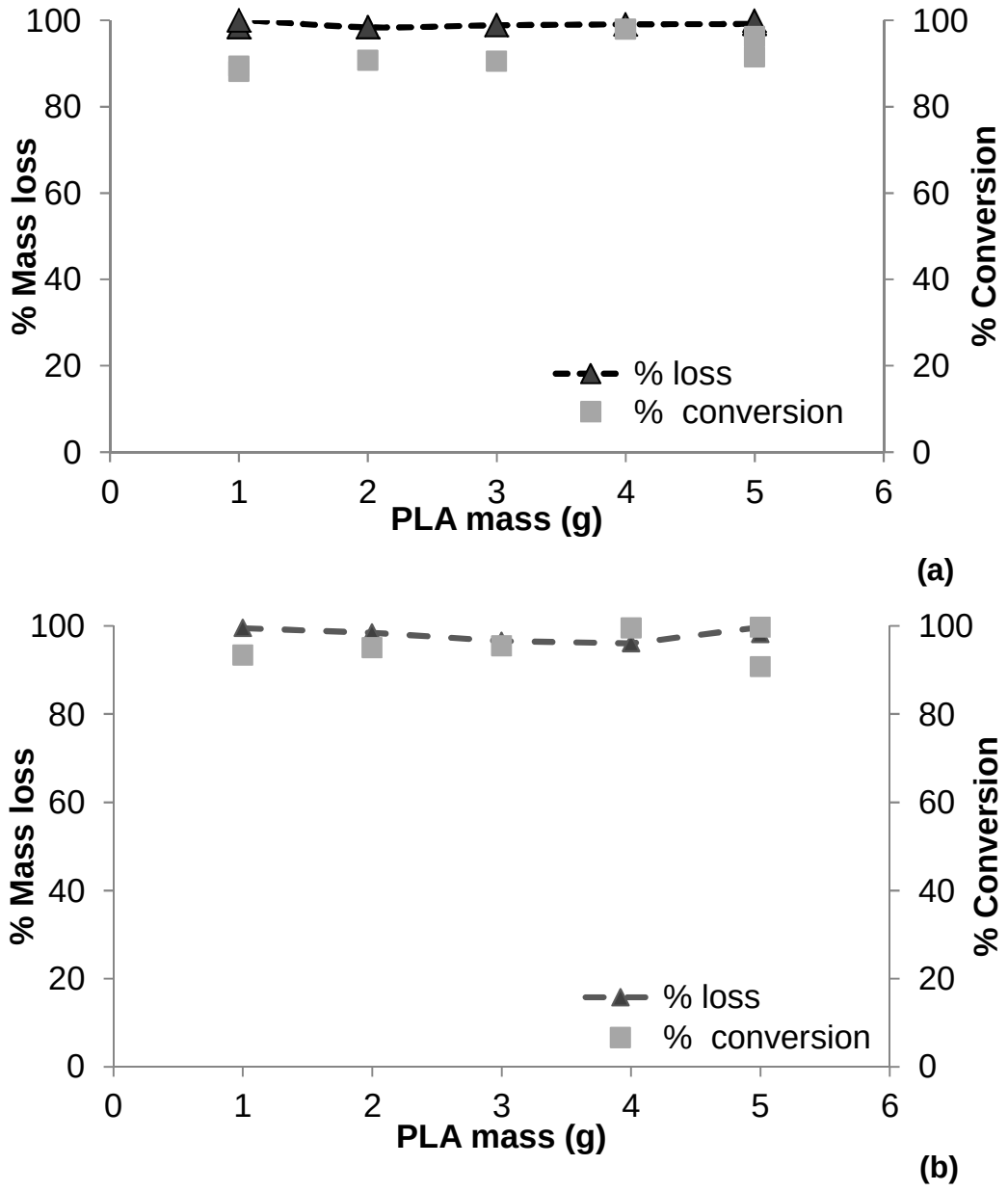

Figure 38 Relative mass loss (%) as a function of PLA mass for MNa experiments (a) for 0.25 g sodium hydroxide and (b) 0.125 g sodium hydroxide

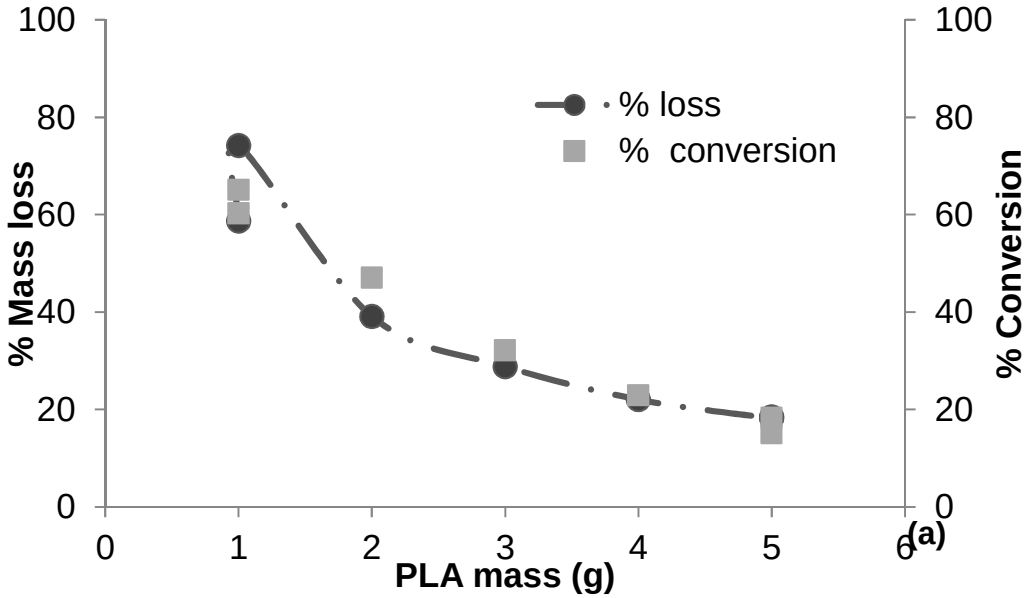

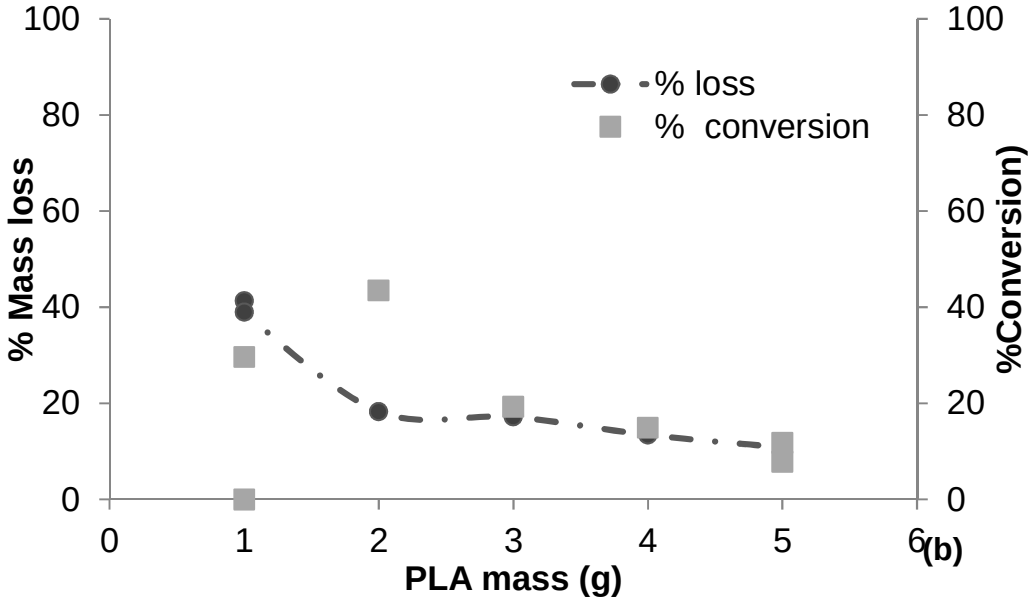

Figure 39 Relative mass loss (%) as a function of PLA mass for ENa experiments (a) for 0.5 g sodium hydroxide and (b) 0.25 g sodium hydroxide

From these results, it is concluded that depolymerization of PLA measured as relative mass loss is a dependent on the salt/catalyst mass (concentration), particularly for the combinations of potassium carbonate with methanol (MK) and sodium hydroxide with ethanol (ENa). This relationship was not seen with sodium hydroxide and methanol over the range of PLA mass that was tested here. In most figures, the data points are connected with a straight line to aid in visualization.

5.3 Results-Phase III

Based on the results of Phase-II, a mass of 5 g of a PLA sample was selected for further optimization of the depolymerization of PLA. Results of ultrasonic experiments of MK, MNa, and ENa, discussed in Phase II, were replicated with hot bath treatment serving as the control group. The temperatures of the hot bath treatment were selected to correspond (match) the temperatures achieved during the ultrasonics treatment in Phase II. These temperatures, were dependent on the treatment medium, and were 55ºC and 65 ºC for methanol and ethanol respectively. The results of Phase III allowed the comparison of ultrasonic and hot bath treatments.

Figure 40 shows a relative mass loss as a function of treatment time for both ultrasonics and hot bath treatments in a methanol with 0.5 g (1) and 0.25 g (2) of potassium carbonate. As expected, mass loss was generally proportional to the catalyst's mass (concentration). In addition, there is little difference between the hot bath treatment (HB) and ultrasonics (US) in terms of mass loss. Note that it is possible to fully depolymerize the 5 g of PLA in 10 min, which is much faster than reported by others [39,40,41,42].

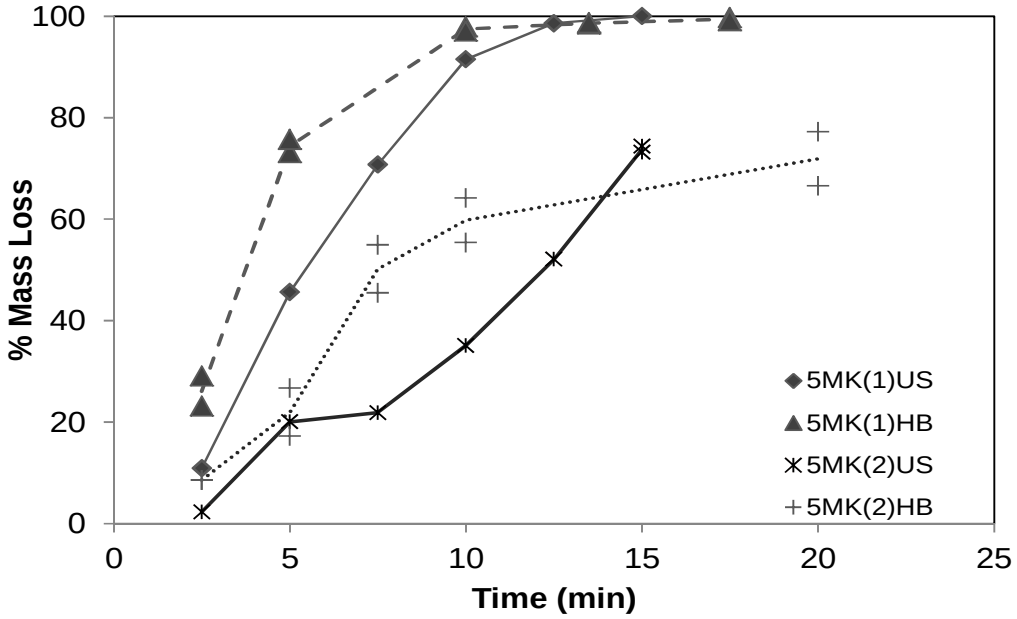

Figure 40 Relative mass loss as a function of treatment time for MK experiments using ultrasonic and hot bath treatments

As shown in Figure 41, with NaOH as catalysts, both mass levels (0.125 g and 0.25 g) resulted in 100% mass loss of PLA within 5 min for both

treatments (ultrasonic and hot bath). The trends of depolymerization for both ultrasonic and hot bath treatments are very similar with the combination of methanol and sodium hydroxide at both mass levels (0.125 and 0.25 g). Again, note that this is much faster than reported by others [39,40,41,42].

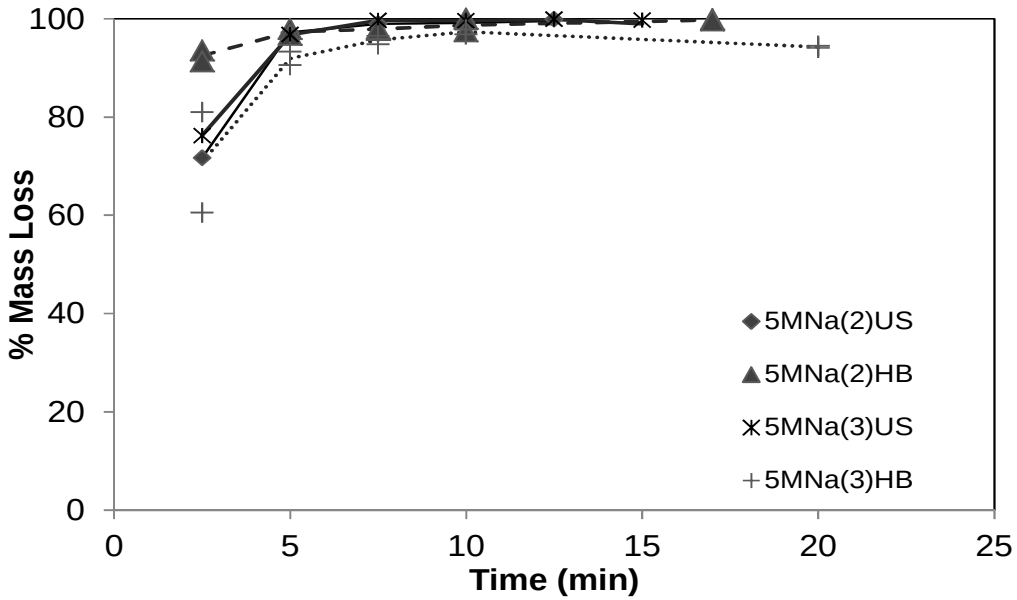

Figure 41 Relative mass loss as a function of treatment time for MNa experiments using ultrasonic and hot bath treatments

Figure 42 shows that with ethanol combined with sodium hydroxide at both mass levels of 0.25 g and 0.5 g, the maximum relative mass loss was 11% and 23% respectively. The depolymerization of PLA nearly stops after 5 min of treatment. The pattern was observed for both ultrasonic and hot bat treatments. It is believed that with this combination of catalysts and media,

the activity of the catalysts is inhibited by the LA and may be the result of a chemical reaction of acid (LA) and base (NaOH). There is no clear explanation why this possible effect is only seen with this combination.

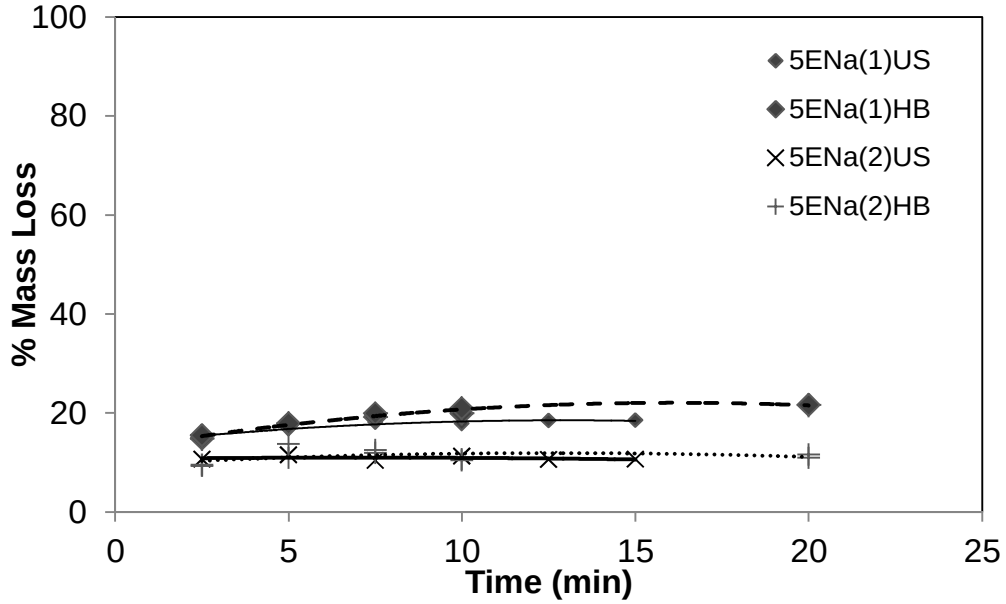

Figure 42 Relative mass loss as a function of treatment time for ENa experiments using ultrasonic and hot bath treatments

The relative conversion of PLA into LA lactic acid as a function of treatment time are seen in Figure 44, 41, and 42 for methanol/potassium carbonate, methanol/sodium hydroxide, and ethanol/sodium hydroxide respectively. The lactic acid conversion (calculated from HPLC results) as a function of treatment time exhibit results similar to relative mass loss, thereby confirming the release of lactic acid (monomer) from the PLA polymer. It is observed that

relative conversion of PLA to LA is lower than 100%, unlike mass loss. This is attributed to the weight contribution by colorants and additives (2.7% w/w) in PLA as confirmed with thermal gravimetric analysis (TGA) as seen in Figure 43, where there is approximately 2.7% residual mass.

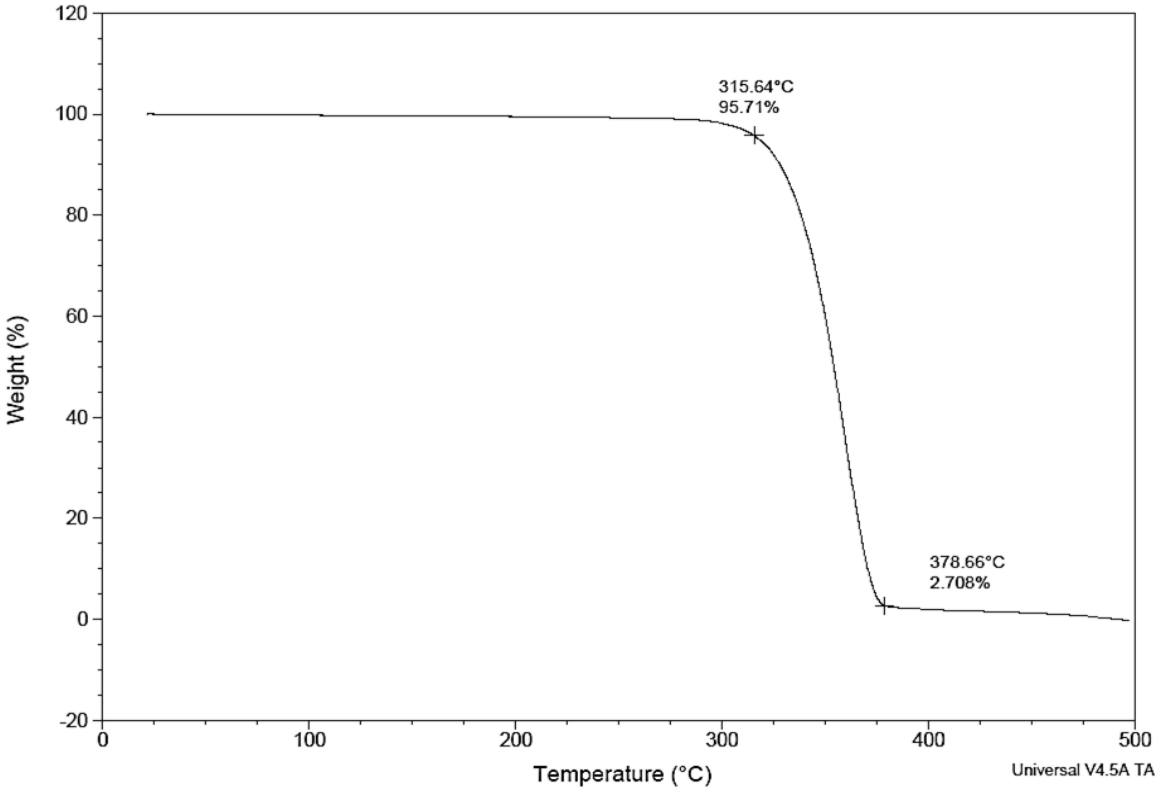

Figure 43 Thermo gravimetric analysis of post-consumer PLA chips from water bottle

It is believed that this difference in mass loss values and relative conversion is a compound effect of additive/colorants with incomplete conversion of PLA into LA.

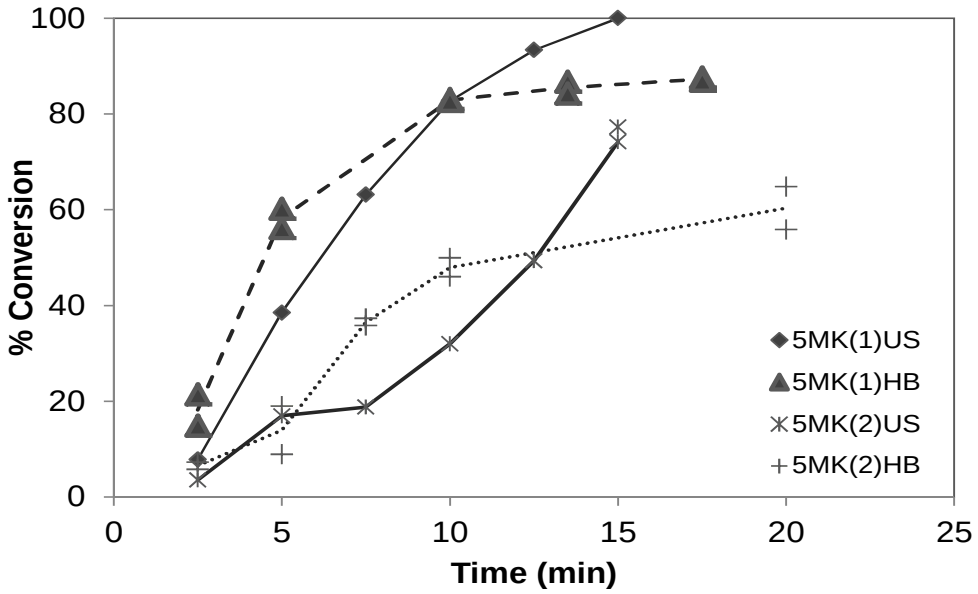

Figure 44 Relative conversion of lactic acid (HPLC) as a function of treatment time for MK experiments using ultrasonic and hot bath treatments

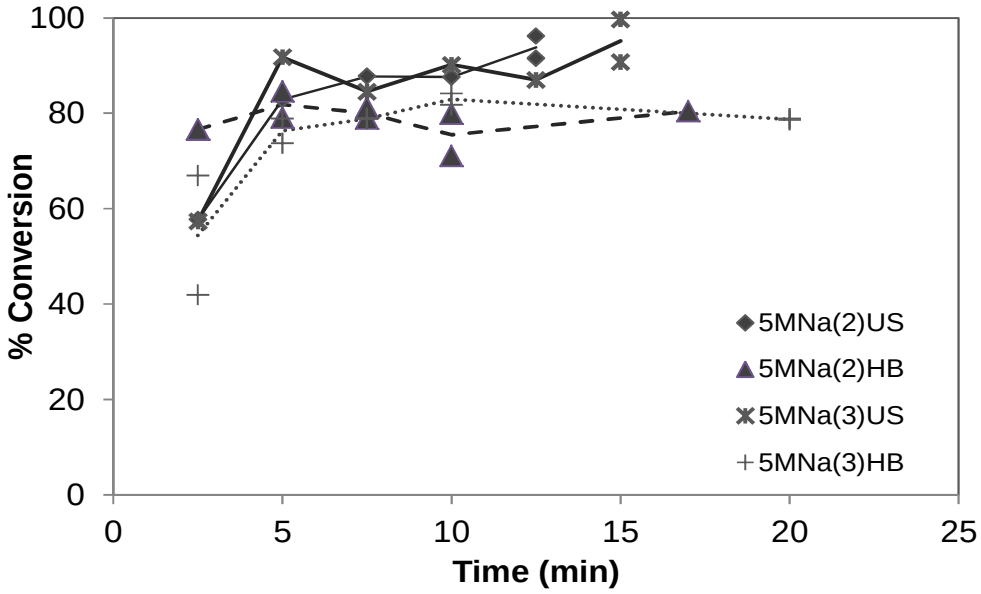

Figure 45 Relative conversion of lactic acid (HPLC) as a function of treatment time for MNa experiments using ultrasonic and hot bath treatments

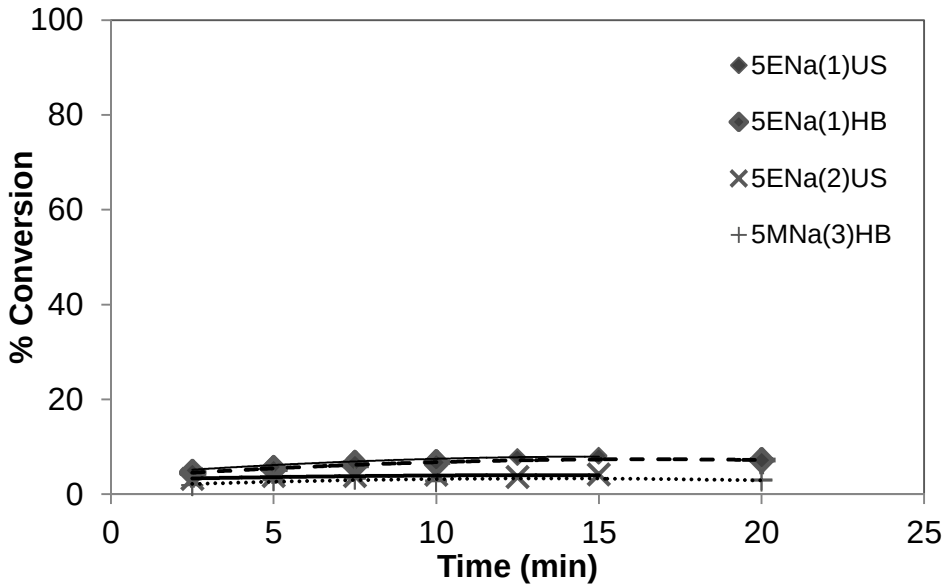

Figure 46 Relative conversion of lactic acid(HPLC) as a function of treatment time for ENa experiments using ultrasonic and hot bath treatments

and the presence of colorants and additives. It is seen from Figures 40 and 41 that the relative conversion values are higher for ultrasonic treatment with respect to hot bath treatment at times near 100% mass loss. This could be because of the mixing effect caused by acoustic streaming in conjunction with cavitation effects. In general, for a majority of the experiments mass loss as a function of treatment time (min) for both ultrasonics treatment and hot bath followed a similar trend.

To further optimize the depolymerization of PLA, additional studies of the effects of temperature on depolymerization (relative mass loss) of PLA were

completed. This was achieved by conducting hot bath experiments at 10ºC above and below the treatment temperature observed during ultrasonic treatment to assure that the temperatures were bracketed. The relative mass losses as a function of time are shown in Figure 47, 44, and 45 and suggest that depolymerization of PLA is generally proportional to temperature. This relationship is more prominent with MK and MNa experiments. In these experiments, care was taken to maintain a constant temperature, but some experimental error occurred as the bath temperature typically increased slightly as a function of time. Further, lines connecting the individual points are added for visualization reasons only.

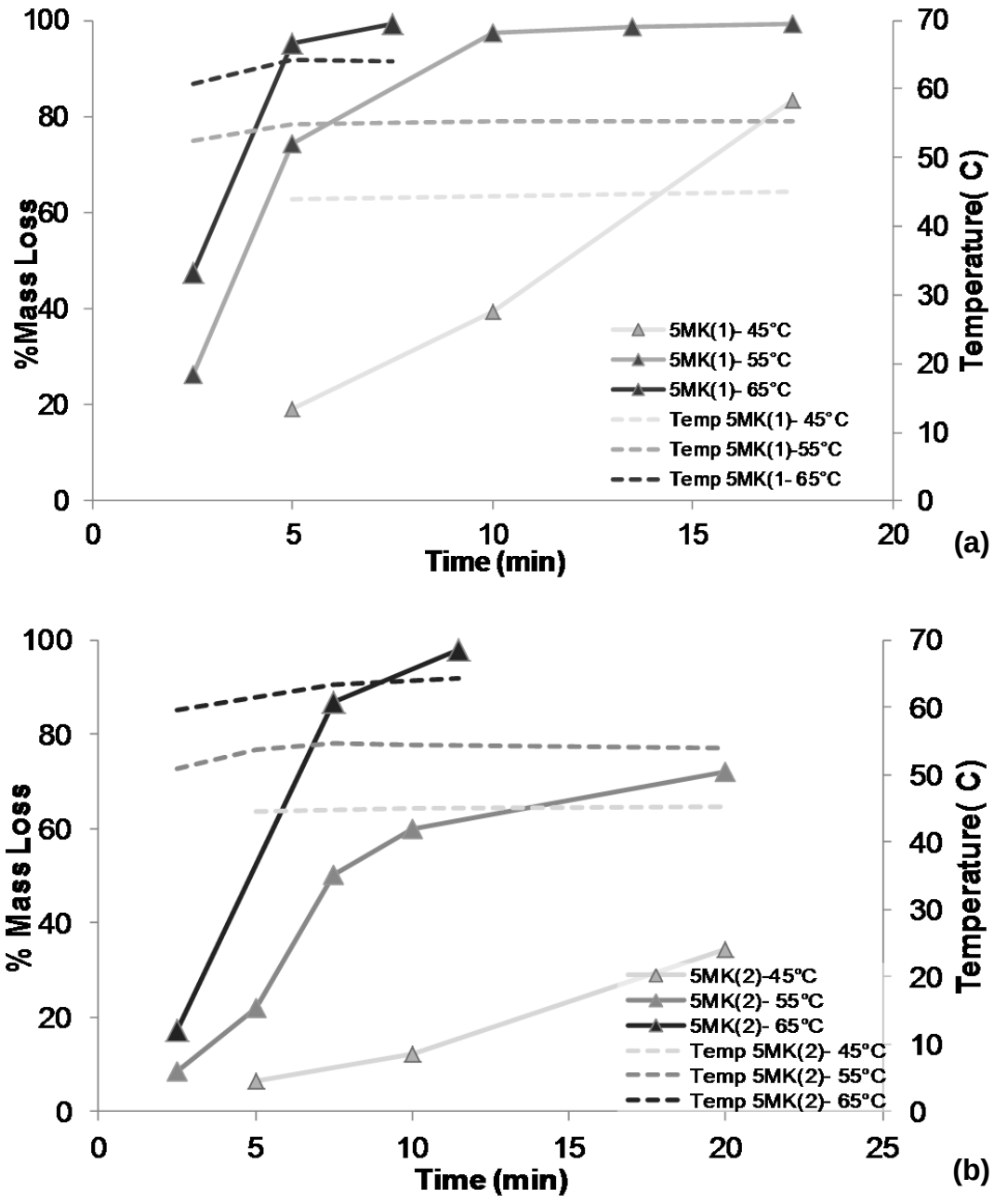

Figure 47 Effect of treatment temperature on relative mass loss as a function of treatment time for (a) MK(1) and (b) MK(2) experiments using hot bath treatments

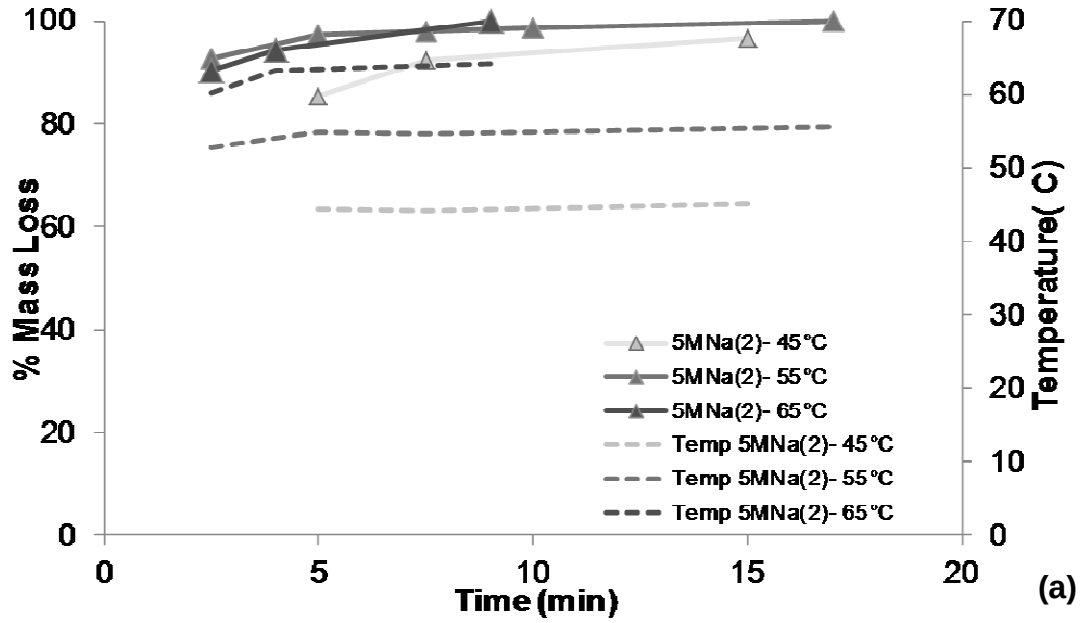

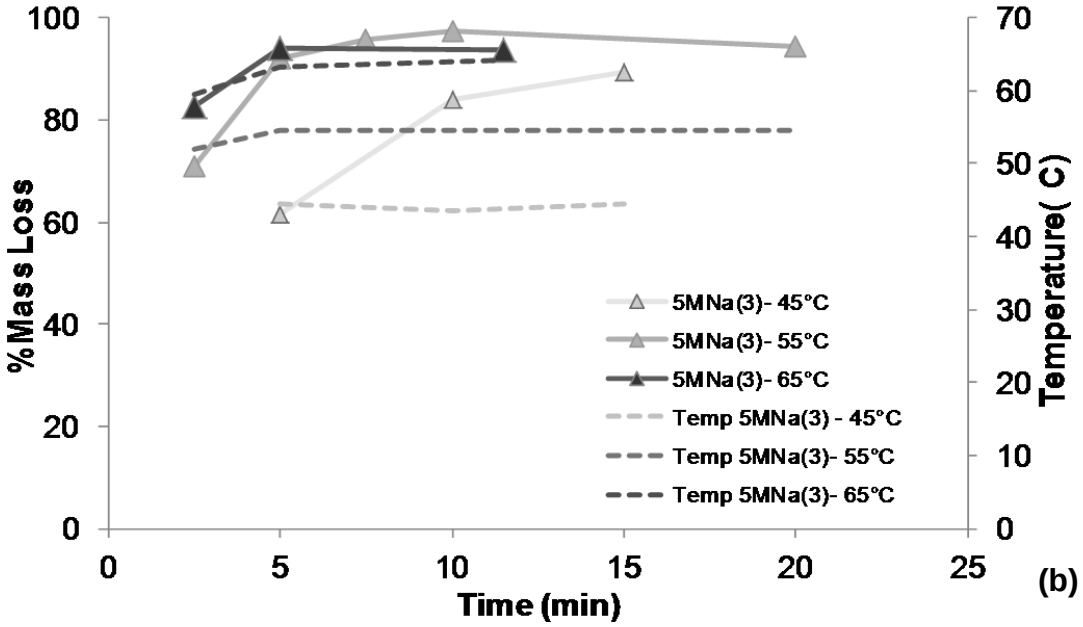

Figure 48 Effect of treatment temperature on relative mass loss as a function of treatment time for (a) MNa(2) and (b) MNa(3) experiments using hot bath treatments

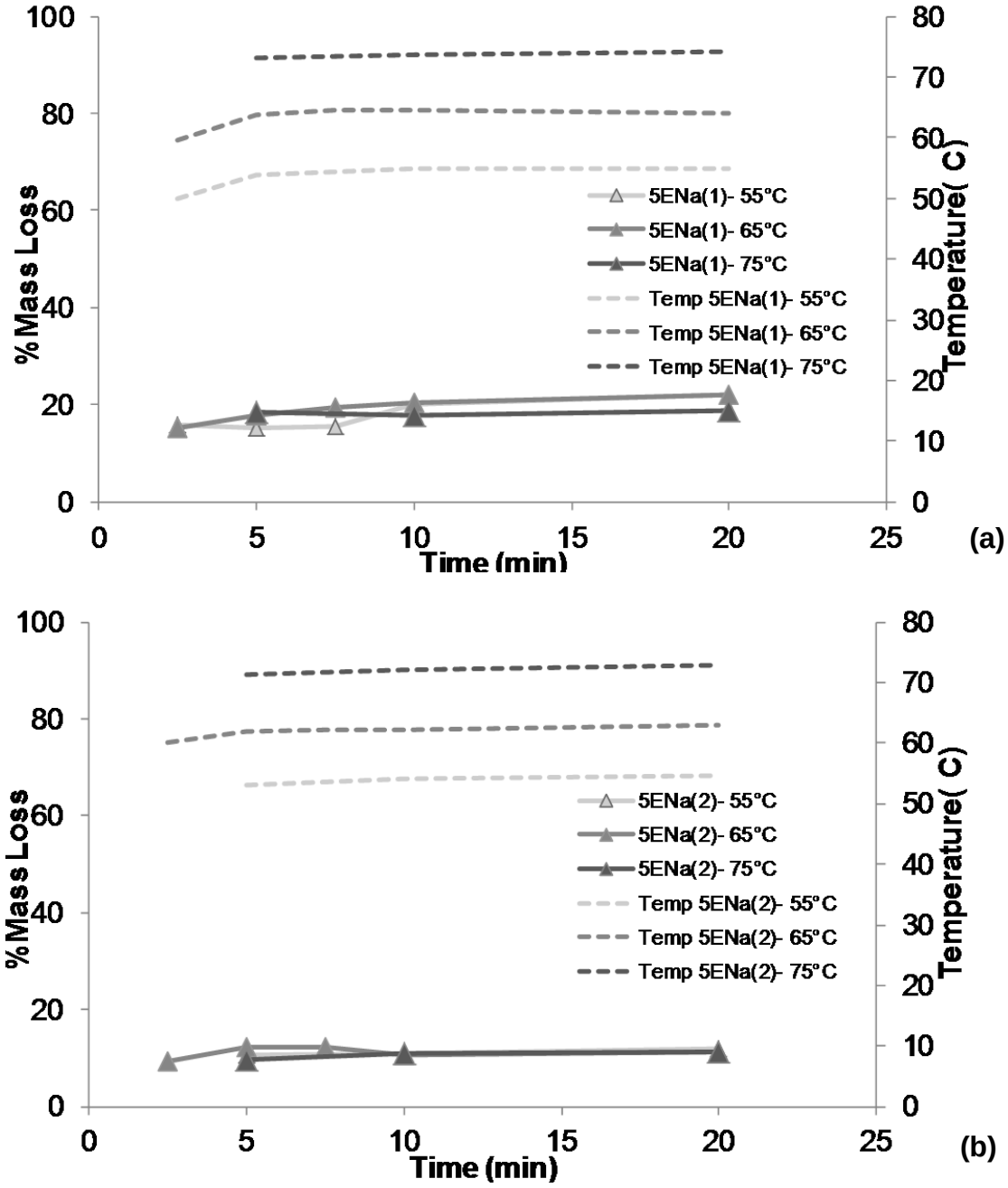

Figure 49 Effect of treatment temperature on relative mass loss as a function of treatment time for (a) ENa(1) and (b) ENa(2) experiments using hot bath treatments

5.4 Results: Scanning electron microscopy (SEM)

To gain insight into the impact (or lack thereof) of ultrasonic treatment, optical and scanning electron microscopy studies were completed. It was visually observed that the particle size was not significantly affected by the ultrasonic treatment. Typically, particle size is reduced by ultrasonics, particularly when particulate substrates (such as chips) are treated in a liquid ultrasonic bath. This increases the surface area to volume ratio and increases the number of reaction sites, thereby increasing reaction rates, such as depolymerization (theorized). This was not seen with the PLA chips, and it is believed to be related to the toughness of the plastic and its ability to absorb the shock waves and jets produced by ultrasonic cavitation.

Figure 50 shows the SEM image of virgin PLA as received. The surface is relatively smooth, but becomes rough after 5 min of depolymerization treatment with sodium hydroxide (0.25 g) and methanol (0.25 g), as shown in Figure 51 (a) with ultrasonic treatment and (b) with hot bath treatments. With ultrasonic treatment, there is a relatively rough texture on the surface, and the alignment of this texture corresponds to the stretch direction of the PLA bottle. In addition, this texture was more pronounced on the inner diameter of the bottle, where the degree of crystalline is higher because of a slower cooling. This texture is also less pronounced with the hot bath treated sample. It is

believed that the ultrasonics enhanced mixing of the liquid and caused some cavitation erosion on the surface. These effects resulted in the rough surface, but the increase in the surface area was not sufficient to accelerate depolymerization.

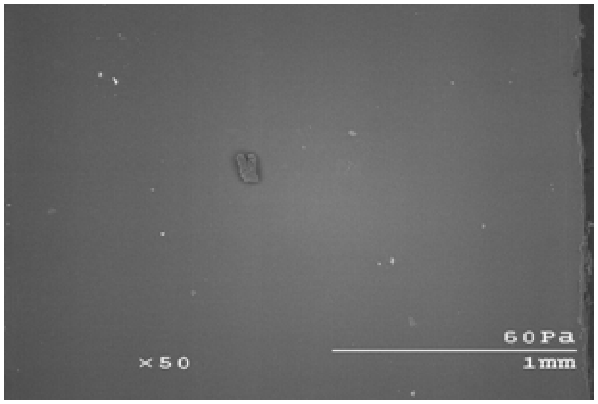

Figure 50 SEM image untreated PLA sample

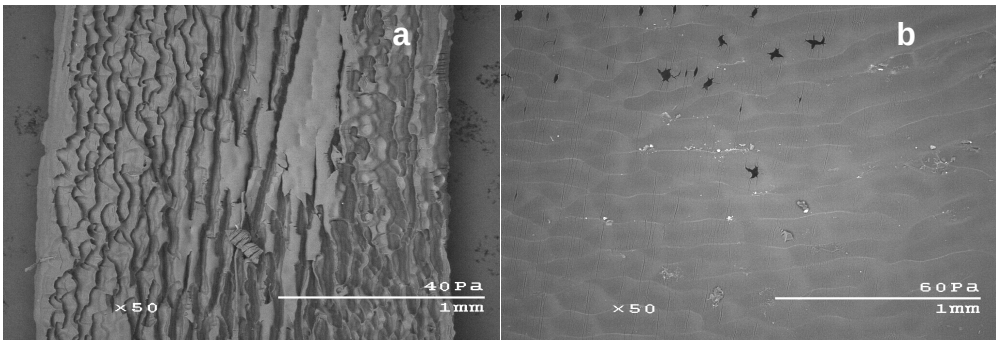

Figure 51 Treated PLA sample at 5 min with NaOH (0.25 g) and methanol media (0.5 g) (a) ultrasonics-13 μm (b) hot bath

A similar effect was seen with potassium carbonate (0.5 g) and methanol (0.5 g) as shown in Figure 52, but both the hot bath (b) and the ultrasonic (a) surfaces had a similar roughness, even though the ultrasonically treated samples appear slightly rougher. Again, it is believed that the mixing effects of ultrasonics promoted surface erosion but was not sufficient to accelerate the chemical rates.

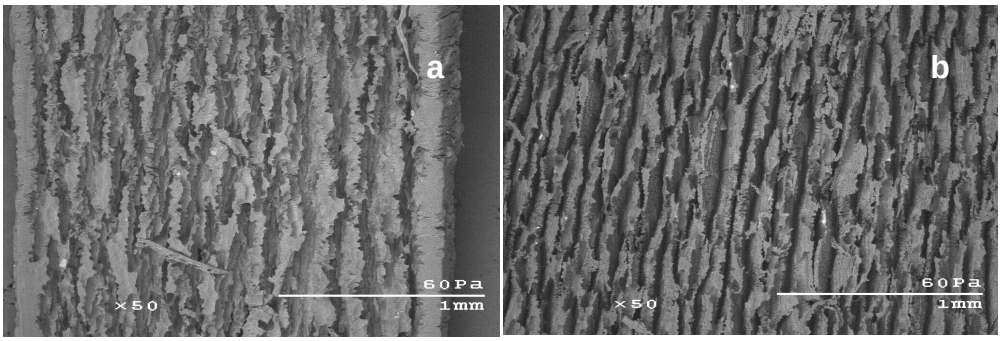

Figure 52 Treated PLA sample at 5min with K_2CO_3 -0.5g and methanol media (0.5 g) (a) ultrasonics13μm (b) hot bath

As confirmed in the next section, the laminar structure is the result of varying regions of crystallinity that are caused by the thermal history of the plastic as well as its stretching (molecular alignment) during the formation of the water bottles. That is, during the formation of the water bottles (i.e., the stretching of the bottles), the molecules are aligned in the hoop direction of the bottle.

This produces regions of crystallinty with amorphous regions between them. The amorphous regions are depolymerized faster (seen as valleys), while the crystalline regions depolymerized slower (seen as peaks). This is constant with the observation that the outer diameter (faster cooling) of the PLA sheets was even less textured as a result of less crystallinity.

5.5 Confirmation of depolymerization selectivity: Effect of crystallinity

To characterize the effect of crystallinity on depolymerization, relatively crystalline and relatively amorphous samples of PLA were depolymerized under optimum conditions with the hot bath treatment. Two samples of PLA chips, each with a mass of 5 g, were prepared by heating them above the T_g (75 ºC) for 30 min in a platen heater to mobilize the polymers. The first 5 g samples were then quickly removed from the heater and rapidly cooled in dry ice and methanol. This rapid cooling should have prevented crystallinity and resulted in samples that were nearly 0% crystiniline (~100% amorphous). The balance of the samples was then allowed to cool slowly by turning the heaters off of the platen heaters. It took approximately 120 min for the platen heater (and PLA samples) to cool to room temperature. This slow cooling should have promoted crystallinity. The balance of the samples was then depolymerized for various lengths of time to study the rate and morphology of the sample during depolymerization.

In those experiments where the effect of crystallinity on depolymerization was studied, the slowly cooled PLA samples shrank and warped, whereas the amorphous samples remained flat and unaltered. This is consistent with the fact that with more crystallinity, there is more shrinkage (less free volume). Both samples, when observed under cross-polarized light, exhibited different transmittance of light (see Figure 53) and, as expected, suggested a higher level of crystallinity with the slowly cooled sample. As seen in Figure 53 (a) the birefringence patterns are indicative of a semicrystalline structure. These samples were treated with MK(1) the hot bath technique (55°C) to observe the difference in progressive depolymerization for a cumulative time of 15 min.

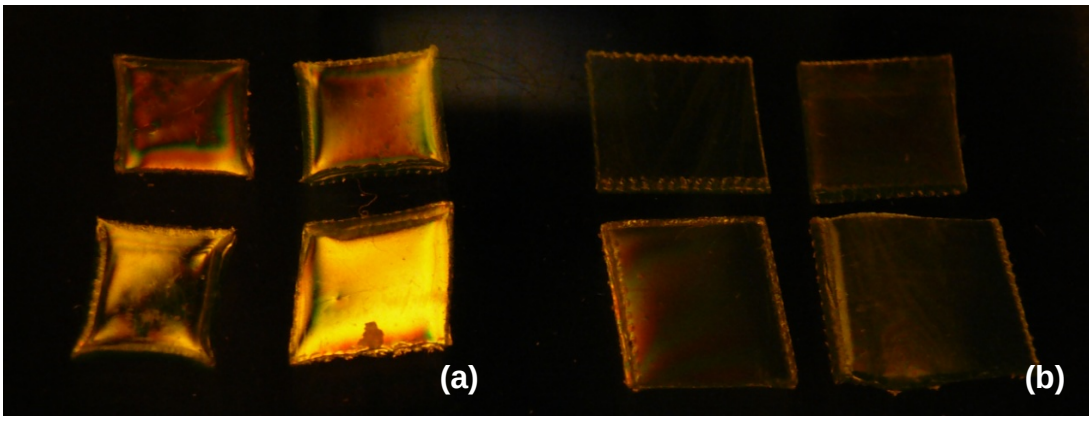

Figure 53 Photographs of PLA samples with cross polarized light (a) slowly cooled sample (b) rapidly cooled sample

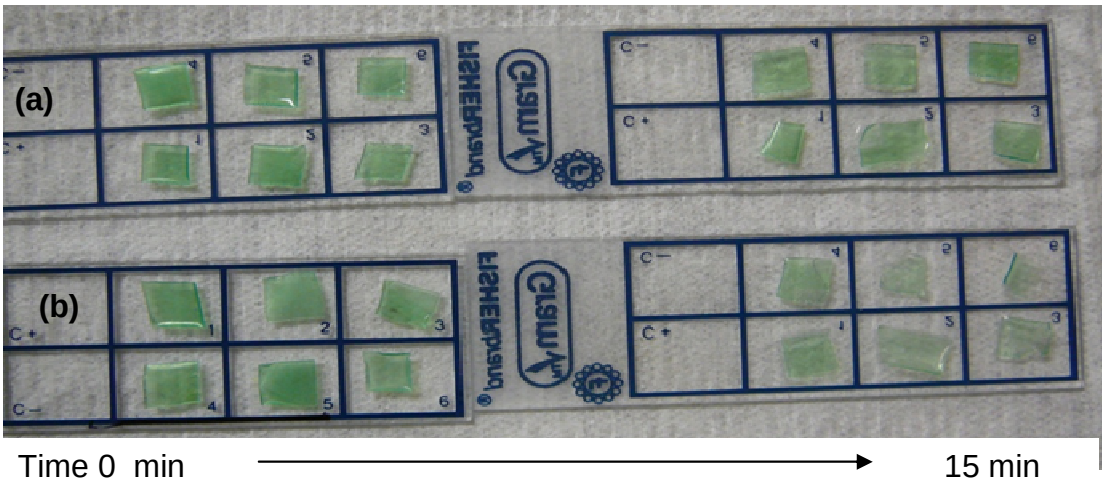

Figure 54 Photograph of PLA samples at different times from MK(1) hot bath treatment (a) slowly cooled sample (b) rapidly cooled sample (more depolymerization observed)

It was visually observed that rapidly cooled samples (amorphous) depolymerized faster when compared to slowly cooled samples (see Figure 54), where the mass losses of these samples is higher when compared to the slowly cooled samples.

This suggests that the degree of crystallinity affects the rate of depolymerization, a finding that is consistent with free-volume theories. The crystalline samples have less free volume between the polymer chains, which limits the rate and depth of diffuse (penetration) of catalysts into the samples.

In contrast, the amorphous samples had more free volume, thereby allowing the catalysts to penetrate into the bulk of the material. This allowed for more reaction sites and higher rates of depolymerization.

5.6 Statistical analysis of poly lactic acid (PLA) yield data

The PLA yields were categorized into sets of data, each of which correlated to a particular relationship between dependent and independent variables, such as sample size (g), media/solvent type, alkali compound (catalysts), amount of alkali compound, and ultrasonic amplitude and the response variable: LA yield. For each of the smaller sets of data, one or two explanatory (independent) variables were changed while the others were maintained at a constant value.

5.6.1 Effect of amplitude on yield

For a PLA sample (5 g) in methanol with 0.5 g of potassium carbonate, there were two values (two data points) of mass loss for each amplitude value (7, 13, and 19 µm (p-p)). The resulting data are detailed in Table 4.

Table 4 Summary of statistical data for the various ultrasonic amplitudes and effect of percentage mass loss

	Amplitude (µm (p-p))		
	7	**13**	**19**
	72	100	100
	70	99	99
Mean	71	99	100
Std. Dev.	1.5	1.0	0.38

There was a statistically significant difference between the mean yields for amplitude values 7,13, and 19 μm_{p-p} (F = 460.96, P value = 0.0002). The difference between the 7 and 13 μm_{p-p} showed a P-value near zero and a large F-factor. The 95% least significant difference (LSD) was 3.44. This means that if a difference in mean yields between two amplitudes was greater than or equal to 3.44, as seen with the 7 and 13 μm_{p-p} and 13 and 19 μm_{p-p}, that difference was significant. The procedure has a 95% confidence level. Thus, while the amplitude did affect depolymerization yield, this effect was only seen at the lower amplitude and not at the highest amplitude, as detailed in Table 5.

Table 5 Tabulated summary of the statistical difference among ultrasonic amplitudes

Comparison (Amplitude)	Difference in means	Statistically significant?
25 to 50	28.246 > 3.44	Yes
25 to 75	28.586 > 3.44	Yes
50 to 75	0.340 < 3.44	No

5.6.2 Effect of sample size and amount of NaOH on yield in ethanol

For samples treated in ethanol with NaOH, there were two values of yield for the four combinations of sample size (1 g and 5 g) and amount of sodium hydroxide (0.25 g and 0.50 g). This allowed for a two-factor model with interaction to be characterized by the effect of each factor individually measured.

Some combinations of sample size and amount of sodium hydroxide had a statistically significant effect on the mean LA yield. ($F = 40.95$, P-value = 0.0018). The honestly significant difference (HSD) was 22.50. The HSD is similar to the LSD and is used when making larger number of cross-comparisons. With four treatment combinations, there were 6 possible pair-wise comparisons. The HSD allows all of these values to be compared and maintain a 95% confidence. The difference in mean LA yield for the various

treatment combinations, if and when greater than 22.50, correlates to a statistically significant difference.

Table 6 Tabulated data of combinations of PLA mass (1 g and 5 g) and catalysts mass(0.25 g and 0.5 g) on the statistical difference of LA yield. The statistical difference in treatment is indicated by differing alphabets (A, B, and C)

Treatment Combination				Mean Yield
1 g, 0.50 g	A			66.461
1 g, 0.25 g		B		40.151
5 g, 0.50 g		B	C	18.376
5 g, 0.25 g			C	10.752

In Table 6, treatment combinations sharing the same letter were not significantly different. For example 1 g, 0.50 g was significantly different than any other population, while 1 g and 0.25 g and 5 g and 0.5 g were not statistically different. In other words, the 1 g PLA sample with 0.500 g NaOH produced the highest mean yield, and this mean yield was significantly greater than the mean yields for all other combinations of size of sample and amount of NaOH.

The individual factors were also evaluated. The sample mass was statistically significant (F = 98.29, P-value = 0.0006) on LA yield. The 1 g mass had a statistically higher mean yield (53.3) compared to the 5 g size (14.6). Therefore, for the same amount of salt/catalyst mass, note that as the sample mass increases, the mean yield decreases significantly. The amount of NaOH was statistically significant (F = 18.9, P-value = 0.0122) on LA yield. The larger amount of NaOH (0.50 g) produced a significantly higher mean yield (42.4) compared to the smaller amount of NaOH (0.25 g), which had a mean yield of 25.5. Therefore, the yield was generally proportional to the amount of NaOH. The interaction between sample mass and amount of NaOH was not statistically significant (F = 5.72, P-value = 0.0751).

5.6.3 Effect of sample size and amount of NaOH or K_2CO_3 on LA yield in methanol

Because the amounts of K_2CO_3 were different from the amounts of NaOH, two separate analyses were performed.

1. Sample mass and amount of K_2CO_3 in methanol
2. 2. Size of sample and amount of NaOH with methanol

These two are detailed below.

Sample mass and amount of K_2CO_3 in methanol

For samples in methanol with K_2CO_3 there were at least two values of yield for the four combinations of sample mass (1 g and 5 g) and amount of potassium carbonate (0.25 g and 0.50 g). This allowed a two factor model to be generated with interaction as well as the effect of each factor individually.

Some combinations of sample mass and amount of potassium carbonate had a statistically significant effect on mean yield of LA. ($F = 29.62$, P-value = 0.0013). The honestly significant difference (HSD) was 14.53.

Note that once again treatment combinations not connected by the same letter are significantly different. Table 7 shows that both combinations are significantly different from 1 g PLA and 0.25 g K_2CO_3. The 5 g PLA sample with 0.250 g K_2CO_3 produces the lowest mean yield, and this mean yield was significantly lower than the mean yields for all other combinations of size of sample and amount of K_2CO_3.

Table 7 Tabulated data of combinations of PLA mass (1 g and 5 g) and potassium carbonate catalysts mass (0.25 g and 0.5) on the statistical difference of LA yield. The statistical difference in treatment is indicated by differing alphabets (A, B, and C)

Treatment Combination			Mean Yield
1 g, 0.500 g	A		99.6
1 g, 0.250 g	A		99.5
5 g, 0.500 g	A		99.3
5 g, 0.250 g		B	73.2

The individual factors were also evaluated. The test was statistically significant (F = 24.76, P-value = 0.0042). The 1 g size had a statistically higher mean yield (99.5) compared to the 5 g sample (86.3, the average of 99.3 and 73.2). Therefore, the mean yield is generally inversely proportional to sample mass. The amount of K_2CO_3 was statistically significant (F = 24.15, P-value = 0.0044). The larger amount of K_2CO_3 (0.50 g) produced a significantly higher mean yield (99.4) compared to the smaller amount of K_2CO_3 (0.25 g), which had a mean yield of 86.3. Therefore, LA yield is generally proportional to the amount of K_2CO_3. The interaction between sample mass and amount of K_2CO_3 was also statistically significant (F = 23.79, P-value = 0.0046). This increase in mean yield was seen when the amount of K_2CO_3 was increased from 0.25 g to 0.50 g. However, this increase

in yield is not the same (statistically) for the various sample masses (1 g and 5 g). The interaction plot below demonstrates this interaction. For 1 g samples, the amount of K_2CO_3 had virtually no effect on yield. However, with 5 g samples, increasing the amount of K_2CO_3 dramatically increases average yield.

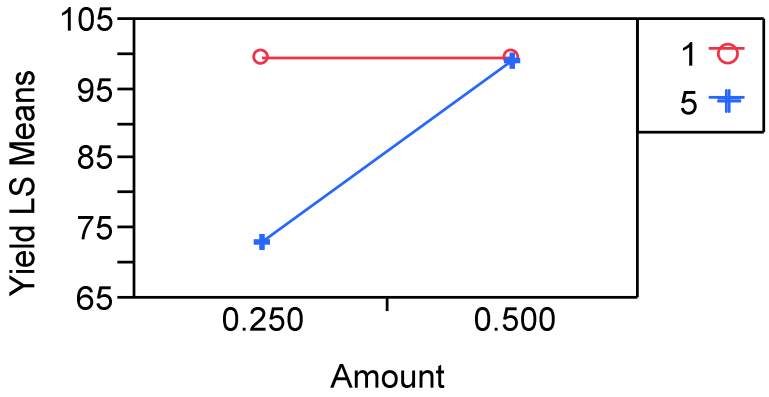

Figure 55 Interaction plot for catalyst concentration and yield/ % mass loss

Size of sample and amount of NaOH with methanol

For samples in methanol with NaOH, there were at least two values of yield for the four combinations with sample mass (1 g and 5 g) and amount of sodium hydroxide (0.125 g and 0.250 g). This allows a two-factor model with interactions generated by the effect of each factor individually.

None of the combinations of sample masses and amount of sodium hydroxide had a statistically significant effect on mean LA yield. (F = 0.37, P-value = 0.7768).

Table 8 Tabulated data of combinations of PLA mass (1 g and 5 g) and sodium hydroxide catalysts mass(0.25 g and 0.5 g) on the statistical difference of LA yield. The statistical difference in treatment is indicated by differing alphabets (A, B, and C)

Treatment Combination		Mean Yield
1 g, 0.125 g	A	98.800
1 g, 0.250 g	A	99.467
5 g, 0.125 g	A	98.970
5 g, 0.250 g	A	99.570

Treatment combinations not connected by the same letter are significantly different. Table 8 shows that all other combinations are not significantly different from each other. The individual factors can also be evaluated. The size of the sample is not statistically significant (F = 0.44, P-value = 0.5370). The amount of NaOH is not statistically significant (F = 0.06, P-value =

0.8173). The interaction between size of sample and amount of NaOH is not statistically significant (F = 0.47, P-value = 0.7721).

5.7 Validation of finite element analysis modeling with particle image velocimetry (PIV)

The FEA models were validated by comparing the predicted fields with measured velocity fields. The velocity field was measured using a laser illuminated tracking technique with natural buoyancy particles (TiO_2) with a diameter of 1 µm. It was assumed that the beads had insignificant inertia and that their velocity would correspond to the water velocity. The images of the illuminated particles were captured with a CCD and the sequential images processed with a proprietary software package. Based on spatial locations of the particles from frame to frame the software calculated the velocities of the particles. These velocities were then plotted as contour plots. Figure 56 shows the contour plot and a single frame of the images recorded for the ultrasonic amplitude of $13\mu m_{p\text{-}p.}$

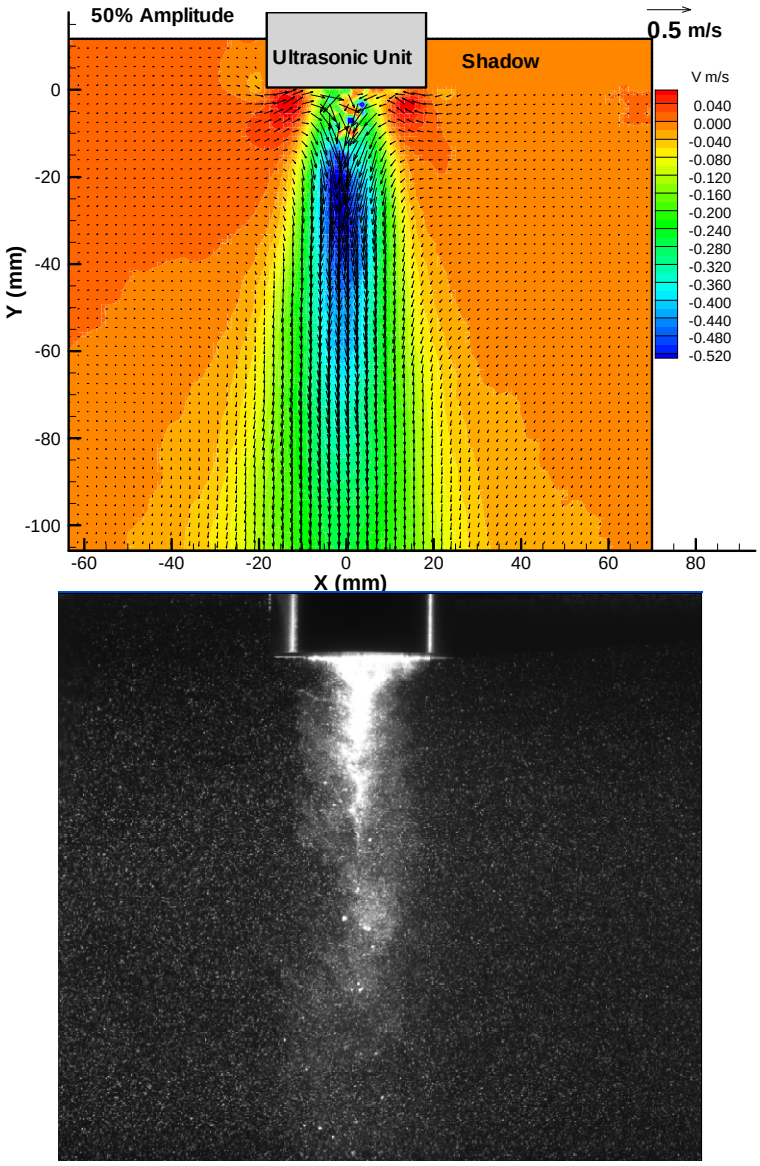

Figure 56 Photograph of ultrasonics turbulence as capture by PIV

These experiments were conducted for several seconds at three ultrasonic amplitudes: 7, 13, and 19 µm. Figure 57 shows the contour plot of velocities predicted by FEA analysis

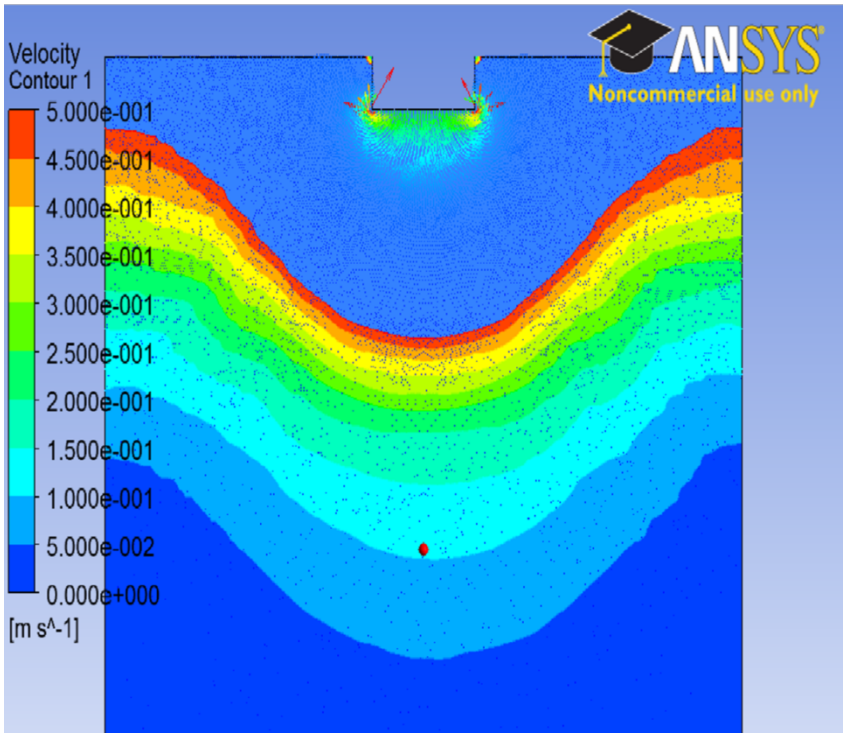

Figure 57 Predicted velocity of water in beaker with FEA

While the maximum velocities are in agreement, the velocity fields are not. For example, in the experimental velocity fields, the maximum velocity contour map forms an inverter “cone”-shaped field below the horn. However, in the model, this maximum field has a “bowl” shape below the horn at a relatively large distance. It is believed that this is because water is assumed

to be incompressible, while at the accelerations observed (~1000 g), water is compressible.

The flow patterns as observed from both PIV analysis and Ansys FEA model are in concurrence with near-field and far-field effects of ultrasound diffraction. A classical explanation of these effects for a circular disc source is as depicted in Figure 58

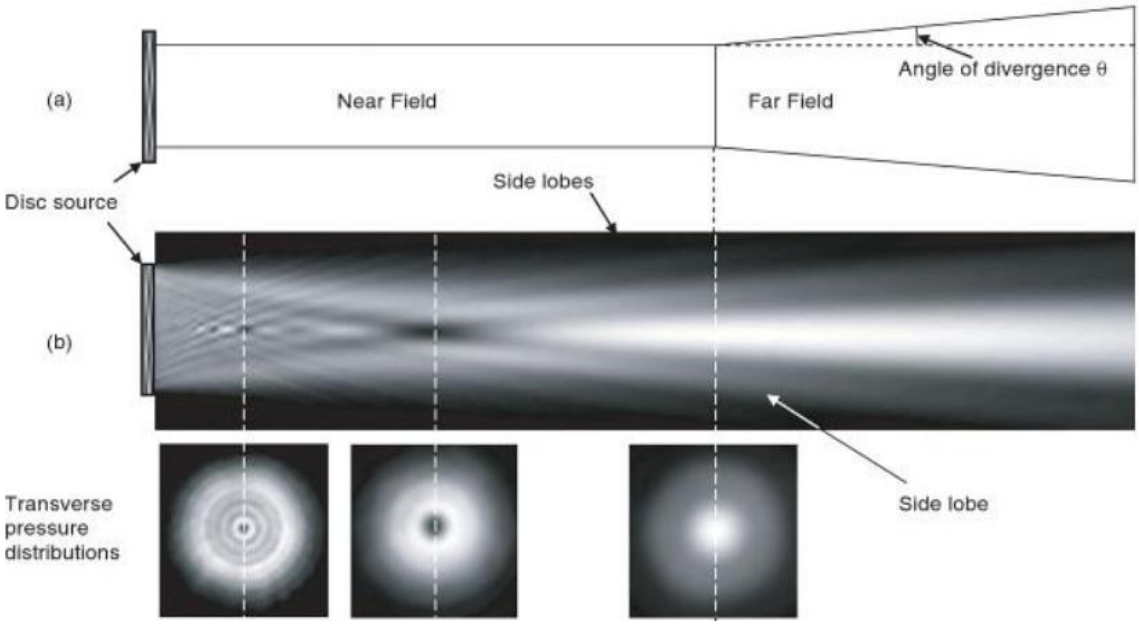

Figure 58 Near field and far field effects of ultrasound from a planar disc source [52]

The ultrasound follows a cylindrical beam shape with the similar cross-sectional geometry as the vibration source within the near field region. It

should be noted that the pressure is uniform in the near field region of the medium. The length over which near field effects prevail can be determined based on the Rayleigh distance. In the far field region, constructive and destructive interference lead to maximum intensities (toward center) and near zero intensity regions. In the far field region, the pressure difference caused by ultrasound interference results in turbulence and mixing in the medium. The Rayleigh distance for the ultrasonic source is determined from the Eq. 13 [53] where 'a' is the radius of circular horn face (19.5 mm) and λ (74.2 mm) is the wave length of the ultrasound in a water medium (speed of sound in water c_{water}=1484 m/s)

$$R= \pi a^2/\lambda \qquad \text{[Eq. 13]}$$

Utilizing previously mentioned values, the distance R is calculated to be 16mm and this is shorter than 25mm, the average distance between the ultrasonic horn surface and bottom of the treatment beaker. The Rayleigh distance and velocity vector contour plots from PIV indicate that both near and far field effects exists during the ultrasonic treatment in the utilized treatment vessel(150 ml beaker). Further change in vessel geometry for ultrasonic treatment will alter the final effects. However, because strong

mixing of the chips was visually observed, it was assumed that the PLA was uniformly treated.

5.8 Energy and conversion efficiency.

Polylactic acid as an alternative for petroleum plastics has a heating value of only 19 MJ /kg [54, 55] . The energy consumption for production of PLA is 82.5 MJ /kg of which 54 MJ/KJ [56] is derived from fossil fuel and the balance is from corn and its cultivation which considered to be biorenewable energy. Considering these energy values, it can be seen that energy recovery as low as 25 % can be achieved by incineration of PLA. Though composting is considered an effective route, the production of new PLA will effect further consumption of fossil energy (54MJ/kg of PLA) and result in additional greenhouse gas (GHG) emissions.

The average amount of energy utilized per ultrasonic treatment to achieve complete depolymerization was observed to range between 1.83-2.25 MJ/kg (22-27 KJ/ 12 g from trials) of PLA depending on treatment parameters such as medium and catalyst concentration. In comparison, for hot bath technique the combination of methanol as treatment medium with sodium hydroxide at 0.25 g the amount of energy required for depolymerization was calculated based on adiabatic heating. In more detail, the treatment medium methanol

with volume of 50ml corresponds (40g at a density of 0.79g/cm^3) to 1.25 Moles of methanol. The specific heat or heat capacity (C_p) of methanol is 79 J/(mol K). The amount of energy required to raise the temperature of the methanol medium from 25ºC to 55ºC (depolymerization temperature) can be calculated by Eq. 14, where M is the number of moles and ΔT is the change in temperature

$$E_{(25\text{-}55)} = M \times C_p \times \Delta T \qquad \text{[Eq. 14]}$$

From the above expression for a ΔT=55-25C = 30K, the energy was determined to be 0.26 MJ/ kg of PLA for effectively depolymerization (neglecting energy required to maintain constant temperature). Similar calculations for HTHP process with water as a medium (C_p water=75.6 J/(mol K)) and ΔT=160-25ºC and assuming the same concentration of 12g/50ml (PLA/water) the energy consumption is 2.34 MJ/kg of PLA. Comparison of these energy values indicates that the newly developed hot bath process with methanol as treatment medium along with sodium hydroxide utilizes 10 fold less energy than the investigated ultrasonic treatment or the HTHP process developed by other researchers.

5.9 Conclusions

When this research began, it was believed that the use of ultrasonics could enhance and/or accelerate the depolymerization of PLA and that ultrasonics could decrease the energy required to depolymerize (enhance) and/or reduce the time required to depolymerize PLA. However, this did not prove to be the case over the range of parameters studied. While ultrasonics resulted in surface erosion of the PLA samples (chips), the effect was insignificant compared to bulk erosion/depolymerization with proper media and catalysts over the range of treatment parameters studied.

The most significant finding of this work was the identification of a catalyst (K2CO3 and NaOH) that could depolymerize PLA within 5 to 7 min at moderate conditions (60°C). This is in contrast to previously reported results that required long cycle times (30 min to 24 h), as well as others that required intense conditions, including high temperatures and pressures. This reduced cycle time may allow the realization of recovery of lactic acid from postconsumer PLA products, reducing greenhouse gas emissions (less need to process biofeedstocks) as well as the food/stuff concern with bioplastics. The research also showed that the depolymerization of PLA was accelerated by temperature and limited by the degree of crystallinity. Finally, it is also concluded that simple models based on fundamental principles can be used

to predict acoustic streaming velocities. These models were validated with experimental values from particle tracking techniques.

Other conclusions that can be drawn from this research include:

1) Water is not an effective media/solvent for PLA depolymerization.
2) MgO,$CuCO_3$, $CACO_3$, and $ZnCO_3$ are not effective catalysts for PLA depolymerization.
3) A mass of 0.25 g of catalysts, such as NaOH in 50 ml of methanol and 5 g of PLA, is sufficient to fully depolymerize PLA in 5 to 7 min
4) Other catalysts, such as K_2CO_3, require higher concentrations to fully depolymerize PLA, and require depolymerization times between 10 and 15 min.
5) The combinations of K_2CO_3 and NAOH with methanol respectively form a rapid depolymerizing chemistry for PLA.
6) It is hypothesized that alkoxide radicals generated from K_2CO_3 and methanol were that create a highly basic pH environment leading to effective depolymerization of PLA.
7) It is theorized that Alkoxide radicals along with optimum temperatures (55 ºC to 75ºC) were found to affect depolymerization faster at lower energy (temperature) inputs compared to previous research. This

might favor the regeneration of optically pure stereoisomer as indicated by previous research[40,41,42,43]

8) The combination of NaOH with methanol in particular was effective because of the added presence of hydroxly radical in the reacting media. This ultimately leads to a further increase in basic pH.

9) The is difference in maximum percent mass loss value and percent conversion value and this is attributed to compounder effects of additive/colorants present in the sample along with incomplete conversion of PLA to LA.

REFERENCES

1 Weekly weight crude oil prices. Published by U.S. Energy Information Administration (http://www.eia.doe.gov/dnav/pet/hist/LeafHandler.ashx?n=PET&s=WTOTWORLD&f=W) (visited 3/20/2011)

2 Municipal Solid Waste Generation, Recycling, and Disposal in the United States: Facts and Figures for 2009. Pg 4. Published by U.S . Environmental Pollution Agency (http://www.epa.gov/osw/nonhaz/municipal/pubs/msw2009-fs.pdf) (visited 03/20/2011)

3 Municipal Solid Waste In The United States 2009 Facts and Figures (full report). Pg 51 Published by U.S. Environmental Pollution Agency (http://www.epa.gov/osw/nonhaz/municipal/pubs/msw2009rpt.pdf) (visited 03/20/2011)

4 Performance Evaluation of Environmentally Degradable Plastic Packaging and Disposable Food Service Ware - Final Report (2007) (http://www.calrecycle.ca.gov/publications/Plastics/43208001.pdf) (visited 06/06/2011)

5 'Advanced Materials And Chemicals' Published by NatureWorks LLC (formerly Cargill, Inc.) (http://statusreports.atp.nist.gov/reports/94-01-0173PDF.pdf) (visited 11/02/2010)

6 'Sun Chips Bag to Lose Its Crunch' Web article by The Wall Street Journal. (http://online.wsj.com/article/SB10001424052748703843804575534182403878708.html) (visited 05/26/2011)

7 Narayanan, Niju; Roychoudhury, Pradip K.; Srivastava, Aradhana. Pg 167 " L-(+)- lactic acid fermentation and its product polymerization". Electronic Journal of Biotechnology; Vol.7(2) (2004).

8 Davis. W.A.; Allen. A.H., Pg 429. "Allen's commercial organic acid analysis" ;Vol 7 (1912).

9 Dubos. R.J., Pg 360-61, "Louis Pasteur, freelance of science" (1950).

10 Benninga. H., Pg 77, "A history of lactic acid making: a chapter in the history of biotechnology" (1990)

11 1893 :Process for Manufacturing lactic acid discovered, (http://www.boehringer-ingelheim.com/corporate_profile/history/history1.html) (visited 03/21/2011)

12 Rafael. A., Loong-Tak. L., Susan. E. M. Selke, Hideto Tsuji, Pg 4, "Poly(lactic Acid): Synthesis, Structures, Properties, Processing, and Application"; (2010).

13 Robergs, RA; Ghiasvand, F; Parker, D. Pg 502, "Biochemistry of exercise-induced metabolic acidosis". American Journal of physiology-Regulatory, Integrative and Comparative Physiology., Vol 287 (3) (2004).

14. Vaidya A. N , Pandey .R. A., Mudliar .S., Suresh Kumar .M., Chakrabarti .T. and Devotta .S., Pg 429, "Production and Recovery of Lactic Acid for Polylactide—An Overview", Critical Reviews in Environmental Science and Technology, Vol 35,(2005)

15 Dworkin. M. (Editor-In-Chief), Falkow .S., Rosenberg. E., Schleifer. KH., Stackebrandt. E. (Editors), P 239-250, "The Prokaryotes: A Handbook on the Biology of Bacteria, Third Edition Vol1: Symbiotic Associations, Biotechnology, Applied Microbiology" (2005)

16 Tamime. A.Y., Pg 18 , "Fermented milks" Society of Dairy Technology (2006).

17 Kulp.K, Loren .K.J, Pg 328, "Handbook of Dough Fermentation" ; (2003).

18 Goswami. B.C, Anandjiwala. R.D, Hall.D.M, Pg 80, "Textile sizing"; (2005).

19 Scott. G., Pg 200, "Degradable polymers: principles and applications" 2nd edition; (2002).

20 Mohanty, A.K., Misra. M, Drzal, L.T.; "Natural Fibers , Biopolymers , and Biocomposites."; (2005).

21 Lunt. J., Pg142, "Large - scale production , properties and commercial applications of polylactic acid polymers." Polymer Degradation and Stability; 59(1-3), (1998).

22 Gonzalez .M. F., Ruseckaite R. A., Cuadrado .T. R., Pg-1222, “Structural Changes of Polylactic-Acid (PLA) Microspheres under Hydrolytic Degradation”, Journal of Applied Polymer Science; Vol. 71, (1999).

23 Ensminger. D., Bond. L., Pg 2, “Ultrasonics: Fundamentals, Technologies and Applications”’; Third Edition (2008).

24 Leighton T.G, Pg 3. “The acoustic bubble”; Volume 10 (1997)

25 Baldev. R., Palanichamy. P., Rajendran. V., Pg 10 “Science and technology of ultrasonics” (2003)

26 Sen.S.N, Pg 27 ,“Acoustics, waves and oscillations”; (1990)

27 Iowa state University coursework – AE/ TSM 590 by Dr. David Grewell

28 Magnetostrictive versus piezoelectric transducers for power ultrasonics applications by Blackstone~Ney ultrasonisc inc. (http://www.blackstone-ney.com/pdfs/T_Mag_Vs_Piezo.pdf)(visited 5/11/2011.)

29 Patranabis.D., Pg-48, “Sensors and Transducers”; (2004).

30 Tooley. M, Toole. M.H, Pg 78,”Electronic circuits: fundamentals and applications”;(2006)

31 Nano cavitation for algal oil harvesting- web article (http://alfin2300.blogspot.com/2010_01_01_archive.html) (visited 5/13/2011)

32 Suclick. K., Pg 7, “Ultrasound: Its Chemical, Physical, and Biological Effects” (1988).

33 Storz doulth shock wave : web image for Ultrasonic shock wave therapy equipment. (http://www.lockstockuae.com/products/_storz_duolith_shockwave) visited on 5/13/2011

34 Chiellini. E; Solaro, R., Editors. “Biodegradable Polymers and Plastics”;(2003)

35 NAPCOR concerned about impact of PLA bottles on PET recycling. Article by Plastics News
(http://plasticsnews.com/headlines2.html?id=1248447732) (visited July 8th 2010)

36 Using Near-Infrared Sorting to Recycle PLA Bottles.
(http://www.natureworksllc.com/the-ingeo-journey/end-of-life-options/recycling/recycling-sortation.aspx) (visited July 8th 2010)

37 Noda, M; Okuyama. H. Pg 497, "Thermal catalytic depolymerization of poly (L - lactic acid) oligomer into LL - lactide : effects of Al, Ti, Zn and Zr compounds as catalysts". Chemical & Pharmaceutical Bulletin 47(4). (1999).

38 Morita. M; Hirama, Yasuko; Liew, M. K. H., Pg 467 , "Separation and purification of lactic acid from fermentation broth. Thermal catalytic depolymerization of poly (lactic acid) into lactide". Kagaku Kogaku Ronbunshu 22(3) (1996).

39 Muhammad.F., Takashi. S, Hideto, T; Hiroyuki.D; Koichi.F. Pg 1714, "Depolymerization of poly (L- lactic acid) under hydrothermal conditions." Asian Journal of Chemistry 19(3), (2006),

40 Watanabe.M , Kawai.F, Tsuboi.S., Nakatsu,S., Ohara,H., Pg 619, "Study on Enzymatic Hydrolysis of Polylactic Acid by Endogenous Depolymerizaion Model. Macromolecular Theory and Simulation.", vol 16 (2007).

41 Yagihashi, M., Funazukuri.T., Pg 1247, "Recovery of L-Lactic Acid from Poly(L-lactic acid) under Hydrothermal Conditions of Dilute Aqueous Sodium Hydroxide Solution". Industrial & Engineering Chemistry Research, 49, (2010).

42 Motoyama. T, Tsukegi. T, Shirai. Y., Nishida.H., Endo. T. Pg 1350, " Effects of MgO catalyst on depolymerization of poly - L - lactic acid to L , L - lactide." Polymer Degradation and Stability, 92(7), (2007).

43 Tsuji, H., Saeki. T., Tsukegi. T., Daimon. H.; Fujie, K., Pg 1956 “Comparative study on hydrolytic degradation and monomer recovery of poly (L - lactic acid) in the solid and in the melt”. Polymer Degradation and Stability , 93(10), (2008).

44 Sutokskaya, I. V. , Pg 431 “Effect of ultrasonics on microbial cells (fungi and bacteria).“ Eur. Biophys. Congr., Proc., 1st (1971),

45 Flint, E. B., and Suslick, K. S. Pg 1397. “The temperature of cavitation, Science”, 253,(1991).

46 Faraday, M. Pg 299. “On peculiar class of acoustical figures; and on certain form assumed by groups of particles upon vibrating elastic surfaces.” Phil. Trans. Roy Soc. London, 121,. (1831)

47 Kuttruff, H. “Ultrasonics Fundamentals and Applications”. Elsevier Science Publishers Ltd., Essex, England. (1991).

48 Grippaudo F R; Matarese R M; Macone A; Mazzocchi M; Scuderi N Pg 197, “Effects of traditional and ultrasonic liposuction on adipose tissue: a biochemical approach. Plastic and reconstructive surgery” (2000), 106(1),

50 Sun, Ximei; Isayev, A. I. Pg19 “Continuous ultrasonic devulcanization : comparison of carbon black filled synthetic isoprene and natural rubbers.” Rubber Chemistry and Technology (2008), 81(1).

51 Recycling PLA (http://biocor.org/?page_id=5) (visited 5th Nov 2010)

52 Hoskins. P. R., Martin. K, Thrush A. Pg 16, “Diagnostic Ultrasound: Physics and Equipment” (2010)

53 University of South Hampton, UK, “Fundamentals of Ultrasonic wave propagation”, Humphrey V (2011).

54 “Life Cycle Inventory Of Five Products Produced From Polylactide (Pla) And Petroleum-Based Resins” Technical report

(http://www.athenasmi.ca/projects/docs/Plastic_Products_LCA_Technical_Rpt.pdf) (visited- 06/10/2011)

55 Cornelissen T., Yperman J,, Reggers G., Schreurs S. and Carleer R. Pg 1031, “Flash co-pyrolysis of biomass with polylactic acid. Part 1: Influence on bio-oil yield and heating value”, Fuel, Volume 87, Issue 7, June 2008.

56 Vinka E.T.H., Ra´bagob K.R., Glassnerb G.A., Gruberb P. R. Pg 403, “Applications of life cycle assessment to NatureWorksTM polylactide (PLA) production”, Polymer Degradation and Stability 80 (2003)